JAEA-Review
2011-034

JAEA-Review

# Annual Report of R&D Activities in Center for Computational Science & e-Systems from April 1, 2009 to March 31, 2010

Center for Computational Science & e-Systems

October 2011

Japan Atomic Energy Agency

日本原子力研究開発機構

本レポートは独立行政法人日本原子力研究開発機構が不定期に発行する成果報告書です。
本レポートの入手並びに著作権利用に関するお問い合わせは、下記あてにお問い合わせ下さい。
なお、本レポートの全文は日本原子力研究開発機構ホームページ（http://www.jaea.go.jp）
より発信されています。

独立行政法人日本原子力研究開発機構　研究技術情報部　研究技術情報課
〒319-1195　茨城県那珂郡東海村白方白根 2 番地 4
電話 029-282-6387, Fax 029-282-5920, E-mail:ird-support@jaea.go.jp

This report is issued irregularly by Japan Atomic Energy Agency
Inquiries about availability and/or copyright of this report should be addressed to
Intellectual Resources Section, Intellectual Resources Department,
Japan Atomic Energy Agency
2-4 Shirakata Shirane, Tokai-mura, Naka-gun, Ibaraki-ken 319-1195 Japan
Tel +81-29-282-6387, Fax +81-29-282-5920, E-mail:ird-support@jaea.go.jp

JAEA-Review 2011-034

# Annual Report of R&D Activities in Center for Computational Science & e-Systems from April 1, 2009 to March 31, 2010

Center for Computational Science & e-Systems

Japan Atomic Energy Agency
Tokai-mura, Naka-gun, Ibaraki-ken

(Received August 5, 2011)

This report overviews the activity of research and development (R&D) in Center for Computational Science & e-Systems (CCSE) of the Japan Atomic Energy Agency (JAEA), during the fiscal year 2009 (April 1, 2009 - March 31, 2010). The work has been accomplished by the Simulation Technology R&D Office and Computer Science R&D Office in CCSE. The activity includes researches of secure computational infrastructure for the use in atomic energy research, which is based on the grid technology, a seismic response analysis for the structure of nuclear power plants, materials science, and quantum bioinformatics. The materials science research includes large scale atomic and subatomic simulations of nuclear fuels and materials for safety assessment, large scale quantum simulations of superconductor for the design of new devices and fundamental understanding of superconductivity. The quantum bioinformatics research focuses on the development of technology for large scale atomic simulations of proteins.

Keywords: Nuclear Engineering, R&D Activity, CCSE, Computer Technology, Computational Mechanics, Computational Materials Science, Computational Quantum Bioinformatics

JAEA-Review 2011-034

# 平成 21 年度　システム計算科学センター研究開発　年報

日本原子力研究開発機構
システム計算科学センター

（2011 年 8 月 5 日 受理）

本報告書では、平成 21 年度(2009 年 4 月 1 日～2010 年 3 月 31 日)の日本原子力研究開発機構・システム計算科学センターにおける研究開発活動について報告する。これらの研究開発は、高度計算機技術開発室とシミュレーション技術開発室により執り行われた。主な研究開発内容は、グリッド技術に基づく安全な計算環境の開発、原子炉施設全体の耐震構造解析、原子炉材料および核燃料の安全評価のための大規模物性計算、新奇デバイス開発、および、超伝導現象解明のための大規模量子シミュレーションと、たんぱく質の大規模分子シミュレーション手法の開発等である。

原子力科学研究所(駐在)：〒319-1195 茨城県那珂郡東海村白方白根 2-4

## Contents

# 目　次

# Foreword

Computational science and technology has become a vital part of nuclear energy research, owing to the rapid expansion of computational capabilities which enabled many breakthroughs for the most demanding problems. The mission of the Center for Computational Science and e-Systems (CCSE) is to develop state-of-the-art computational techniques and infrastructure for nuclear energy research, and to promote cross-cutting computational research activities in Japan Atomic Energy Agency (JAEA). To achieve this mission, CCSE is carrying out vigorous research and development in the field of computational science for nuclear energy.

The R&D activities of CCSE during the fiscal year 2009 are presented in the subsequent sections, and they can be summarized as follows:

**1 Computer Science in Nuclear Engineering:** Secure computational infrastructure for nuclear energy research based on the grid technology, V&V technology, and visualization technology

**2 Computational Mechanics:** Vibration and structural simulations for an entire structure of a nuclear power plant

**3 Computational Materials Science:** Large scale atomic and subatomic simulations of nuclear fuels and materials for safety assessment, and large scale quantum simulations of superconductor for the design of new devices and fundamental understanding of superconductivity

**4 Computational Quantum Bioinformatics:** Development of large scale numerical simulation technology for proteins

The CCSE will keep accelerating computational science R&D in the field of nuclear energy.

Ken Muramatsu
Director
Center for Computational Science and e-Systems,
Japan Atomic Energy Agency

This is a blank page.

# 1. CCSE Research and Development Activity

## 1.1 Computer Science in Nuclear Engineering

This is a blank page.

1.1.1 Grid Computing Technology for Vibration Simulations of a Nuclear Power Plant

## (1) A Script Generator API for the Full-Scale Three-Dimensional Vibration Simulation of a Nuclear Power Plant on AEGIS: Atomic Energy Grid InfraStructure

Guehee Kim, Yoshio Suzuki, Naoya Teshima, Akemi Nishida, Tomonori Yamada, Fumimasa Araya, Hiroshi Takemiya, Norihiro Nakajima and Makoto Kondo [1)]

1) O-arai Research and Development Center, JAEA

CCSE has developed grid-enabled client APIs (Application Program Interfaces) to let AEGIS (Atomic Energy Grid InfraStructure) users develop their own grid-enabled applications by themselves. The APIs are a library providing its basic functionalities to access and use AEGIS computing resources such as authentication, authorization, secure communication, file and job control, and so on. Utilizing the APIs, AEGIS users can develop and manipulate their own applications without understanding how to manage complex facilities of grid infrastructure.

In this work, we developed the grid-enabled script generator API based on the previously developed basic APIs to realize multiple job executions (simultaneous and cooperative execution of jobs). Usually, workflow tools are used for a job execution on grid environments. It is useful to execute successive jobs with step by step (a next job is executed after finishing a current job). In some cases, however, it is needed to execute a next job by receiving data at a certain point of the current job unless waiting the end of the current job. It is difficult to control such cases by using previous workflow tools. To control such jobs, the generation of script for each job and their cooperative execution are required. The grid-enabled script generator, API automatically generates a script for each job [1].

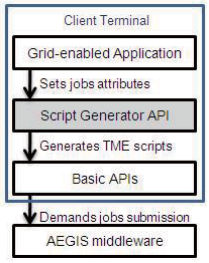


Fig. 1: User development procedure with the API in AEGIS

Figure 1 shows a user's procedure to develop a workflow for multiple job executions with the API. To develop a grid-enabled application based upon multiple jobs' execution by using the developed API, a user sets job attributes, which are an executable file (name and path), arguments, server name, queue name, input file (name and path), output file (name and path), CPU number, and so on . The script generator API generates scripts by using those attributes and describing a script for job execution with the former language of TME (Task Mapping Editor), a workflow tool on AEGIS, in stead of that user describes. By using the language of TME, the difference of description to execute a job among heterogeneous computers need not be considered. Users can develop their own applications to control multiple job executions by putting together script generator APIs and basic APIs.

To verify the functionality of API, we have installed the developed API to a grid-enabled application for 3D structural analysis of a nuclear power plant. Figure 2 shows the three jobs; CONNECT, partPARA, and FIESTAsolver for the 3D structural analysis are listed for multiple job executions, which are sequentially proceeded in the same part, but paralley carried out for the different part. We confirmed the functionality of developed API through this test that we could control submissions and to execute multiple job executions.

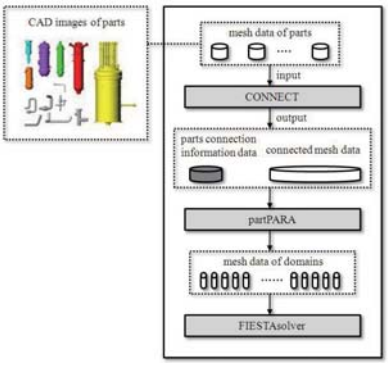


Fig. 2: Flow chart of 3D structural analysis of a nuclear power plant [1]

**References**

[1] G. Kim, Y. Suzuki, N. Teshima, A. Nishida, T. Yamada, F. Araya, H. Takemiya, N. Nakajima and M. Kondo, Proceedings of 1st International Conference on Parallel, Distributed and Grid Computing for Engineering (PARENG) (Pécs, Hungary, 2009.4.6-8) (CD-ROM) (2009)

## 1.1.1 Grid Computing Technology for Vibration Simulations of a Nuclear Power Plant

### (2) Network Computing Infrastructure to Share Tools and Data in GNEP

Guehee Kim, Yoshio Suzuki and Naoya Teshima

GNEP (Global Nuclear Energy Partnership) is U.S. Global nuclear strategy aiming at reducing global dependency on fossil fuels and providing emission-free and abundant nuclear energy. To acceralate this activity, 5 working groups, WGs are organized, namely, Fast Reactor Technology WG, Fuel Cycle Technology WG, Small & Medium Reactor WG, Safeguards & Physical Protection WG, Waste Management WG, and, Simulation & Modeling WG, SMWG [1].

SMWG had a mission to carry out developing simulation tools as a cross-cutting technology for other WGs. To develop tools and for efficient cooperations, a grid computing environment is proposed to share tools and data between U.S. and Japan.

SMWG considered that a grid computing environment provides tools and data sharing environment for R&D communication & collaboration with consideration of nuclear nonproliferation. As a minimum requirement to start sharing tools and data as fast as possible, we focus on three issues: security (access control and data encryption), accessibility (access via FW), and usability. This work suggests its security as a methodology to realize a grid computing environment for GNEP activity and an implementation of a prototype system to share tools and data in AEGIS (Atomic Energy Grid InfraStructure).

Since WGs are organized by persons in various institutes of U.S. and Japan, it is desirable to set the access control in detail, at least, for each research group (community). Unintentional outflow of information is also an important issue to keep information security.

Figure 1 shows the overview of prototype system of information sharing function. Firstly users who try to access the disk from the Internet are restricted by the security policy of each institute. The security is heightened by using a digital certificate installed in a hardware key for the authentication. Secondly, users who try to access the storage unit after connecting into an intranet are secured by the developed authentication gateway. The authentication gateway authenticates only users who have a valid digital certificate and a valid IP address of their machine. Since this authentication gateway is located as a wall for the AEGIS community network which includes the storage unit, users in the intranet are also authenticated in the same manner. Thirdly the information sharing server checks the community in which users belong to. By taking theses sequential procedures, users can access only their own community's file space. Every user who can access the information sharing server may generate one's community. To avoid the unintentional outflow, users belonging to a same community can encrypt (and also decrypt) files in their community space with each other by using a shared key.

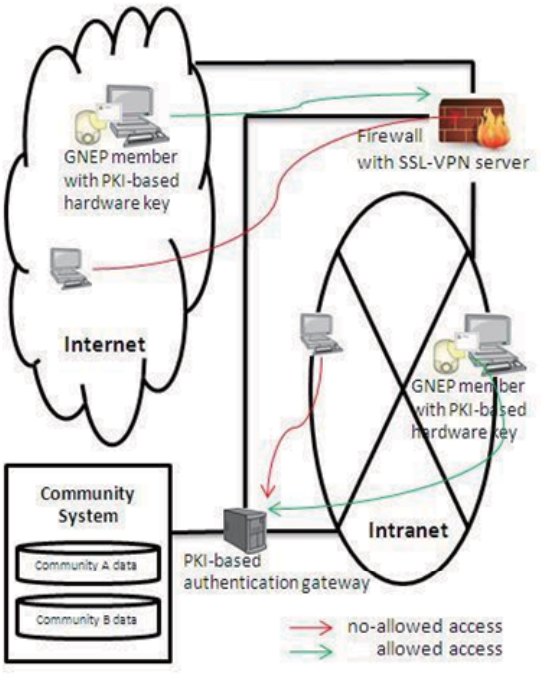


Fig. 1: The overview of prototype system of information sharing function.

We have established the trial environment by implementing the prototype system between U.S. and Japan. Members of Simulation & Modeling WG shares files using the prototype system. The co-chairs meeting by using a video meeting function of AEGIS between U.S. and Japan was held using the implemented prototype system in 9th May 2008.

**References**

[1] G. Kim, Y. Suzuki and N. Teshima, Proceedings of 17th International Conference on Nuclear Engineering (ICONE-17) (Brussels, Belgium, 2009.7.12-16) (CD-ROM) (2009)

## 1.1.2 Verification & Validation Technology for Large Scale Simulations

### (1) Design of Scientific Concept Vocabulary for Cognitive Methodology Based on Data Analysis System

Chiaki Kino, Yoshio Suzuki, Hiroko Nakamura Miyamura, Hiroshi Takemiya and Norihiro Nakajima

Recently, researchers must analyze ever-larger amounts of data because techniques of computer have higher performance. It is difficult to analyze whole data because of constraints of research resources. So, researchers must put analysis targets down to limited area. However, researchers often make oversights and have misunderstandings in the process [1].

We have been developing a data analysis system that interprets physical meanings of result data output from a numerical simulation and annotates meaningful information aiming at supporting a choice of interested region from large scale numerical simulation data. The system stores various data analysis processes to interpret physical meanings and to annotate meaningful information from a scientific viewpoint. Researchers can choose an interested region by using the meaningful information suggested by the system. To actualize the system, we need establish a methodology to make a system recognize physical meanings.

In this paper, we have proposed Scientific Concept Vocabulary (SCV) that is a framework to numerically treat physical meanings. The basic idea of SCV is that physical meaning is described by combination of scientific concepts. Since the vocabularies are defined by substantial information (for example, numerical data, algorism and so on) to express the concept, a system is able to numerically treat abstract concepts. The description manner of SCV is similar to RDF (Resource Description Framework) [2] that is composed of subject resource, object resource and property.

Scientific concept Vocabulary consists of “data”, and “method”. Data is numerical information to define the concept and is categorized into 4 types, namely “Physical distribution”, “Region”, “Physical condition” and “Object”. Method is an algorism which products the substantial data by using data input from object resources.

In this study, we applied Scientific Concept Vocabulary to data of computational fluid dynamics and evaluated the effectiveness. Analysis target of the numerical simulation is the reduced-moderation water reactor (RMWR) [3] core which adopts a hexagonal tight-lattice arrangement with about 1mm gap between adjacent fuel rods. List 1 shows an example of data analysis process which is described by Scientific Concept Vocabulary. A vocabulary of first line defines a concept that extract break-up region. A vocabulary of third line defines liquid film region. This process indicates extraction of a region where liquid film break-up.

```
1<scv:Description
        scv:about="urn:Analysis_process:Break">
2 <ap:target>
3 <scv:Description
        scv:about="urn:Physical_phenomena:Thickness">
4 </scv:Description>
5 </ap:target>
6 </scv:Description>
```

List 1 Example of Scientific Concept Vocabulary

The visualization result which is extracted from the numerical simulation data by the process is shown in Fig. 1. We can see a region which liquid film break-up in the extracted result. So we can say that Scientific Concept Vocabulary describes scientific information which means “liquid film break-up”. In the future, we will extend Scientific Concept Vocabulary in order to describe wider physical meaning.

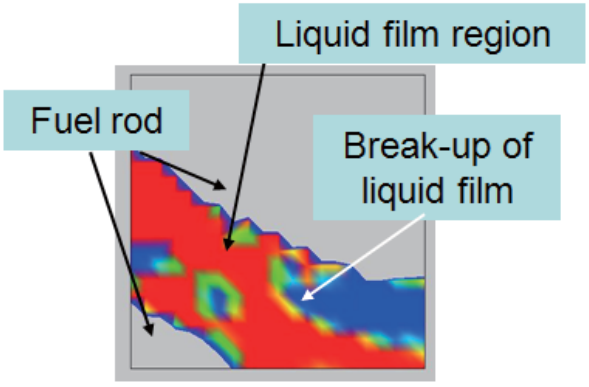


Fig. 1 Visualization result suggested from the present system [1]

**References**

[1] C. Kino et al. Transaction of JSCES, Vol.2009 No.22 p.12 (2009)

[2] World Wide Web Consortium (W3C): Resource Description Framework, http://www.w3.org/RDF/

[3] H. Yoshida and K. Takase, Journal of Fluid Science and Technology Vol.3, No.2, pp.311-322, (2008)

## 1.1.3 Visualization Technology for Large Scale Simulations

### (1) Visualization of Runtime Behavior of Branch-and-Bound Algorithms

Hiroko Nakamura Miyamura, Yuji Shinano [1)], Ryuhei Miyashiro [2)] and Takafumi Saito [2)]

1) Zuse Institute Berlin

2) Tokyo University of Agriculture and Technology

In branch-and-bound algorithms for integer programming, runtime behavior of the algorithms depends much on its branching strategy. However, from a huge computation log of a large program, it is difficult to explore key factors for effective branching. To analyze which factor of branching strategy is essential, we develop a system for visualization of growing process of a large branch-and-bound tree. The proposed system provides intuitive understanding how branching strategy affects branch-and-bound process.

When visualizing large-scale branch-and-bound tree, cluttering and occlusion occur. This can be avoided if different tree graph styles are used at a given node. We consider effective node arrangement and link representation [1].

Node Arrangement: When nodes and the link do not overlap, each node is arranged by conventional tree layout algorithms. The value determined as the division of the window width by the total number of leaf nodes is defined as the area of one leaf node. For each node, the area of the descendant node is determined by multiplying the number of leaf nodes in the descendant nodes by the area of one leaf node. To show the parent-child relationship between the nodes clearly, the parent nodes are sequentially relocated at the center of the child nodes starting from the bottom. This node arrangement is called "Center arrangement". The node arrangement before relocating is called the "Starting point arrangement". Furthermore, the hierarchical depth can be determined from the *y* coordinate.

Link representation: For the representation of links, three different link visualization styles are used. The first link style is the "Straight line" style, which, as its name suggests, results in a straight line connection between the nodes. Therefore, we propose the second link style, "Straight line with corner" style, which connects the nodes by a straight line that moves some number of units in the *x* coordinate in a line along the hierarchy. The final representation is a "Drawing" style, which links the nodes using adjacent areas.

Tree Graph Variation: We implemented the following two node styles, "Center arrangement" and "Starting point arrangement" with the following three link styles, "Straight line", "Straight line with corner", and "Drawing" for our visualization system. Fig.1 shows the results of application to the branch-and-bound tree. The color indicates objective value of nodes. The effects of each style are discussed below. Fig.2 shows an example of visualization result. Our system has tree graph drawing function and another information visualization functions.

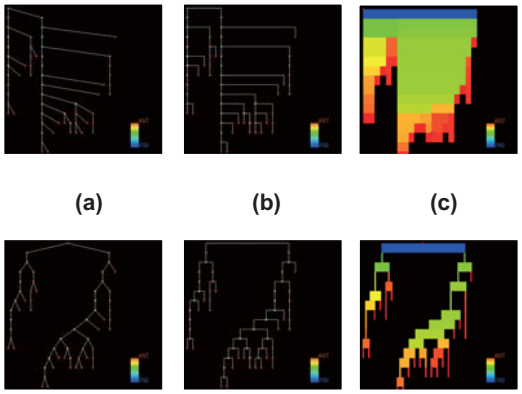


Fig. 1: Tree Graph Variation [1]: “Starting point arrangement” style is (a), (b), and (c); and “Center arrangement” style is (d), (e), and (f). “Straight line” style is (a) and (d); “Straight line with corner” style is (b) and (e); and “Drawing” style is (c) and (f).

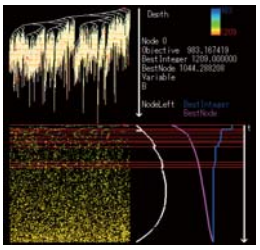

Fig. 2 A Visualization result for branch-and-bound tree [1].

**References**

[1] H. N. Miyamura, Y. Shinano, R. Miyashiro and T. Saito, “Visualization of Runtime Behavior of Branch-and-Bound Algorithms”, IPSJ; TOM, Vol. 12, No. 12, pp. 103-112 (2009)

# 1.2 Computational Mechanics

This is a blank page.

## 1.2.1 Vibration Analysis Technology to Handle a Different Wavelength

### (1) Wave Propagation Analysis of Piping Structures

Akemi Nishida

Generally, it is difficult to predict the occurrence of natural disasters such as earthquakes. Therefore, a performance management system that constantly maintains the safety and functionality of structures is imperative, particularly for critical structures like nuclear power plants. In order to realize such a system, it is becoming important to carry out detailed modeling procedures and analyses to better understand the actual phenomena. Such details are also important in understanding the phenomena occurring in frame structures such as piping systems, which are considered to be among the weakest and most vulnerable components of nuclear power plants. The aim of our research is to develop detailed analysis tools and to determine the dynamic behavior of piping systems in nuclear power plants, which are complicated assemblages of different parts [1].

The elastic wave theory has been primarily used to investigate the response of a structure subjected to an impact load in a structural field. The Laplace transformation is generally used to analyze the wave equation, which is expressed by a partial differential equation. However, it is difficult to analytically perform the inverse transformation for the solution in the frequency domain, except in some special cases. Due to this difficulty, many approximate methods have been proposed. Doyle proposed another method that uses Fourier transformation instead of Laplace transformation and showed that the method is applicable to the analysis of structures with multiple degrees of freedom. This analytical method is called the spectral element method or finite spectral element method and has an advantage with regard to its ability to use the FFT algorithm. Nishida et al. extended this method for three-dimensional frame structures including shear and torsional deformation effects.

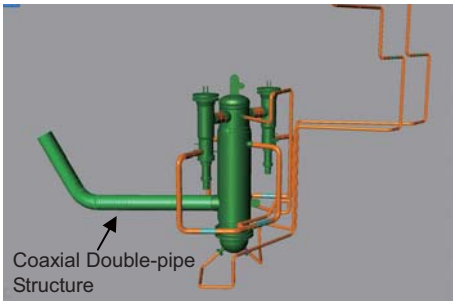


Fig. 1 Auxiliary cooling system of HTTR[1]

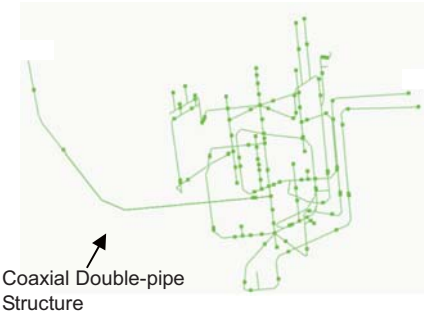


Fig. 2 Analytical model of piping structures of auxiliary cooling system of HTTR [1]

In this paper, a detailed dynamic analysis method by using SEM and its application to piping structures of a nuclear power plant are shown. A comparison of the Bernoulli–Euler beam theory and Timoshenko beam theory shows the necessity of the latter in piping structure analyses of nuclear power plants. Further, it is shown that the SEM is effective for resolving the frequency response problem. Finally, the application of the SEM for a multi-connected frame structure was shown and the results were compared with the experimental results. It was found that the spectral element could effectively represent the wave propagation phenomena and that the modeling of the boundary condition was crucial for estimating the phase properties of a multi-connected frame structure. As a topic for future study, we are preparing to conduct the numerical simulation of more complicated piping structures in a nuclear plant system.

**References**

[1] A. Nishida, Proceedings of the 17th International Conference on Nuclear Engineering (ICONE17), 2009

## 1.2.2 Fundamental Technology for 3D Vibration Simulations of an Entire Nuclear Plant

### (1) Parallel Distributed Seismic Analysis of a Real Component in Assembled Nuclear Power Plant

Tomonori Yamada

The modeling and reduction of parallel computation cost for seismic analysis of nuclear power plants are discussed. The safety requirement of nuclear power plant is extremely high enough to perform real experiments to evaluate the structural integrity of mechanical components. However, such experiments are performed on independent sets of components because the ability of experimental facilities is limited. Hence, a numerical simulation, which can treat whole assembled plant, attracts more and more attentions with the growing computational technologies. To simulate such complex assembled structures, meshfree modeling technology [1] and hierarchical simulation strategy [2] was introduced and implemented as a simulation framework. In hierarchical simulation strategy, large mechanical components such as pressure vessels and small ones such as pipes are loosely coupled because the displacement transferred from the small component to the large one approaches zero as the size difference increases. The computation cost for seismic simulation of nuclear power plant is drastically reduced with this strategy. The balancing domain decomposition method is also investigated to reduce the computation cost of large mechanical components [3]. Because the computation cost of balancing domain decomposition method depends much on the number of subdomains, a prediction curve for optimal number of subdomains is introduced. Numerical validation is performed with a component of an actual nuclear power plant as is illustrated in Fig.1. The number of degrees of freedom in this numerical example is 80 million. The optimal number of subdomains on 512 processor elements (PE) is approximately 10,000. The measured computation cost is summarized in table 1. The results coincided with the predicted optimal number of subdomains successfully.

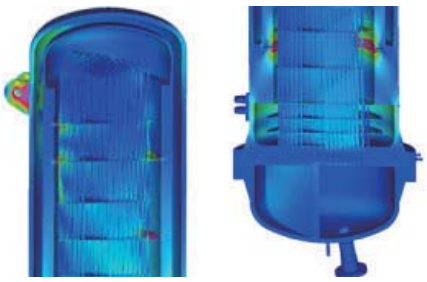

Fig. 1: Obtained von Mises stress distribution of a component of an actual nuclear power plant

Tab. 1: Computation time on 512PE

| Number of Subdomains | Computation Time |
|---|---|
| 5120 | 3305sec. |
| 10240 | 1810sec. |
| 20480 | 2370sec. |
| 30720 | 3138sec. |

**References**

[1] T. Yamada, Parallel Distributed Seismic Analysis of an Assembled Nuclear Power Plant, Parallel, Distributed and Grid Computing for Engineering, pp. 439-454, 2009

[2] T. Yamada and T. Nagashima, An Integration Scheme of Boundary Elements for Meshfree Finite Element Analysis with Structured Grid, Transaction of JSCES, Vol. 2009, No. 6, p. 7, 2009

[3] T. Yamada, M. Ogino and S. Yoshimura, Prediction and Numerical Validation of Optimal Number of Subdomains on Balancing Domain Decomposition Method, Transaction of JSCES, Vol. 2009, No. 14 p. 7, 2009

## 1.2.2 Fundamental Technology for 3D Vibration Simulations of an Entire Nuclear Plant

### (2) High Speed Eigenvalue Solver on the Cell Cluster System for Controlling Nuclear Fusion Plasma

Noriyuki Kushida, Hiroshi Takemiya and Shinji Tokuda

The International Thermo-nuclear Experimental Reactor (ITER) project, which is being led by seven countries including Japan, is testing the feasibility of a Tokamak type fusion reactor for burning plasma for long periods. It has been noted that the operation efficiency of a Tokamak fusion reactor can be degraded by the existence of plasma instabilities. One of the encouraging methods for plasma stabilization is that of control of the plasma by changing the external magnetic field when signs of the plasma instabilities appear (Fig.1) [1]. However, the period between the time the signs appear and the time limit to stabilization is quite short (such as only five seconds, even in a reactor as large as ITER). Thus, fine control based on accurate plasma state analysis has been considered technically challenging, because it requires higher processing power than what is provided by today's supercomputers. Recently the computational power of supercomputers has been increased by connecting many CPUs. This method is suitable for reducing calculations from one week to one day. However, it cannot be adapted to a one-minute calculation, because communication overheads can become large. Moreover, supercomputers are not suitable for use in constant monitoring use, because many users share them and we cannot exclusively use them for monitoring use [2].

We introduced the Cell processor [3] into our computing environment, to obtain more processing power beyond that of supercomputers. Moreover, the Cell processors are highly cost-effective, and this enables us to build a dedicated computing environment. On the other hand, it also requires sophisticated programming techniques for high performance.

As a first step, we focused on the eigenvalue solver, because it consumes the most of computational time. In order to achieve high performance with the Cell processor, we reduced communication time by introducing a hierarchical parallelization technique (Fig. 2). Furthermore, we developed a novel eigenvalue solver that only requires mathematically inevitable communication. As a result, our eigensolver performs well, with high computational stability, although there is a trade-off between these qualities in traditional methods. Taking these techniques together, we can complete the eigenvalue within one second. We believe that we may open the way toward real time plasma stabilization. Additionally, our newly developed method can be applied to other applications in the nuclear field.

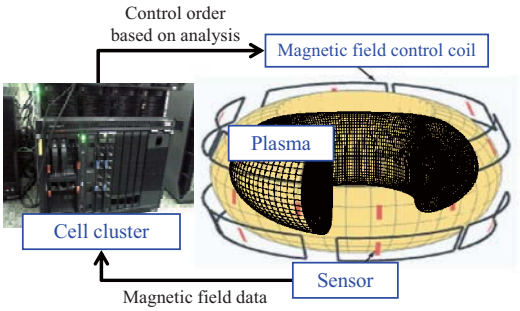


Fig.1 Illustration of plasma stabilizing system

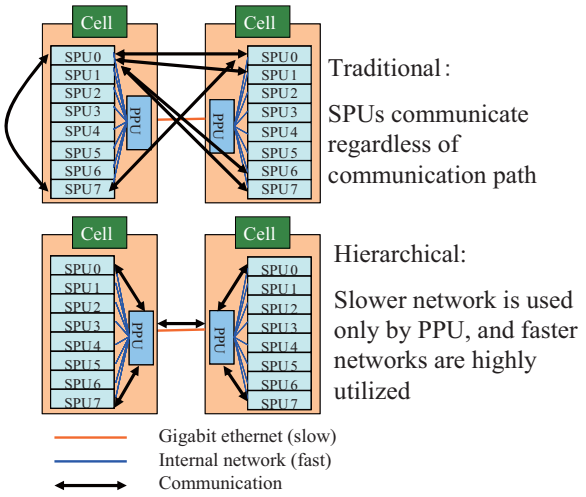


Fig.2 Overview of Cell cluster and hierarchical parallelization

**References**

[1] S.Tokuda, "Development of Eigenvalue Solver for an MHD Stability Analysis Code", 5th Burning Plasma Simulation Initiative Annual Meeting, 2006.

[2] N. Kushida, H. Takemiya and S. Tokuda, High speed eigenvalue solver on the Cell cluster system for controlling nuclear fusion plasma, DOI 10.1109/PDP.2010.22, p. 482-488, 2010

[3] Cell Broadband Engine processor based systems White Paper, available at http://www.irisa.fr/orap/Constructeurs/Cell/cell_be_systems_whitepaper.pdf

This is a blank page.

# 1.3 Computational Materials Science

This is a blank page.

## 1.3.1 Multiscale Simulations for Materials and Fuels

### (1) Interatomic Potentials for Hydrogen in Alpha-Iron Based on Density Functional Theory

Ashwin Ramasubramaniam [1)], Mitsuhiro Itakura and Emily Carter [1)]

1) Princeton University

We have developed two interatomic potentials for hydrogen in alpha–iron [1] based on the embedded atom method potentials for iron developed by Mendelev et al. and Ackland et al. Since these latter potentials are unique among existing iron potentials in their ability to produce the same core structure for screw dislocations as density functional theory (DFT) calculations, our interatomic potentials for hydrogen in iron also inherit this important feature. We use an extensive database of energies and atomic configurations from DFT calculations to fit the cross interaction of hydrogen with iron. Detailed tests on the dissolution and diffusion of hydrogen in bulk alpha–iron, as well as the binding of H to vacancies, free surfaces, and dislocations, indicate that our potentials are in excellent overall agreement with DFT calculations, as shown in Table 1.

Tab. 1: Comparison of interatomic potentials with PAW-PBE-GGA (fitting targets in italics) for binding of H at (100) and (110) surfaces at coverages of 0.11 and 0.08 monolayers, respectively. “min” indicates stable minimum; “ts” indicates transition state; “hos” indicates higher-order saddle. All energies are in eV and distances in Å (Taken from Ref. [1]).

| | PAW-PBE-GGA | EAM[a] | Potential A | Potential B |
|---|---|---|---|---|
| | | Binding energies | | |
| (100) surface | | | | |
| Hollow | *0.775* (min) | 0.627 (hos) | 0.700 (hos) | 0.717 (hos) |
| Quasi-threefold | *0.768* (min) | 0.628 (min) | 0.727 (min) | 0.749 (min) |
| $\delta$ [d] | *0.19* | 0.16 | 0.55 | 0.55 |
| Bridge | *0.655* (min) | 0.624 (min) | 0.665 (ts) | 0.690 (ts) |
| (110) surface | | | | |
| Threefold | *1.003* (min) | 0.630 (min) | 0.672 (min) | 0.734 (min) |
| Long bridge | 0.970 (ts)[e] | 0.601 (ts) | 0.624 (ts) | 0.678 (ts) |
| Short bridge | 0.823 (ts)[e] | 0.599 (min) | 0.564 (ts) | 0.621 (ts) |
| | | Distance from surface to H | | |
| (100) surface | | | | |
| Hollow | *0.38* | 0.20 | 0.20 | 0.21 |
| Quasi-threefold | *0.38* | 0.43 | 0.28 | 0.29 |
| Bridge | *1.20* | 0.74 | 0.74 | 0.74 |
| (110) surface | | | | |
| Threefold | *0.98* | 0.84 | 0.83 | 0.84 |
| Long bridge | 0.95[g] | 0.83 | 0.82 | 0.84 |
| Short bridge | 1.14[g] | 1.05 | 0.83 | 0.84 |

We have also tested the quality of our potentials with respect to the dissolution and diffusion of H in bulk alpha-Fe as well as the binding of H to vacancies, free surfaces, and dislocations. The overall agreement of our potentials with DFT calculations is very encouraging and suggests that these potentials might be used with confidence in the future to simulate H-defect interactions, grain-boundary diffusion, and hydrogen embrittlement of iron, among other problems. Between the two potentials developed in this work, Potential B is seen to reproduce DFT fitting targets with slightly greater accuracy than Potential A, although both potentials present several improvements over existing Fe-H potentials. Therefore, the choice of which potential to employ is probably best decided on the basis of the properties of Fe that one wishes to model with greater accuracy.

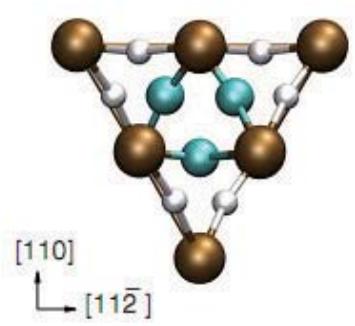


Fig. 1: Binding sites for H atoms at a screw dislocation core. The blue and white spheres represent the first and second shell of binding sites around the core. The “bonds” are merely a guide for visualization (Taken from Ref. [1]).

**References**

[1] A. Ramasubramaniam, M. Itakura and E. Carter, Physical Review B, Vol. 79, 174101 (2009)

## 1.3.1 Multiscale Simulations for Materials and Fuels

### (2) Understanding Covalent Mechanochemistry

Jordi Ribas-Arino [1)], Motoyuki Shiga and Dominik Marx [1)]

1) Ruhr Universitaet Bochum

Most chemical reactions must be activated by some form of energy. The oldest approach is to use fire, that is, thermal energy leading to thermochemistry, but other “chemistries” are activated by light or electricity, that is, photochemistry or electrochemistry. In general, different ways of activation lead to different reaction pathways and products. A prominent example are pericyclic reactions, which are either thermochemically or photochemically forbidden or allowed, according to the Woodward-Hoffmann rules [1]. Although pioneering work dates back more than a century [2], the field of mechanically induced covalent chemistry, dubbed here “covalent mechano-chemistry”, is still in its infancy [3-5]. Most recently, however, intriguing experiments have opened the door to applying forces on covalent bonds by exploiting atomic force microscopy (AFM) [6-9], force-clamp [10,11] and sonochemical [5,12,13] techniques. Despite promising case studies [6,14-20], theory is in arrears when it comes to understanding the underlying concepts of nano-mechanics. Here, we devise a most general theoretical framework that allows one to investigate covalent mechanochemistry both in terms of concepts and applications. This is achieved by exploiting the notions of force-transformed potential energy surfaces connected by Legendre transforms and isotensional versus isometric activation of covalent bonds, and by generalizing Fukui’s Intrinsic Reaction Coordinate concept [21] to embody mechanical forces. Using a cyclobutene derivative [12,5] as a demonstration we delineate the limits of commonly used models, find topological rules that explain why certain pathways are mechanochemically allowed or forbidden, uncover differences between isotensional and isometric activation, and find topological irreversibility in stretching-compression cycles.

**References**

[1] R. B. Woodward and R. Hoffmann, Angew. Chem. 81, 797 (1969); Angew. Chem. Int. Ed. Engl. 8, 781 (1969)
[2] M. Carey Lea, Philos. Mag. 34, 46 (1892)
[3] M. K. Beyer and H. Clausen-Schaumann, Chem. Rev. 105, 2921 (2005)
[4] S. Granick, S. C. Bae, Nature 440, 160 (2006)
[5] B. M. Rosen, V. Percec, Nature 446, 381 (2007)
[6] M.Grandbois, M. Beyer, M. Rief, H. Clausen-Schaumann and H. E. Gaub, Science 283, 1727 (1999)
[7] T. Hugel, N. B. Holland, A. Cattani, L. Moroder, M. Seitz and H. E. Gaub, Science 296, 1103 (2003)
[8] A. S. Duwez, S. Cuenot, C. Jerome, S. Gabriel, R. Jerome, S. Rapino and F. Zerbetto, Nat. Nanotechnol. 1, 122 (2006)
[9] S. W. Schmidt, M. K. Beyer and H. Clausen-Schaumann, J. Am. Chem. Soc. 130, 3664 (2008)
[10] A. P. Wiita, S. R. K. Ainavarapu, H. H. Huang and J. M. Fernandez, Proc. Natl. Acad. Sci. USA 103, 7222 (2006)
[11] A. P. Wiita, R. Perez-Jimenez, K. A. Walther, F. Gr− ter, B. J. Berne, A. Holmgren, J. M. Sanchez-Ruiz and J. M. Fernandez, Nature 450, 124 (2007)
[12] C. R. Hickenboth, J. S. Moore, S. R. White, N. R. Sottos, J. Baudry and S. R. Wilson, Nature 446, 423 (2007)
[13] G. Cravotto and P. Cintas, Angew. Chem. 119, 5573 2007); Angew. Chem. Int. Ed. 46, 5476 (2007)
[14] A. M. Saitta, P. D. Soper, E. Wasserman and M. L. Klein, Nature 399, 46 (1999)
[15] U. F. Roehrig, I. Frank and J. Chem. Phys. 115, 8670 (2001)
[16] D. Aktah and I. Frank, J. Am. Chem. Soc. 124, 3402 (2002)
[17] D. Krueger, H. Fuchs, R. Rousseau, D. Marx and M. Parrinello, Phys. Rev. Lett. 89, 186402 (2002)
[18] M. K. Beyer, Angew. Chem. 115, 5062 (2003); Angew. Chem. Int. Ed. 42, 4913 (2003)
[19] D. Krueger, R. Rousseau, H. Fuchs and D. Marx, Angew. Chem. 115, 2353 (2003); Angew. Chem. Int. Ed. 42, 2251 (2003)
[20] M. Konopka, R. Turansky, J. Reichert, H. Fuchs, D. Marx and I. Stich, Phys. Rev. Lett. 100, 115503 (2008)
[21] K. Fukui, Acc. Chem. Res. 14, 363 (1981)

1.3.1 Multiscale Simulations for Materials and Fuels

## (3) Quantum Effects on Vibrational and Electronic Spectra of Hydrazine Studied by "On-The-Fly" Ab Initio Ring Polymer Molecular Dynamics

Anna Kaczmarek [1)], Motoyuki Shiga and Dominik Marx [1)]

1) Ruhr Universitaet Bochum

Structural and electronic properties of the hydrazine molecule, it being prone to large-amplitude motion, have been studied by a series of classical and quantum ab initio simulations at room temperature. In particular, ab initio molecular dynamics, ab initio path integral molecular dynamics, and ab initio ring polymer molecular dynamics (RPMD) simulations have been carried out using the MP2 method “on-the-fly” to access thermal and quantum fluctuation effects on molecular properties at finite temperatures, which can be compared to static calculations on the basis of the equilibrium structure. In addition to structure, the respective broadening effects on ultraviolet (UV), ionization, and infrared (IR) spectra have been decomposed in comparison to both stick spectra obtained using the same electronic structure method as well as experimental results.

It has been shown that using ab initio path integral molecular dynamics (PIMD) simulations, thus taking proper account of skeletal vibrations at finite temperatures due to both thermal and quantum effects, it is possible to reproduce the overall shape of the continuous UV spectrum. Classical dynamics, in contrast, yields a UV spectrum that is overstructured compared to that of experiment, characterized by a few structureless peaks on a broad background. When it comes to the stick spectrum obtained at the static equilibrium structure, unphysical a posteriori broadening procedures seem to be required to reproduce experiment. In addition, nuclear quantum effects offer a natural explanation of the pronounced tail of the single-photon ionization efficiency that is observed to extend to energies much lower than the vertical ionization energy at the equilibrium structure. Again, such quantummechanical fluctuation effects are shown to considerably improve the result obtained with classical ab initio molecular dynamics (MD) whereas the respective “stick spectrum” obtained at equilibrium cannot explain the phenomenon at all by definition. Moreover, ab initio RPMD simulations, providing a sort of quasi-classical approximation to quantum dynamics, were proven to be useful to compute the fully coupled anharmonic IR spectra from the Fourier transform of dipole autocorrelation functions in the room temperature regime. Thus, “...something is to be learned by ’observing’ the motion of different isotopic species on the same potential surface.” [1] considering classical nuclei as “infinitely heavy isotopes”, vide ante. Along these lines, it would be most interesting to probe quantum effects on the kinetics and possibly on the mechanism of the intramolecular isomerization reaction that interconverts the two enantiomeric forms in view of internal soft modes along either rotation or inversion pathways, using hydrazine and perdeuterated hydrazine. Although this requires neither further methodological development nor additional implementations beyond ab initio RPMD, it would call for a considerable investment of computer time to sample these rare events without accelerating artificially (and thus destroying) the physical time evolution.

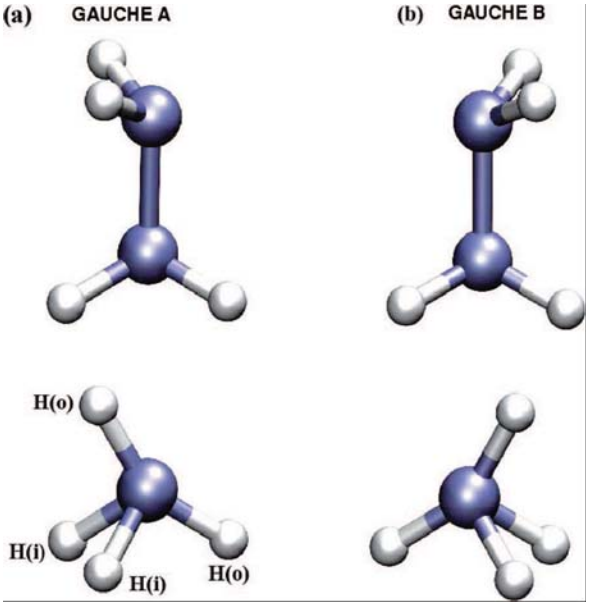


Fig. 1: Hydrazine enantiomers: side and top views.

**References**

[1] M. Wolfsberg, Annu. Rev. Phys. Chem. 20, 449, (1969)

1.3.1 Multiscale Simulations for Materials and Fuels

## (4) Path-Integral Molecular Dynamics Simulations of Small Hydrated Sulfuric Acid Clusters $H_2SO_4$ $(H_2O)_n$ (n=1-6) on Semiempirical PM6 Potential Surfaces

Akira Kakizaki [1)], Haruki Motegi [1)], Takehiro Yoshikawa [1)], Toshiyuki Takayanagi [1)], Motoyuki Shiga and Masanori Tachikawa [2)]

1) Saitama University
2) Yokohama-City University

Sulfuric acid is one of the key substances controlling climate change in atmospheric chemistry. $H_2SO_4$ is a principal component of acid rain and is an effective nucleation agent significantly enhancing the homogeneous nucleation rate of water [1,2]. It is also known that $H_2SO_4$ plays an important role in the formation of sulfate aerosols, which can catalyze heterogeneous reactions contributing to ozone depletion in the polar stratosphere [3,4]. Recently, it is proposed that overtone excitation of the OH stretching vibration of the hydrated $H_2SO_4$ can lead to dissociation of the system into $SO_3$ and water and that this process plays a role in the troposphere [5-7].

In this report, we have studied the ability of the semiempirical PM6 method in describing the electronic structures of the hydrogen-bonded $H_2SO_4$ $(H_2O)_n$ clusters. Various low-lying isomeric structures of the $H_2SO_4$ $(H_2O)_n$ (n = 1-9) clusters were examined using the PM6 method and compared to previous DFT results. Although the PM6 method seems to somewhat overemphasize bifurcated hydrogen-bonded structures, where two protons of one water molecule form a hydrogen-bond to the same acceptor atom, moderately good agreement was obtained for structures and energetics of the $H_2SO_4$ $(H_2O)_n$ clusters. Thus, the use of the PM6-level calculations would be quite attractive in performing direct dynamics simulations of hydrated sulfuric acid clusters. We have then carried out direct PIMD simulations in order to understand the effect of quantum mechanical nature of nuclei on thermal equilibrium structures of the $H_2SO_4$ $(H_2O)_n$ (n = 1-6) clusters. By comparing the PIMD result of the $H_2SO_4$ $(H_2O)_6$ cluster to classical MD results at the same temperature, we have demonstrated that nuclear quantization significantly enhances thermal fluctuations presumably due to larger zero-point vibrational amplitudes of hydrogen atoms. As a result, the PIMD results showed liquid-like structures for the $H_2SO_4$ $(H_2O)_n$ (n = 3-6) clusters even at T = 250 K while the corresponding classical MD results gave solid-like structures around the global minimum of the potential energy surface. It was found that the acid dissociation probability increases with an increase of the cluster size, as expected. The contact-ion-pair structures are dominant in the ionized clusters. Two-dimensional contour plots were also presented in order to understand nuclear distributions in the hydrated clusters from a microscopic viewpoint. An interesting transient behavior between the ionic and non-ionic structures was seen in the $H_2SO_4$ $(H_2O)_5$ cluster. In addition, it was found that the water environment around an excess proton depends upon the cluster size as well as the solvation shell. It should be emphasized that such cluster size-dependent features cannot be easily obtained from the MD simulations in bulk phase. Although the present PIMD simulations show several interesting features for small hydrated sulfuric acid clusters, it should be mentioned that all the observed features may depend upon the accuracy of the PM6 potential energy surfaces.

**References**

[1] R. J. Charlson, S. E. Schwartz, J. M. Hales, R. S. Cess, J. A. Coakley, J. E. Hansen and D. J. Hofmann, Science 255, 423 (1992)

[2] A. Laaksonen, V. Talanquer and D.W. Oxtoby, Ann. Rev. Phys. Chem. 46, 489 (1995)

[3] R. Bianco and J. T. Hynes, Theor. Chem. Acc. 111, 182 (2004)

[4] R. Bianco and J. T. Hynes, Acc. Chem. Res. 39, 159 (2006)

[5] V. Vaida, H. G. Kjaergaard, P. E. Hintze and D. J. Donaldson, Science 299, 1566 (2003)

[6] D. J. Donaldson, A. F. Tuck and V. Vaida, Chem. Rev. 103, 4717 (2003)

[7] Y. Miller and R. B. Gerber, J. Am. Chem. Soc. 128, 9594 (2006)

1.3.1 Multiscale Simulations for Materials and Fuels

## (5) Path-Integral Molecular Dynamics Simulations of Hydrated Hydrogen Chloride Cluster $HCl(H_2O)_4$ on a Semiempirical Potential Energy Surface

Toshiyuki Takayanagi [1], Kenta Takahashi [1], Akira Kakizaki [1], Motoyuki Shiga and Masanori Tachikawa [2]

1) Saitama University

2) Yokohama-City University

Properties of $HCl(H_2O)_n$ clusters have extensively been studied from both experimental and theoretical sides in the past decade. This is largely because $HCl(H_2O)_n$ clusters are playing a key role in ozone depletion cycles in polar stratospheric clouds above Antarctica. It is generally accepted that ozone depletion processes are initialized by HCl dissociation on ice surface or in small water clusters [1,2]. In addition to this atmospheric context, microscopic understanding of the solvation and dissociation phenomena of strong acids in water systems has previously been the subject of fundamental interest. In particular, an important question is to understand how many water molecules are required to cause ionic dissociation of the HCl molecule in water environment.

In this work we focus on the role of quantum mechanical nature of nuclei in a $HCl(H_2O)_4$ cluster using path-integral molecular dynamics (PIMD) method. In our previous research, the PIMD approach combined with the ab initio electronic structure method and the corresponding computer code have been established [3]. This method generates the PIMD trajectory calculating potential energy and its derivatives on-the-fly using ab initio electronic structure codes. Due to recent advances in computer power as well as in parallelizing techniques, ab initio (or first-principles) PIMD calculations are becoming feasible; however, it is still very expensive to use ab initio PIMD method to study the present $HCl(H_2O)_4$ system especially for the temperature range that structural rearrangement is important. We have then decided to implement the semiempirical PM3-MAIS (Parameterized Model 3 Method Adapted for Intermolecular Studies) method, which has recently been developed by Bernal-Uruchurtu and Ruiz-Lopez [4], into our code. In the PM3-MAIS method, only the core-core interaction terms in the semiempirical PM3 Hamiltonian [5] are modified so as to accurately reproduce interaction potential energies especially for hydrogen-bonded systems. In their most recent paper [6], numerical parameters used in the PM3-MAIS calculations have been developed to describe HCl dissociation in water clusters. Although the PM3-MAIS method predicts a slightly overestimated HCl acidity in water environment, they found that the overall agreement with previous ab initio MO as well as density functional theory (DFT) calculations is satisfying. Therefore, it is quite encouraging for us to employ the PM3-MAIS method in the present PIMD simulations from the viewpoint of computational efficiency.

So far, $HCl(H_2O)_4$ cluster has been studied by molecular dynamics without taking account of nuclear quantum effect where nuclei have been assumed to be classical point charges. In this paper, we use the PIMD method to investigate the possible role of quantum mechanical fluctuations in proton-transfer processes and hydrogen-bond rearrangement processes in the $HCl(H_2O)_4$ cluster. The PIMD simulations are carried out for different temperatures ranging from 100 K to 300 K. Comparing the results for quantum and classical simulations, we indeed found quantum description has strong influence on the structure of the $HCl(H_2O)_4$ cluster. It is found that the $HCl(H_2O)_4$ cluster has structural rearrangement above the temperature of 300 K showing a liquid-like behavior. Quantum mechanical fluctuation of hydrogen nuclei plays a significant role in structural arrangement processes in this cluster.

**References**

[1] S. Solomon, R. R. Garcia, F. S. Rowland and D. J. Wuebbles, Nature 321, 755 (1986)

[2] R. Bianco and J. T. Hynes, Acc. Chem. Res. 39, 159 (2006)

[3] M. Shiga, M. Tachikawa and S. Miura, Chem. Phys. Lett. 332, 396 (2000)

[4] M. I. Bernal-Uruchurtu and M. F. Ruiz-Lopez, Chem. Phys. Lett. 330, 118 (2000)

[5] J. J. P. Stewart, J. Comput. Chem. 12, 320 (1991)

[6] O. I. Arillo-Flores, M. F. Ruiz-Lopez and M. I. Bernal-Uruchurtu, Theor. Chem. Acc. 118, 425 (2007)

1.3.1 Multiscale Simulations for Materials and Fuels

## (6) On the Applicability of Centroid and Ring Polymer Path Integral Molecular Dynamics for Vibrational Spectroscopy

Alexander Witt [1)], Sergei Ivanov [1)], Motoyuki Shiga, Harald Forbert [1)] and Dominik Marx [1)]

1) Ruhr Universitaet Bochum

Over the past two decades, “classical” ab initio molecular dynamics (MD) methods [1] have had success in simulating such complex many-body systems. One possible route to include quantum effects on nuclear motion that are mandatory for a description of the most complicated and, therefore, most interesting classes of systems is provided by formalisms based on Feynman’s path integral (PI) quantum statistical mechanics [2,3] in an elegant and, in principle, exact fashion. Numerical PI simulation techniques [4-6] are based on the isomorphism [7] between the quantum partition function, represented as an imaginary time PI [2,3,8,9] and the classical configurational integral of a system of interacting “ring polymers” subject to specific harmonic nearest neighbor interactions. Static properties of quantum objects can thus be obtained by simulation of more complicated, but classical objects (independently of the way the electrons are treated) using and extending the full power of the well established classical simulation techniques. Monte Carlo (MC) and MD consequently yield most powerful PIMC [10] and PIMD [11,12] algorithms, as well as derived variants such as hybrid MC [14] or Langevin MD.

Nevertheless, computation of dynamic properties in the framework of PIs is not straightforward and requires additional effort. Centroid molecular dynamics (CMD) [14] and ring polymer molecular dynamics (RPMD) [15] are two conceptually distinct extensions of path integral molecular dynamics that are able to generate approximate quantum dynamics of complex molecular systems. Both methods can be used to compute quasiclassical time correlation functions which have direct application in molecular spectroscopy; in particular, to infrared spectroscopy via dipole autocorrelation functions. The performance of both methods for computing vibrational spectra of several simple but representative molecular model systems is investigated systematically as a function of temperature and isotopic substitution. In this context both CMD and RPMD feature intrinsic problems which are quantified and investigated in detail. Based on the obtained results guidelines for using CMD and RPMD to compute infrared spectra of molecular systems are provided.

**References**

[1] D. Marx and J. Hutter, Ab Initio Molecular Dynamics: Basic Theory and Advanced Methods (Cambridge University Press, Cambridge, 2009)

[2] R. P. Feynman and A. R. Hibbs, Quantum Mechanics and Path Integrals (McGraw-Hill, New York, 1965)

[3] R. P. Feynman, Statistical Mechanics (Addison-Wesley, Redwood City, 1972)

[4] L. D. Fosdick, J. Math. Phys. 3, 1251 (1962)

[5] L. D. Fosdick and H. F. Jordan, Phys. Rev. 143, 58 (1966)

[6] H. F. Jordan and L. D. Fosdick, Phys. Rev. 171, 128 (1968)

[7] D. Chandler and P. G. Wolynes, J. Chem. Phys. 74, 4078 (1981)

[8] M. Kac, Trans. Am Math. Soc. 65, 1 (1949)

[9] H. Kleinert, Path Integrals in Quantum Mechanics, Statistics, Polymer Physics and Financial Markets (World Scientific, Singapore, 2004)

[10] D. M. Ceperley, Rev. Mod. Phys. 67, 279 (1995)

[11] M. E. Tuckerman and A. Hughes, in Classical and Quantum Dynamics in Condensed Phase Simulations, edited by B. J. Berne, G. Ciccotti, and D. F. Coker (World Scientific, Singapore, 1998)

[12] M. E. Tuckerman, in Quantum Simulations of Complex Many-Body Systems: From Theory to Algorithms, NIC Series Vol. 10, edited by J. Grotendorst, D. Marx and A. Muramatsu (John von Neumann Institute for Computing, Julich, 2002), p. 269

[13] M. E. Tuckerman, B. J. Berne, G. J. Martyna and M. L. Klein, J. Chem. Phys. 99, 2796 (1993)

[14] J. Cao and G. A. Voth, J. Chem. Phys. 100, 5106 (1994)

[15] I. R. Craig and D. E. Manolopoulos, J. Chem. Phys. 121, 3368 (2004)

1.3.1 Multiscale Simulations for Materials and Fuels

## (7) Speed-Up of Ab Initio Hybrid Monte Carlo and Ab Initio Path Integral Hybrid Monte Carlo Simulations by Using an Auxiliary Potential Energy Surface

Akira Nakayama [1)], Tetsuya Taketsugu [1)] and Motoyuki Shiga

1) Hokkaido University

Computer simulations via molecular dynamics (MD) and Monte Carlo (MC) methods are widely used in a variety of fields ranging from drug design to materials science [1]. Instead of using empirical force fields, ab initio molecular dynamics or ab initio Monte Carlo methods, which solve the electronic Schroedinger equation for nuclear potential energy (or its derivatives) as needed, are now being widely used to investigate static and also dynamic properties of molecular systems from first principles. The computational cost for such ab initio simulations is, however, still highly expensive when combined with statistical simulations where $10^5$-$10^6$ simulation steps are usually required, thus limiting their applicability to relatively small system sizes. Recently, we have proposed an efficient sampling scheme for ab initio Monte Carlo calculations by employing an approximate potential constructed by an interpolation method, and it has been shown that the computational cost is reduced significantly by almost an order of magnitude [2]. In this letter, we introduce a simple scheme for ab initio hybrid Monte Carlo (HMC) calculations, which enhance sampling efficiency by utilizing an auxiliary potential for updating the system configuration. This is similar in spirit to an approximate potential method [3,4] reported previously. The hybrid Monte Carlo method combines the advantages of both the MD and MC methods, allowing the global update of the system configuration with reasonable acceptance ratio [5,6]. It is an exact method and does not suffer from the finite step-size errors of MD simulations. In an update process of the system configuration, the time-reversible and area-preserving MD algorithm needs to be used to ensure the detailed balance, and the commonly used velocity Verlet algorithm satisfies this requirement.

In this paper, efficiency of the ab initio hybrid Monte Carlo and ab initio path integral hybrid Monte Carlo methods is enhanced by employing an auxiliary potential energy surface that is used to update the system configuration via molecular dynamics scheme.

We employ a computationally inexpensive potential energy surface and its gradient for an MD update but uses the same acceptance probability given above to ensure that the target distribution is still determined under the potential. In the context of ab initio simulations, one can use energy gradients of less expensive ab initio potentials for an MD update. The numerical evaluation of the energy gradients requires additional computational cost, which could be several times higher than that of the energy calculation, thus there would be a great saving in computational effort if the above approach is utilized.

As a simple illustration of this method, a dual-level approach is introduced where potential energy gradients are evaluated by computationally less expensive ab initio electronic structure methods. It is noted that the similarity of the target and auxiliary potentials is of course a key factor which determines the efficiency of the method. One needs to find a compromise between accuracy of an auxiliary potential and computational cost for evaluating energy gradients. One of the notable advantages of the present method is again that it does not require energy gradient calculations for target (high-level) ab initio potentials. This is particularly useful for simulations with highly correlated electronic structure methods such as CCSD(T), where the evaluation of energy gradients is highly demanding or a module for analytical gradients is not available. Finally, the limiting factor of the present simulation is still the numerical cost of ab initio calculations.

**References**

[1] D. Frenkel and B. Smit, Understanding Molecular Simulation, Academic Press, San Diego, 1996

[2] A. Nakayama, N. Seki and T. Taketsugu, J. Chem. Phys. 130, 024107 (2009)

[3] R. Iftimie, D. Salahub, D. Q. Wei and J. Schofield, J. Chem. Phys. 113, 4852 (2000)

[4] L. D. Gelb, J. Chem. Phys. 118, 7747 (2003)

[5] S. Duane, A. D. Kennedy, B. J. Pendleton and D. Roweth, Phys. Lett. B 195, 216 (1987)

[6] B. Mehlig, D. W. Heermann and B. M. Forrest, Phys. Rev. B 45, 679 (1992)

1.3.1 Multiscale Simulations for Materials and Fuels

## (8) Unravelling the Mechanism of Force-Induced Ring-Opening of Benzocyclobutenes

Jordi Ribas [1)], Motoyuki Shiga and Dominik Marx [1)]

1) Ruhr Universitaet Bochum

Pericyclic reactions constitute a key class of organic reactions that have been extensively studied, both experimentally and theoretically, for decades. At the end of the 1950's, several seminal papers served to boost the study of electrocyclic reactions [1-3]. In particular, the stereochemistry of electrocyclic ring-opening of cyclobutene was experimentally established for the first time. Some years later stereospecific reactions involving cis and trans benzocyclobutenes were also reported [4,5]. With the principle of the conservation of the orbital symmetry, Woodward and Hoffmann laid down the basis for a satisfactory rationalization of the associated stereospecificity. The accumulated experimental and theoretical data [6-9] over the years provide solid evidence of the fact that the thermal electrocyclic ring-opening of cyclobutene and benzocyclobutene proceeds by a concerted conrotatory pathway. An intriguing recent experiment [10] however, has shown that ring-opening pathways can be altered, in the absence of photoexcitations, when applying mechanical forces. In particular, this experiment has shown that a cis 1,2-disubstituted benzocyclobutene (BCB) derivative yields the corresponding E,E diene as a result of ring-opening instead of the expected E,Z product. Given the fact that this reaction under normal thermal activation conditions would have followed the conrotatory pathway on the electronic ground state potential energy surface (PES), thus yielding the E,Z diene, this landmark work has to be considered the first proof that mechanical forces not only activate reactions [11] but that they also can change qualitatively their course [12].

In the present work we apply our recently introduced theoretical framework [13] to address relevant open questions concerning the mechanism of the force-induced ring-opening reaction of 1,2-disubstituted BCBs, thus transcending significantly our preliminary analysis. In particular, i) we show that the stereochemistry of the products cannot be set after an assumed conrotatory ring-opening via bond rotation, ii) we disclose an unprecedented two-regime behavior associated with the force-dependence of activation energies, iii) based on a newly introduced technique, we explain the disappearance of the conrotatory transition state (TS) of this reaction by visualizing a topological bifurcation between the conrotatory and disrotatory reaction pathways, iv) we rationalize the unexpected finding why both the cis and trans BCBs yield the same product, E,E diene, upon mechanochemical ring-opening. Furthermore, v) we quantitatively disentangle the twofold effect of an external force on chemical reactions: this force not only adds mechanical work along a mechanical reaction coordinate, but it also distorts molecular structures. We also demonstrate vi) that discussing mechanochemistry on the basis of the Born-Oppenheimer potential energy surface, that is, at zero force, can lead to wrong conclusions. Finally, vii) complete breakdown of a commonly used approximation to mechanochemical activation is demonstrated for our specific case.

**References**

[1] W. Cooper and W. D. Walters, J. Am. Chem. Soc. 80, 4220 (1958)

[2] E. Vogel, Liebigs Ann. Chem. 615, 14 (1958)

[3] R. Criegee and K. Noll, Liebigs Ann. Chem. 627, 1 (1959)

[4] R. Huisgen and H. Seidel, Tetrahedron Lett. 46, 3381 (1964)

[5] G. Quinkert, K. Opitz, W. W. Wiersdorff and M. Finke, Tetrahedron Lett. 34, 3009 (1965)

[6] D. C. Spellmeyer and K. N. Houk, J. Am. Chem. Soc. 110, 3412 (1988)

[7] J. Breulet and H. F. Schaefer III, J. Am. Chem. Soc. 106, 1221 (1984)

[8] C. W. Jefford, G. Bernardinelli, Y. Wang, D. C. Spellmeyer, A. Buda and K. N. Houk, J. Am. Chem. Soc. 114, 1157 (1992)

[9] S. Sakai, J. Phys. Chem. A 104, 11615 (2000)

[10] C. R. Hickenboth, J. S. Moore, S. R. White, N. R. Sottos, J. Baudry and S. R. Wilson, Nature 446, 423 (2007)

[11] M. K. Beyer and H. Clausen-Schaumann, Chem. Rev. 105, 2921 (2005)

[12] B. M. Rosen and V. Percec, Nature 446, 381 (2007)

[13] J. Ribas-Arino, M. Shiga and D. Marx, Angew. Chem. 121, 4254 (2009); Angew. Chem. Int. Ed. 48, 4190 (2009)

1.3.1 Multiscale Simulations for Materials and Fuels

## (9) Path-Integral Molecular Dynamics Simulations for Water Anion Clusters $(H_2O)_5^-$ and $(D_2O)_5^-$

Toshiyuki Takayanagi [1)], Takehiro Yoshikawa [1)], Haruki Motegi [1)] and Motoyuki Shiga

1) Saitama University

Water anion clusters $(H_2O)_n^-$ have been extensively studied, since the first observation in mass spectroscopic experiments [1,2], as an important model to understand the solvation phenomena of an excess electron in bulk water. From the experimental side, various sophisticated techniques have recently been applied to study the structures and dynamics of $(H_2O)_n^-$ [3-7]. For example, Johnson and his coworkers [4,5] have provided important information for understanding the excess electron binding motifs for small $(H_2O)_n^-$ clusters using infrared vibrational predissociation spectroscopy. Neumark and his coworkers [6,7] have succeeded in measuring vertical detachment energies (VDEs) for water cluster anions as large as n = 200 using a photoelectron imaging technique. They have also developed a femtosecond time-resolved photoelectron spectroscopic technique to study the photoexcitation dynamics and subsequent relaxation dynamics for $(H_2O)_n^-$ clusters and their related systems such as $I^-(H_2O)_n$ [7].

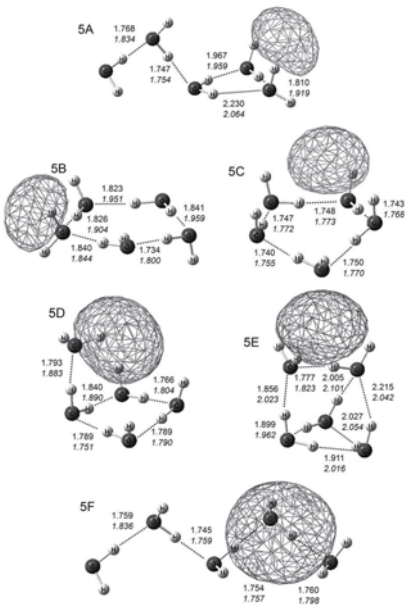


Fig. 1: Stationary points of water $(H_2O)_5^-$ optimized on the TB-RWK potential energy surface. Hydrogen-bond lengths are shown in unit of A and compared to the B3LYP/6-31(1+,3+)G* results (in italic) taken from Ref. [8]. The excess electron distributions are also shown.

In this Letter we have performed quantum-mechanical PIMD simulations for the $(H_2O)_5^-$ and $(D_2O)_5^-$ anion clusters utilizing the semiempirical one-electron pseudopotential model for the description of the excess electron motion in water clusters. We have demonstrated that quantum-mechanical treatment of nuclear motions is quite important for understanding thermal equilibrium water anion cluster structures since the structures are mainly determined by hydrogen-bonding, where light atoms play an essential role. Zero-point vibrational amplitudes affect the O-O hydrogen-bond lengths and thus the hydrogen-bond lengths for $(H_2O)_5^-$ were calculated to be longer than those for $(D_2O)_5^-$ by 0.02 A. We also found that the VDE distribution obtained for $(H_2O)_5^-$ show a broader feature than that for $(D_2O)_5^-$ due to the difference in the zero-point vibrational amplitude.

**References**

[1] H. Haberland, H.-G. Schindler and D. R. Worsnop, Ber. Bunsenges. Phys. Chem. 88, 270 (1984)

[2] H. Haberland, C. Ludewigt, H.-G. Schindler and D. R. Worsnop, J. Chem. Phys. 81, 3742 (1984)

[3] T. Maeyama, T. Tsumura, A. Fujii and N. Mikami, Chem. Phys. Lett. 264, 292 (1997)

[4] W. H. Robertson and M. A. Johnson, Ann. Rev. Phys. Chem. 54, 173 (2003)

[5] N. I. Hammer, J. W. Shin, J. M. Headrick, E. G. Diken, J. R. Roscioli, G. H. Weddle and M. A. Johnson, Science 306, 675, (2004)

[6] J. R. R. Verlet, A. E. Bragg, A. Kammrath, O. Cheshnovsky and D. M. Neumark, Science 307, 93 (2005)

[7] D. M. Neumark, Mol. Phys. 106, 2183 (2008)

[8] J. M. Herbert and M. Head-Gordon, Phys. Chem. Chem. Phys. 8, 68 (2006)

1.3.1 Multiscale Simulations for Materials and Fuels

## (10) Path-Integral Molecular Dynamics Simulations of Glycine-$(H_2O)_n$ (n=1-7) Clusters on Semi-Empirical PM6 Potential Energy Surfaces

Takehiro Yoshikawa [1)], Haruki Motegi [1)], Akira Kakizaki [1)], Toshiyuki Takayanagi [1)] and Motoyuki Shiga

1) Saitama University

It is generally known that quantization of the nuclear degrees of freedom in a molecule or molecular cluster significantly affects its free energy surface and thus its structural and dynamical features due to quantum effects including zero-point vibrations and tunneling. Nuclear quantum effects of hydrogen atoms may play essential roles in hydrogen-bonding as well as proton-transfer phenomena in hydrated acid clusters [1,2].

In this work, we present computational results of quantum path-integral molecular dynamics (PIMD) simulations for hydrated glycine clusters. Glycine is the simplest naturally occurring amino acid and is one of the most fundamental molecules in biological systems. Since glycine has two functional groups of different polarity, an amino group ($-NH_2$) and a carboxylic group (-COOH), it can exist either as nonionized neutral form or as zwitterionic tautomer form with ammonium ion ($-NH_3^+$) and carboxylate ion ($-CO_2^-$) units. More specifically, it is well-known that glycine predominantly exists in its neutral form in the gas phase and that in contrast glycine adopts zwitterionic form in bulk aqueous solution and in crystalline state [3-6]. This fact indicates that polar solvent environments significantly affect a thermodynamic equilibrium between neutral and zwitterionic forms. Therefore, the relative stability of these two forms of glycine depending on the number of explicit solvent molecules has been of particular interest so far.

It is generally difficult to study a very flexible molecular system only by static structural calculations if the system has many lowlying stationary points on its potential energy surface and transitions among these stationary points frequently occur. The PIMD simulations are very useful for understanding both the quantum mechanical effect of nuclei and the effect of thermal motions in equilibrium structures of such a molecular system. In this work we have carried out on-the-fly PIMD simulations for the small glycine-$(H_2O)_n$ (n = 1.7) clusters using the semi-empirical PM6 molecular orbital level in order to understand their structural features from quantum mechanical viewpoints. It has been shown that the PM6 level calculations semiquantitatively reproduce energetics and structures of various low-lying stationary points on the potential energy surfaces of hydrated glycine clusters obtained from more accurate density-functional calculations. The present PIMD simulations have given an interesting cluster size dependence for cluster configurations. In the case of small n = 1-3 clusters, the PIMD simulations show an expected behavior, where water molecules are bound to a neutral form glycine through hydrogen-bond between the COOH carboxylic group of glycine and water. In contrast, in the case of n = 4-6 clusters, proton- exchange processes effectively occur between the $COO^-$ group of the conjugate glycine base and the water cluster moiety although the overall cluster structure essentially corresponds to a complex between a neutral glycine and a water cluster. For the glycine-$(H_2O)_7$ cluster, the zwitterionic glycine structure is readily formed and is maintained during the simulation time even if the simulation was done with an initial structure being a neutral glycine structure. It was also found that the water solvation structure is very different between these two cases, where glycine has a neutral form or a zwitterionic form. Water molecules are mainly bound to the COOH carboxylic group of the neutral form glycine through hydrogen-bond, while the zwitterionic glycine is surrounded by water molecules.

**References**

[1] U. W. Schmitt and G. A. Voth, J. Chem. Phys. 111, 9361 (1999)

[2] S. Raugei and M. L. Klein, Chem. Phys. Chem. 5, 1569 (2004)

[3] R. D. Suenram and F. J. Lovas, J. Mol. Spectrosc. 72, 372, (1978)

[4] G. Wada, E. Tamura, M. Okina and M. Nakamura, Bull. Chem. Soc. Jpn. 55, 3064 (1982)

[5] P. D. Godfrey and R. D. Brown, J. Am. Chem. Soc. 117, 2019 (1995)

[6] R. Ramaekers, J. Pajak, B. Lambie and G. Maes, J. Chem. Phys. 120 4182 (2004)

1.3.1 Multiscale Simulations for Materials and Fuels

## (11) Rate Theory Modeling of Irradiation-Induced Phosphorus Segregation in FCC Nickel Using First Principles Calculations

Kenichi Ebihara, Masatake Yamaguchi, Hideo Kaburaki and Yutaka Nishiyama[1)]

1) Nuclear Safety Research Center, Japan Atomic Energy Agency (JAEA)

Intergranular embrittlement which is induced by segregation of phosphorus (P) to grain boundaries (GBs) is one cause of toughness degradation of materials. GB P segregation is particularly enhanced by self interstitial atoms (SIAs) and vacancies (Vs) created by irradiation. Actually, intergranular embrittlement caused by P at GBs is observed in irradiated reactor pressure vessel steels [1]. Thus, irradiation-induced GB P segregation is evaluated using a rate theory model based on atomic processes which are estimated from first principles. In order to check the validity of such a first-principles-based rate theory model, in this paper [2], we simulated the P distribution in FCC Ni, which is obtained from experiments of ion-irradiation [3], using the rate theory model which was constructed on the basis of the atomic processes identified by the first-principles calculation.

By estimating the atomic processes in [3] by the first-principles calculation code, VASP, we found the following facts concerning the interstitial dumbbell and the vacancy mechanisms that model the transport of P atoms. (1) In the interstitial dumbbell mechanism, the configuration of a self interstitial dumbbell (SID) and a P atom, which is regarded as a stable state in [4], was so unstable that the P atom was pushed into an octahedral interstitial site and that the mixed interstitial dumbbell (MID) was not formed as shown in Fig.1. (2) In the vacancy mechanism, since the exchange energy barrier between a P atom and a V was lower than that reported in [3], the vacancy mechanism was more effective in the P transport than the interstitial mechanism.

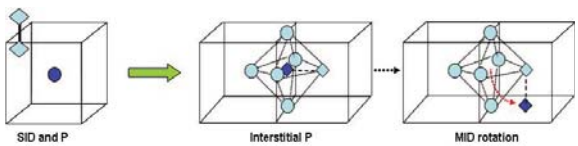


Fig. 1: Change of the interstitial mechanism [2]: Ni and P are represented by light color and dark color, respectively and a substitutional and an interstitial atom are described by a diamond and a circle, respectively.

According to the result (1), we proposed the free migration mode of an interstitial P atom (Fig.2) instead of the rotation of an MID in [3,4] which is shown in Fig.1, and constructed the diffusion rate equation as a rate theory model on the basis of the model described in [3].

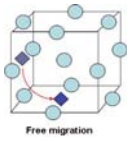


Fig. 2: Interstitial P atom migration mode [2]: The meaning of the symbol is same as Fig.1.

By adjusting the diffusion constant of the interstitial P free migration and the sink strength reducing the amount of Vs and SIAs, we simulated the P distribution under the condition in which the Ni target is irradiated by 100keV Ni ions at 773K after implanted with 60keV P ions. The obtained result in Fig.3(a) was much closer to the experiment result [3] in Fig.3(b) than the previously simulated result [3] in Fig.3(c). In particular, it is noted that the distribution of P near the surface is improved.

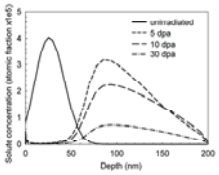


(a)

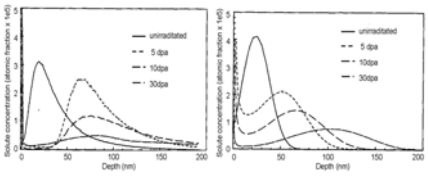

(b) (c)

Fig. 3: (a) Our simulation result [2] (b) Experimental result [3] (c) Simulation result reported in the paper[3]

**References**

[1] Y. Nishiyama, K. Onizawa, M. Suzuki, J. W. Anderegg, Y. Nagai, T. Toyama, M. Hasegawa and J. Kameda, Acta Materialia 56, (2008)

[2] K. Ebihara, M. Yamaguchi, H. Kaburaki and Y. Nishiyama, Mater.Res.Soc.Sym.Proc.Vol.1125, (2009)

[3] S. M. Murphy and J. M. Perks, J. Nucl. Mater. 171, (1990)

[4] A. Barbu, Acta Metallurgica 28, 499-506 (1980)

1.3.1 Multiscale Simulations for Materials and Fuels

## (12) Numerical Simulation of Irradiation-Induced Grain-Boundary Phosphorus Segregation in Reactor Pressure Vessel Steels Using Rate Theory Model with First-Principles Calculations

Kenichi Ebihara, Masatake Yamaguchi, Yutaka Nishiyama[1)], Kunio Onizawa[1)] and Hiroshi Matsuzawa[2)]

1) Nuclear Safety Research Center, Japan Atomic Energy Agency (JAEA)

2) Japan Nuclear Energy Safety Organization (JNES)

The experimental results on neutron-irradiated reactor pressure vessel (RPV) steels have revealed grain boundary (GB) segregation of phosphorus (P) due to neutron irradiation, which may lead to intergranular fracture. Because of the lack of experimental database, however, the dependence of the segregation on variables such as dose, dose-rate, and temperature is not clear. In this paper [1] we incorporated the parameters determined by first-principles calculations into a rate theory model, and applied it to the simulation of irradiation-induced P segregation in RPV steels. We evaluated the GB P coverage and discussed its dependence on dose-rate and irradiation temperature by comparing our results with previously reported results and experimental data.

Since P atoms is transported by the vacancy and the interstitial dumbbell mechanisms, the diffusion and partial diffusion coefficients incorporated into the rate theory model as the simulation parameter are derived from the model correspoinding to both mechanisms. In this paper, we adopted the four frequency model [2] and the model of Barbu and Lidiard [3], and estimated barrier energies of the atomic processes of each model by the nudged elastic band method using the first-principles calculation code, VASP. The rate theory model was applied to the simulation of GB P segregation of three kinds of A533B steels which are the model steels of actual RPV steels and are neutron-irradiated at 290 $^{o}$C in the experiment [4]. The A533B steels have 0.103 at% (PH), 0.047at %(PM), and 0.023 at%(PL) of the P content. The dose and dose rate are 2.5x10$^{19}$n/cm$^{2}$ (0.039dpa) and 5.2x10$^{12}$n/cm$^{2}$/s (8.1x10$^{-9}$dpa/s), respectively. The GB P segregation is measured as the monolayer coverage using the scanning Auger electron microprobe analysis, and the GB P coverage of each un-irradiated A533B steel is 26.81at% for PH, 17.70at% for PM, and 11.73at% for PL [4]. The simulation was carried out in the one-dimensional calculation region and the GB P coverage was calculated by using the method in [5]. The dose, the dose rate, and the temperature dependencies of the GB P coverage of three kinds of A533B steels are shown in Figs.1-3.

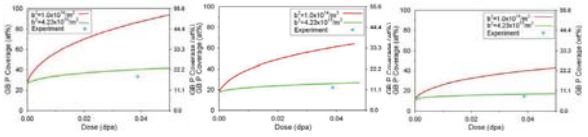

PH PM PL

Fig. 1: The dose dependency of GB P coverage[1]:

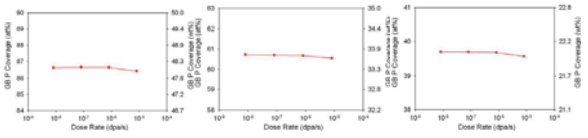

PH PM PL

Fig. 2: The dose rate dependency of GB P coverage[1]:

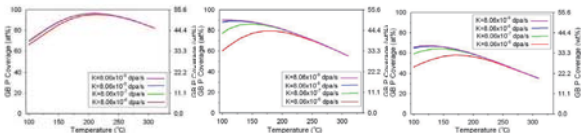

PH PM PL

Fig. 3: The temperature dependency of GB P coverage[1]:

As a result, we found the followings: (i) The dose dependency of the GB P coverage is similar to that in [6], and our results becomes close to the experimental results as the sink strength increases. (ii) The GB P coverage is irrelevant to the dose rate at about 290$^{o}$C. (iii) The temperature dependency of the GB P coverage is very different from that in [6].

**References**

[1] K. Ebihara, M. Yamaguchi, Y. Nishiyama, K. Onizawa and H.Matsuzawa, Proc.ASME 2009 Pressure Vessels and Piping Division Conf., PVP2009, (2009) (CDROM)

[2] M. Jones and A. D. Le Claire, Phil. Mag. 26 (1972)

[3] A. Barbu and A. B. Lidiard, Phil. Mag. A 74 (1996)

[4] Y. Nishiyama, K. Onizuwa, M. Suzuki, J. W. Anderegg, Y. Nagai, T. Toyama, M. Hagesawa and J. Kameda, Acta Mater. 56 (2008)

[5] A. V. Barashev, Phil. Mag. Lett. 82 (2002)

[6] S. G. Druce, C. A. English, A. J. E. Foreman, R. J. McElroy, I. A. Vatter, C. J. Boltor, J. T. Buswell and R. B. Jones, in Effects of Radiation on Materials: 17th International Symposium, ASTM STP1270(1996)

1.3.1 Multiscale Simulations for Materials and Fuels

## (13) A Numerical Study on the Validity of the Local Equilibrium Hypothesis in Modeling Hydrogen Thermal Desorption Spectra

Kenichi Ebihara, Hideo Kaburaki, Tomoaki Suzudo and Kenichi Takai[1)]

1) Department of Engineering and Applied Science, Sophia University

Hydrogen in steels affects significantly their mechanical properties, and, in particular, hydrogen-induced cracking is a problem for the welding process of high-strength steels. Hydrogen atoms in steels are located mostly at trapping defect sites such as vacancies, dislocations, grain boundaries, and phase interfaces. The understanding of these trapping hydrogen states is especially required to predict a delayed fracture process, because hydrogen atoms diffuse in a complex way by being captured by and released from trapping sites depending on the stress and temperature conditions. Each trap site has its own characteristic binding energy, corresponding to the temperature at which hydrogen is released from the trapping site potential. Thus, thermal desorption analysis (TDA) [1] is the most useful experimental method for identifying a hydrogen state in steels to delve into such trapping properties of defects. In this paper [2], we carried out a systematic benchmark study on different numerical models for analyzing hydrogen thermal desorption spectra which is obtained from hydrogen-charged specimens heated constantly in TDA, by focusing on the adoption of the local equilibrium hypothesis in these models.

We compared the following three numerical models: One is a model which is proposed by Wilson and Baskes [3], extended by Turnbull et al. [4]. This model is named Model I, and is described by the one-dimensional mass conservation equation including the releasing and the capturing process of hydrogen by trap sites. The second is Model II which is firstly used by Yamaguchi and Nagumo [5]. This model is described by the one dimensional ordinary diffusion equation with the effective diffusion coefficient renormalized to include the effect of trapping hydrogen. The renormalization is carried out based on the local hydrogen equilibrium hypothesis proposed by Oriani [6]. The last is Model III which is proposed by Ebihara et al. [7]. This model is constructed by aligning cells to which the local hydrogen equilibrium hypothesis is numerically implimented. The last two models include the local hydrogen equilibrium hypothesis mathematically or numerically.

By studying the sensitivity of hydrogen thermal desorption spectra to the specimen size using the three models, as shown in Fig 1, we found that Model I can reproduce the tendency of spectra in the experiment but that the others cannot. In the experiment, the peak of hydrogen desorption shifts to the low temperature side as the specimen width is small but the peak stays under a critical width. Model I shows a similar tendency to the experiment but the peak shift of Model II and Model III is unlimited. We also found that the difference of Model I from the others results from the fact the local hydrogen equilibrium hypothesis is not incorporated in Model I. As a result, it was made clear that Model I is the most fundamental model of TDA.

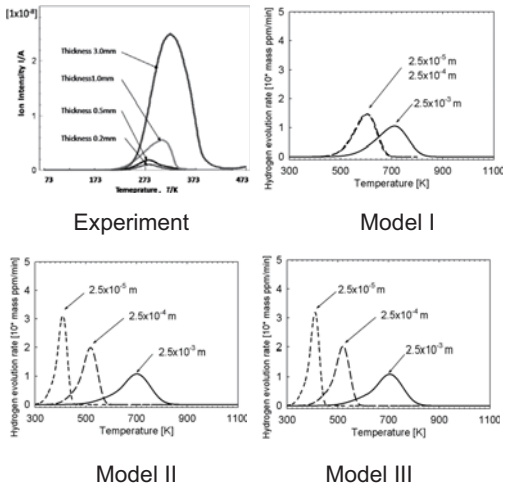


Fig. 1: Comparison of the sensitivity of hydrogen desorption spectra to the specimen width between three models and experimental result [2]

**References**

[1] M. Nagumo, Zairyo-to-Kankyo, 55 (2006)

[2] K. Ebihara, H. Kaburaki, T. Suzudo and K. Takai, ISIJ Int. 49, (2009)

[3] K. L. Wilson and M. I. Baskes, J. Nucl. Mater., 76–77 (1978)

[4] A. Turnbull, R. B. Hutchings and D. H. Ferriss, Mater. Sci. Eng. A, 238A (1997)

[5] T. Yamaguchi and M. Nagumo, ISIJ Int., 43 (2003)

[6] R. A. Oriani, Acta Metall., 18 (1970)

[7] K. Ebihara, T. Suzudo, H. Kaburaki, K. Takai and S. Takebayashi, ISIJ Int., 47 (2007)

## 1.3.2 Computational Design of Superconductor-based Innovative Quantum Devices

### (1) Communication Strategy of Parallel Density-Matrix Renormalization Group Method with Considering Architecture of Multi-Core Cluster

Susumu Yamada, Toshiyuki Imamura [1)] and Masahiko Machida

1) The University of Electro-Communications

The density matrix renormalization group (DMRG) method is a ground-state solver for one-dimensional quantum lattice systems [1]. The DMRG method can keep the number of the relevant quantum states constant by renormalizing the states of the previous step on enlarging the system. However, when the method is extended into two-dimensional models directly, the extended method requires huge memory and CPU resources. Therefore, it is difficult to execute the method on a serial computer. In order to overcome the problem, we have parallelized the extended DMRG method [2]. The parallel DMRG method can simulate *n*-leg quantum lattice models or quasi-two-dimensional models on parallel computers.

The parallel DMRG method requires all-to-all communication operations. Since the all-to-all communication operations communicate between all processes simultaneously (see Figure 1), a wide network bandwidth per process is essential to realize the efficient communication. However, since the network bandwidth of a multi-core system, which is the mainstream of current parallel computers, is not proportional to an increase of cores in general, the communication is unsuitable for the multi-core system.

In this paper, we adopt the two-step communication strategy without the all-to-all communication operation between all processes (see Figure 2), in order to achieve the high performance computing on the multi-core system [3]. We evaluate the performance of the two-step communication on “SGI Altix 3700Bx2" (single-core system) and “T2K Open Supercomputer (Todai Combined Cluster)" (quad-core system) and confirm that the performance is improved by the two-step communication (see Figure 3).

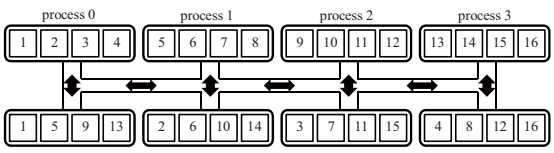


Fig. 1: A schematic figure of all-to-all communication on four processes.

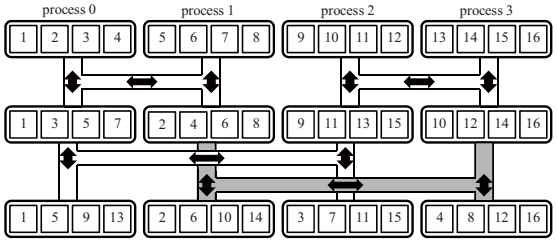


Fig. 2: A schematic figure of two-step communication on four processes.

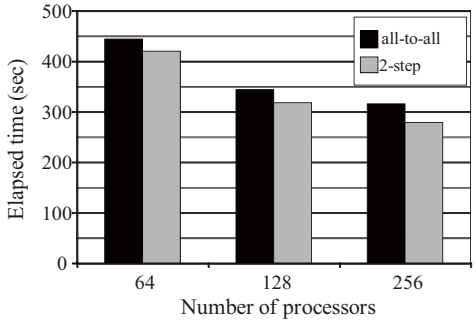


(a) SGI Altix 3700Bx2

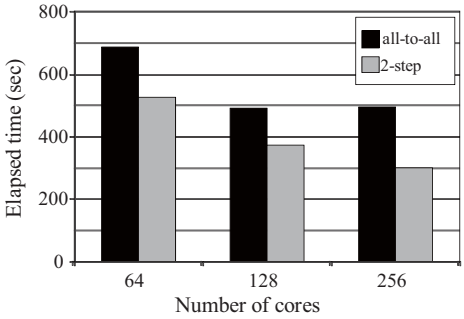


(b) T2K (Todai Combined Cluster)

Fig. 3: Elapsed time of the extended DMRG method for 3x10-site Hubbard model on SGI Altix 3700Bx2 and T2K Open Supercomputer [3].

**References**

[1] S. R. White, Phys. Rev. Lett. 69 (1992)

[2] S. Yamada, M. Okumura and M. Machida, J. Phys. Soc. Jpn., Vol. 78, No. 9 (2009)

[3] S.Yamada, T. Imamura and M. Machida, Trans. of JSCES, Vol. 2009, No. 15, pp. 12 (2009) (Japanese)

1.3.2 Computational Design of Superconductor-based Innovative Quantum Devices

## (2) Direct Extension of Density-Matrix Renormalization Group to Two-Dimensional Quantum Lattice Systems; Studies of Parallel Algorithm, Accuracy and Performance

Susumu Yamada, Masahiko Okumura and Masahiko Machida

The density matrix renormalization group (DMRG) method, which is one of the ground-state solvers for one-dimensional quantum lattice systems, has been proposed by S. R. White [1]. The DMRG method can keep the number of the relevant quantum states constant by renormalizing the states of the previous step on enlarging the system (see Figure 1). Since the DMRG method has been originally developed for 1-D models, many extended method to an *n*-leg model have been proposed. One of the methods for the *n*-leg model is the direct extension DMRG (dex-DMRG) method (see Figure 2). The dex-DMRG method can give simulation results with high precision. However, since the method requires huge memory and CPU resources, it is difficult to execute the method on a serial computer.

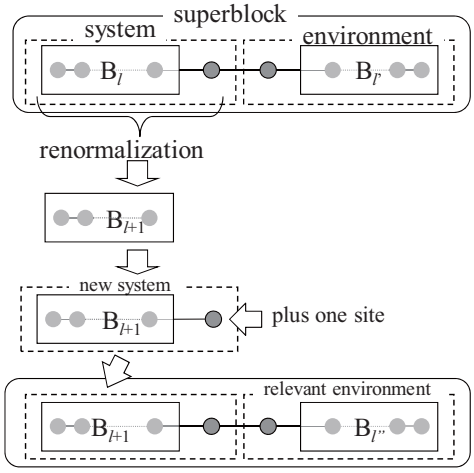


Fig. 1: A schematic figure of the renormalization scheme of DMRG method for a 1-D lattice model [2]. The whole system is called “superblock”, and the “superblock” is split into the "system” and the “environment”. The boxes in the above superblock indicate the blocks which have *l* and *l’* lattice sites, and the dark circles present single sites. The new system block $B_{l+1}$ is formed by renormalizing the system block $B_l$ and adding one site.

In this paper, we propose the parallelization strategy for the dex-DMRG method [2]. The parallelization is performed mainly on the diagonalization for the superblock Hamiltonian since this step requires enormous memory space as the leg number *n* increases. The superblock Hamiltonian is divided into three parts, and the corresponding superblock vectors are transformed into matrices whose elements are uniformly distributed into processors. We evaluate the performance of the parallel dex-DMRG method on SGI Altix 3700Bx2 and confirm that the method achieves the good parallel efficiency (see Figure 3).

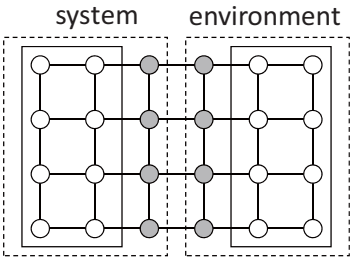


Fig. 2: A superblock configuration of the dex-DMRG method for a 4-leg model [2].

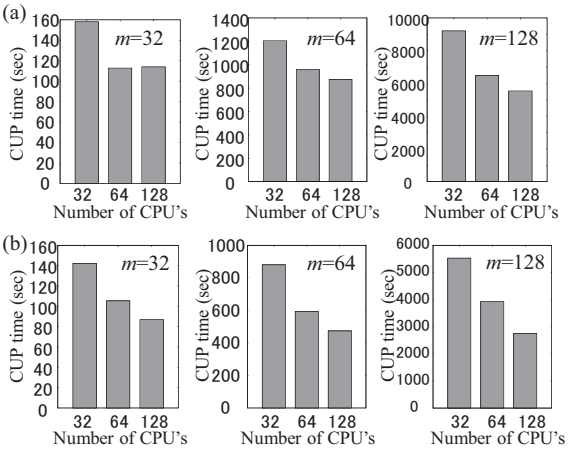


Fig. 3: (a) CPU number dependence of total CPU time for 7 (leg)x10-site Heisenberg model on Altix3700Bx2 with *m* =32, 64, and 128 [2]. (b) Same dependence for 4x10 Hubbard model. Here, *m* means the number of the states kept.

**References**

[1] S. R. White, Phys. Rev. Lett. 69 (1992)

[2] S. Yamada, M. Okumura and M. Machida, J. Phys. Soc. Jpn., Vol. 78, No. 9 (2009)

## 1.3.2 Computational Design of Superconductor-based Innovative Quantum Devices

### (3) Effect of Fermi Surface Topology on Inter-Layer Magnetoresistance in Layered Multiband Systems; Application to $LaFeAsO_{1-x}F_x$

Takao Morinari [1)], Hiroki Nakamura, Masahiko Machida and Takami Tohyama [1)]

1) Yukawa Institute for Theoretical Physics, Kyoto University

It is important to determine the Fermi surface topology since it clarifies the fundamental electronic structure of a superconductor. Angle-resolved photoemission spectroscopy (ARPES) extracts the Fermi surface of layered two-dimensional compounds. Although ARPES is very useful to analyze the map of the Fermi surface, the surface effects are not negligible in ARPES experiments. On the other hand, magnetic quantum oscillations give knowledge of the Fermi surface area perpendicular to the applied magnetic field. The Fermi surface areas obtained by magnetic quantum oscillations contain bulk information of electronic structures, but this method provides only indirect information about the Fermi surface topology. In this paper [1], we suggest interlayer magnetoresistance experiments to obtain the bulk Fermi surface topology in layered multi-band systems and apply this method to the iron-based superconductors. In particular, we concentrate on the first-discovered iron-based superconductor $LaFeAsO_{1-x}F_x$ [2] and discuss the interlayer magnetoresistance for the paramagnetic phase and stripe-ordered antiferromagnetic phases. In the former phase, the superconductivity occurs at a low temperature, while no superconductivity appears in the latter phase.

The Fermi surfaces of the iron-based superconductor are calculated by first-principles calculations for both paramagnetic and antiferromagnetic phases. In the case of paramagnetic phase, two cylindrical Fermi surfaces are constructed. One is a hole pocket around $\Gamma$ point (the center of the Brillouin zone), and the other is an electron pocket around M point (the corner of the Brillouin zone). Because of these discrete Fermi surfaces, superconductivity in this material is suggested to be caused by the spin fluctuation, which brings about so-called “s± gap symmetry”. Note that the Fermi surface structure in the paramagnetic phase keeps tetragonal symmetry. On the other hand, the antiferromagnetic order breaks the tetragonal symmetry as shown in Fig. 1.

Based on these Fermi surface structures, we calculate interlayer conductivity with the new method extended to the multiband system. In the paramagnetic phase, interlayer conductivity as a function of the angle of the applied magnetic field has peaks at every 90 degree, which is originated from the tetragonal symmetry of the Fermi surface. On the other hand, the peaks of the interlayer conductivity in the antiferromagnetic phase are reduced to only one in the range from 0 to 180 degree.

In summary, we have proposed an interlayer conductivity formula under an in-plane magnetic field to study the Fermi surface topology of layered multiband systems. Applications of the formula to one of the iron-based superconductors, $LaFeAsO_{1-x}F_x$, have been discussed. Although the total interlayer conductivity is given by the sum of all band contributions, it is possible to extract information about the Fermi surface topology from the peak positions in the interlayer conductivity as a function of the angle of the magnetic field. We have also discussed the difference between the paramagnetic state and the antiferromagnetic state.

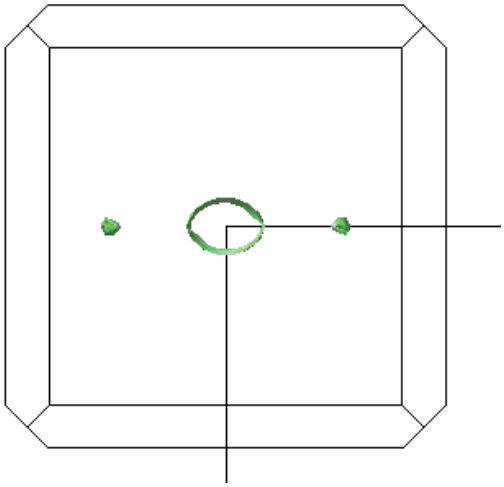

Fig. 1: The Fermi surface structure in the antiferromagnetic phase.

**References**

[1] T. Morinari, H. Nakamura, M. Machida and T. Tohyama, "Effect of Fermi Surface Topology on Inter-Layer Magnetoresistance in Layered Multiband Systems; Application to LaFeAsO1-xFx”, Journal of the Physical Society of Japan, Vol. 78, No. 11, pp. 114702_1-114702_7 (2009).

[2] Y. Kamihara, T. Watanabe, M. Hirano and H. Hosono, Journal of the American Chemical Society, Vol.130, No. 11, pp. 3296–3297 (2008)

## 1.3.2 Computational Design of Superconductor-based Innovative Quantum Devices

### (4) First-Principles Calculations of the Effect of Pressure on the Iron-Based Superconductor LaFeAsO

Hiroki Nakamura and Masahiko Machida

We perform first-principles calculations for an iron-based superconductor LaFeAsO in order to study its pressure effects [1]. In experiments, LaFeAsO shows the antiferromagnetic order instead of the superconducting phase under ambient pressure, while its superconductivity appears at 20 K under 12 GPa.

As the pressure increases, we find a change from monotonic to non-monotonic shrinking manner in lattice constants at 20 GPa, as shown in Fig. 1, and a structural transition from the orthorhombic to the tetragonal crystal with a disappearance of the antiferromagnetically ordered moment at 24 GPa (Fig. 2). The Mössbauer effect of Fe atom under high pressure indicates the disappearance of magnetic moment at 24 GPa [2]. This experimental result agrees with our calculations. Moreover, the calculations reveal that the structural transition is almost the phase transition of the second order.

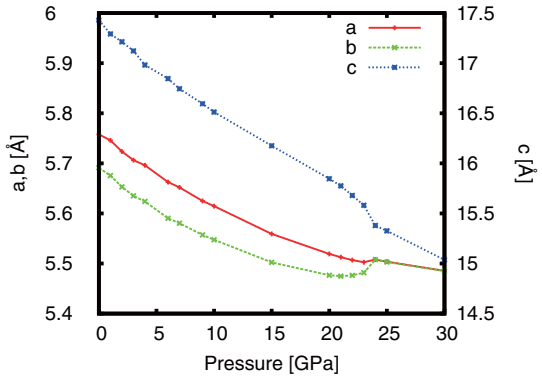


Fig. 1: Calculated lattice constants of LaFeAsO as a function of the external pressure.

In order to investigate the pressure effects on electronic states, we also evaluate density of states (DOS) at various pressure values. In a relatively low-pressure range, where the magnetic moment is still large, a DOS suppression like a pseudogap is found at the Fermi energy. The width of the suppression correlates with the moment value. As the pressure increases, the gap shrinks and finally disappears just at 24 GPa, where the magnetic moment vanishes and the magnetic DOS almost coincides that of the nonmagnetic one. This pressure-induced pseudogap closing is in a qualitative agreement with the pressure dependence of the resistivity in experiments.

We also explore a very high-pressure range and find that the contraction of the distance between As and Fe plane stops above 100 GPa although the c-axis lattice constant continues to shrink.

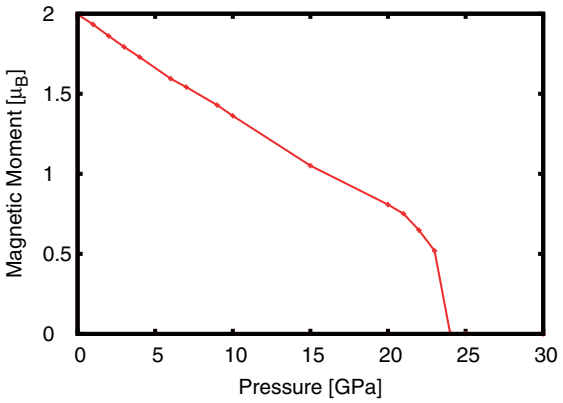


Fig. 2: Calculated magnetic moment of LaFeAsO as a function of the external pressure.

**References**

[1] H. Nakamura and M. Machida, "First-Principles Calculations of the Effect of Pressure on the Iron-Based Superconductor LaFeAsO", Physical Review B, Vol. 80, No. 16, pp. 165111_1-165111_5 (2009)

[2] T. Kawakami, T. Kamatani, H. Okada, H. Takahashi, S. Nasu, Y. Kamihara, M. Hirano and H. Hosono, Journal of the Physical Society of Japan, Vol. 78, No. 12, 123703 (2009)

## 1.3.2 Computational Design of Superconductor-based Innovative Quantum Devices

### (5) Highly Two-Dimensional Electronic Structure and Strong Fermi-Surface Nesting of the Iron-Based Superconductor $Sr_2ScFePO_3$; A First-Principles Study

Hiroki Nakamura and Masahiko Machida

The first-principles calculations are carried out for a newly discovered iron-based superconductor $Sr_2ScFePO_3$ whose blocking layer is a very thick perovskite-based oxide ($Sr_2ScO_3$) as in Fig. 1 [1]. This material brings about superconducting transition at 17 K, which is the highest critical temperature of all the FeP-based superconductors [2].

We systematically compare the calculated results of $Sr_2ScFePO_3$ with those of other typical iron-based superconductors such as LaFeAsO. We find that the thick blocking layer ($Sr_2ScO_3$) gives almost perfectly cylindrical hole and electron Fermi surfaces compared to other types whose Fermi surfaces wind along $k_z$-axis as shown in Fig. 2. This high two-dimensionality can bring about the best nesting condition between the Fermi surfaces. This explains why $Sr_2ScFePO_3$ exhibits an exceptionally high-Tc among non-arsenic iron-based superconductors and suggests a strategy to enhance the superconducting transition temperature.

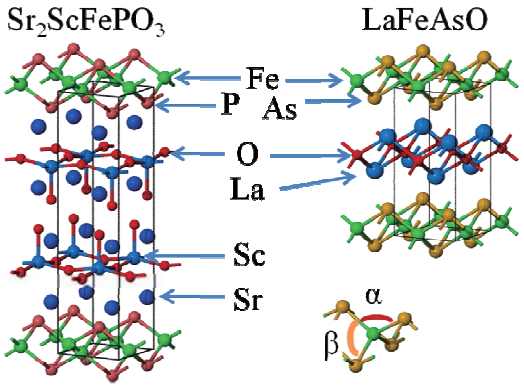


Fig. 1: Crystal structure of $Sr_2ScFePO_3$ and LaFeAsO.

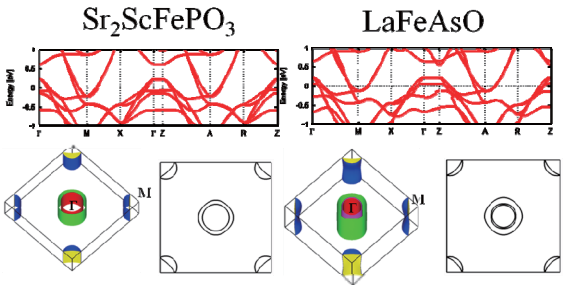


Fig. 2: Band structures and Fermi surfaces of $Sr_2ScFePO_3$ and LaFeAsO.

Lee et al. reported in Ref. [3] that there is a relationship between Tc and the angle α of Pn–Fe–Pn (see inset of Fig 1.), where Pn is a pnictogen atom, in iron-based superconductors. In the case of so-called “1111-family” such as LaFeAsO, the critical temperature as a function of α takes a cusp-like curve with maximum at α = 109.47°. Although α of $Sr_2ScFePO_3$ is 188° which is far from the optimal value, Tc of $Sr_2ScFePO_3$ is larger than that of 1111-family at α = 188°. This implies that Tc of this family with thick blocking layers exceeds the highest Tc of 1111-family if the angle reaches the optimal value.

**References**

[1] H. Nakamura and M. Machida, "Highly Two-Dimensional Electronic Structure and Strong Fermi-Surface Nesting of the Iron-Based Superconductor Sr2ScFePO3; A First-Principles Study”, Journal of the Physical Society of Japan, Vol. 79, No. 1, pp. 013705_1-013705_4 (2010)

[2] H. Ogino, Y. Matsumura, Y. Katsura, K. Ushiyama, S. Horii, K. Kishio and J. Shimoyama, Superconductor Science and Technology, Vol. 22, No. 075008 (2009)

[3] C. H. Lee, A. Iyo, H. Eisaki, H. Kito, M. T. Fernandez-Diaz, T. Ito, K. Kihou, H. Matsuhata, M. Braden and K. Yamada, Journal of the Physical Society of Japan, Vol. 77, No. 083704 (2008)

## 1.3.2 Computational Design of Superconductor-based Innovative Quantum Devices

### (6) First-Principles Study for the Anisotropy of Iron-Based Superconductors toward Power and Device Applications

Hiroki Nakamura, Masahiko Machida, Tomio Koyama [1] and Noriaki Hamada [2]

1) Institute for Materials Research, Tohoku University

2) Faculty of Science and Technology, Tokyo University of Science

With the use of the first-principles density functional theory, we evaluate the anisotropy in the superconducting state of iron-based superconductors to gain an insight into their potential applications [1]. The quasi two-dimensionality of the electronic states due to the layer structure of the iron-based superconductors is important for their applications, since it brings about anisotropy in superconducting properties. A useful quantity characterizing the superconducting anisotropy is the anisotropy parameter $\gamma$ defined as the ratio of the penetration depths perpendicular and parallel to the two-dimensional plane. Due to the values of $\gamma$, one can determine the potential applications of superconductors. For instance, superconductors with small $\gamma$ are suitable for power applications using superconducting wires, tapes or cables. On the other hand, extremely large $\gamma$ achieves the intrinsic Josephson junctions which will be promising as a THz emission device.

In Tab. 1, we show the calculated anisotropy ratio $\gamma$. It is relatively small in $BaFe_2As_2$ and LiFeAs, i.e., $\gamma$~3. On the other hand, in iron-based superconductors having perovskite type blocking layers such as $Sr_2ScFePO_3$, we find a very large value, $\gamma \geq 200$, comparable to that in strongly anisotropic high-$T_c$ cuprate $Bi_2Sr_2CaCu_2O_{8-\delta}$. The value of anisotropy is caused by the shape of the Fermi surface. As shown in Fig. 1, $BaFe_2As_2$ and LiFeAs have winding Fermi surface along longitudinal direction. Meanwhile, the Fermi surface of $Sr_2ScFePO_3$ is perfectly cylindrical. This difference causes the large discrepancy in the calculated anisotropy.

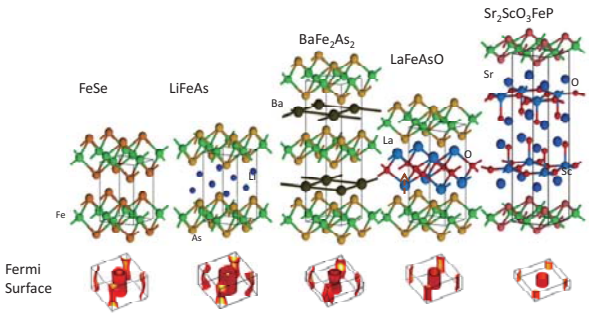


Fig. 1: Crystal structures and Fermi surfaces of various types of iron-based superconductors.

The large anisotropy in perovskite-blocking superconductors infers that the intrinsic Josephson junction stacks are expected to be formed along the c-axis. In addition, the new phase oscillation modes caused by multi-gap [2] will enrich the physics in the intrinsic Josephson junctions expected in the new compounds.

Tab. 1: Calculated anisotropy of various types of iron-based superconductors.

| Compounds | anisotropy $\gamma$ |
|---|---|
| FeSe | 4.29 |
| LiFeAs | 3.01 |
| $BaFe_2As_2$ | 3.27 |
| LaFePO | 4.16 |
| LaFeAsO | 10.81 |
| $Sr_2ScFePO_3$ | 248 |

**References**

[1] H. Nakamura, M. Machida, T. Koyama and N. Hamada, "First-Principles Study for the Anisotropy of Iron-Based Superconductors toward Power and Device Applications", Journal of the Physical Society of Japan, Vol. 78, No. 12, pp. 123712_1-123712_4 (2009)

[2] Y. Ota, M. Machida, T. Koyama and H. Matsumoto: Physical Review Letters, Vol. 102, No. 237003 (2009)

## 1.3.2 Computational Design of Superconductor-based Innovative Quantum Devices

### (7) First-Principle Electronic Structure Calculations for Magnetic Moment in Iron-Based Superconductors; An LSDA + Negative U Study

Hiroki Nakamura, Nobuhiko Hayashi, Noriyuki Nakai, Masahiko Okumura and Masahiko Machida

After the discovery of iron-based superconductors [1], several intensive studies have focused on their magnetic properties. LaFeAsO, which is a mother compound of the superconductor $LaFeAsO_{1-x}F_x$, shows an antiferromagnetic spin density wave (SDW) ordering with the tetragonal-to-orthorhombic structural transition at 150 K [2]. The other mother compounds, such as $BaFe_2As_2$ also show similar SDW. This SDW state is consistent with the ground state by the first-principle calculations. However, the calculated magnetic moment (~$2\mu_B$) of an Fe atom is much larger than the observed one (~$0.3\mu_B$) in experiments [2]. We suggested that the discrepancy can be resolved by expanding Hubbard U to a negative value in the LSDA + U method. In this paper [3], we discuss the discrepancy of magnetic moment and make clear why the negative correction on U is essential.

LSDA+U method is often used to correct the electronic structure of the strongly-correlated electrons on compounds including transition metals. The parameter U is theoretically re-expressed as $U_{eff}$=U-J, where U is the Hubbard U and J is the atomic-orbital intra-exchange energy (Hund's coupling parameter). The parameter $U_{eff}$ is usually positive. The positivity enhances the localized character of d-electrons and sometimes raises the magnetic moment. In LSDA+U calculations, one can principally extend the parameter $U_{eff}$ to a negative region. Although the negative case is rare, it is known that the negative U appears in some cases. For instance, when the screening is unusual, e.g., an overscreening occurs, the estimation of $U_{eff}$ may not simply give a positive value, and it can be negative.

Let us show the results. We focus on the compounds, LaFeAsO and $LaFeAsO_{1-x}F_x$. Figure 1(a) describes $U_{eff}$ dependence of the energy difference between the non-magnetic and the SDW states, and Fig. 1(b) shows the magnetic moment of an Fe atom in the SDW state as a function of $U_{eff}$. At $U_{eff}$=0, the magnetic moment becomes ~$2\mu_B$ and the SDW state is more stable than the non-magnetic one with the energy difference ~90 meV. For $U_{eff}$ > 0, the moment increases by the positive correction. As expected, the positive $U_{eff}$ enhances the localization of d-orbital electrons, and overemphasizes the inconsistency with the experiments. Meanwhile, the moment decreases with decreasing $U_{eff}$ and coincides with the experimental results around $U_{eff}$ =−1. Note that the energy difference becomes very small around $U_{eff}$ = −1 eV, as seen in Fig. 1(a). This indicates that the SDW state becomes not as strongly stable as that at $U_{eff}$=0.

In summary, we evaluated electronic structures of iron-based superconducting compound $LaFeAsO_xF_{1-x}$ with the use of the LSDA + U method with extending the range of $U_{eff}$ from the positive to the negative value. As a result, we found that the magnetic moment calculated in the negative $U_{eff}$ range agrees well with the experimental results.

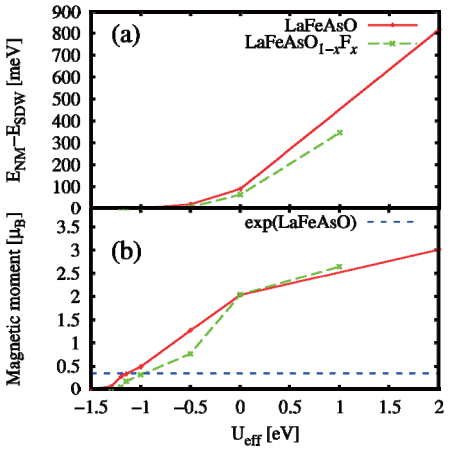


Fig. 1: $U_{eff}$ dependence for LaFeAsO and $LaFeAsO_{1-x}F_x$ (x = 0:125) on (a) the total energy difference between the SDW and the non-magnetic state, and (b) the SDW magnetic moment of an Fe-atom. Horizontal line describes experimental data.

**References**

[1] Y. Kamihara, T. Watanabe, M. Hirano and H. Hosono, Journal of the American Chemical Society, Vol.130, No. 11, pp. 3296–3297 (2008)

[2] C. de la Cruz, Q. Huang, J.W. Lynn, J. Li, W. Ratcliff II, J.L. Zarestky, H.A. Mook, G.F. Chen, J.L. Luo, N.L. Wang and P. Dai, Nature, Vol. 453, pp. 899 (2008)

[3] H. Nakamura, N. Hayashi, N. Nakai, M. Okumura and M. Machida, "First-Principle Electronic Structure Calculations for Magnetic Moment in Iron-Based Superconductors; An LSDA + Negative U Study", Physica C, Vol. 469, No. 15-20, pp. 908-911 (2009)

## 1.3.2 Computational Design of Superconductor-based Innovative Quantum Devices

### (8) First-Principle Calculation for the Phonon Structure on Iron-Based Superconductors

Hiroki Nakamura, Nobuhiko Hayashi, Noriyuki Nakai and Masahiko Machida

The first discovery of superconductivity in $LaFeAsO_{1-x}F_x$ has opened an intensive research streamline for high-Tc iron-based superconductors. After this discovery, various iron-based superconductors were found, such as K-doped $BaFe_2As_2$ and FeSe. They have the universal FeAs(or Se) layer. Hence, it is clear that the layer of Fe and As(Se) atoms is responsible for the superconductivity and its intra-layer electronic structure is deeply connected to the superconducting mechanism. Tha recent detection of an isotope effect on the Fe atom implies that phonon may be a key issue in the mechanism of the iron-based superconductors. Moreover, the isotope effect on O atoms is reported to be very weak. Thus, we concentrate on the optical phonons including Fe vibrations.

We evaluate phonon structures of three typical iron-based superconductors, i.e., LaFeAsO; $BaFe_2As_2$, and FeSe by using the first-principles calculations [1]. The phonon dispersions and densities of states of them are shown in Fig. 1, with their crystal structures. Although these dispersions are slightly different from one another due to the crystal structure variations, the optical modes related to Fe vibrations show almost similar features.

Recently, in the case of RFeAsO (R: rare earth element), X-ray inelastic scattering measurements [2] have potined out that the calculated peak around 8 THz in the phonon DOS as shown in Fig. 1(a) shifts to 7.5 THz. The variation of $T_c$ may be correlated to the phonon softening if the optical mode is crucial for the superconductivity.

An enhancement of $T_c$ in FeSe has been observed under high pressure. Fig. 1(c) shows the phonon dispersions of FeSe at 1.48 GPa and 0 GPa. The dispersions between around 6 and 10 THz, which mainly come from Fe atoms, shift upwards with increasing the pressure. This hardening can be also seen in the phonon DOS. Generally, the existence of the high frequency phonon is crucial for high superconducting critical temperature. This results may support this importance of the phonon.

In summary, we calculated the phonon dispersions and their density of states for three typical iron-based superconductors. Although details of the phonon dispersions are different from each other, the optical modes related to Fe atoms are almost equivalent. We also investigated the pressure effect on the superconductor FeSe. We show that the external pressure makes the phonon frequencies associated with Fe shift upwards, which may be related to $T_c$ enhancement.

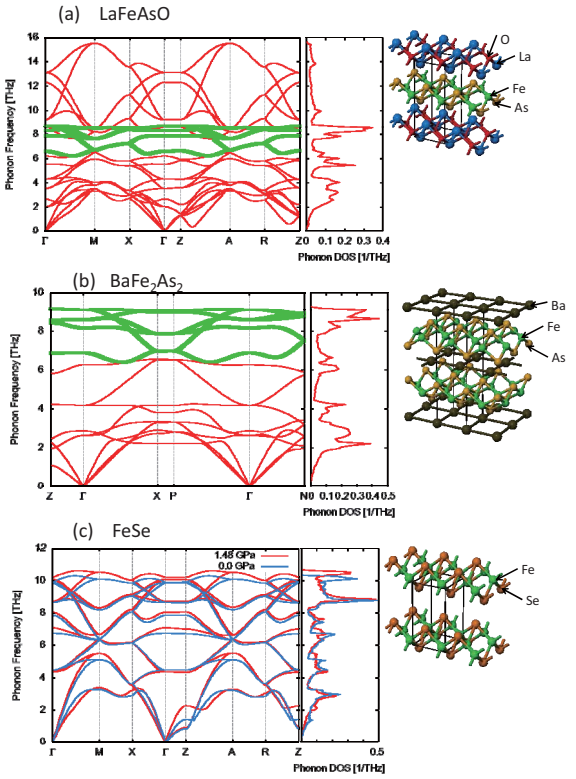


Fig. 1: Phonon dispersions and densities of states for (a) LaFeAsO, (b) $BaFe_2As_2$, and (c) FeSe. Insets show the crystal structure. Thick curves in (a) and (b) show Fe-dominant modes. Red and blue curves in (c) correspond to external pressure 1.45 GPa and zero pressure, respectively.

**References**

[1] H. Nakamura, N. Hayashi, N. Nakai and M. Machida, "First-Principle Calculation for the Phonon Structure on Iron-Based Superconductors", Physica C, Vol. 469, No. 15-20, pp. 1024-1026 (2009)

[2] T. Fukuda, A.Q.R. Baron, S. Shamoto, M. Ishikado, H. Nakamura, M. Machida, H. Uchiyama, S. Tsutsui, A. Iyo, H. Kito, J. Mizuki, M. Arai, H. Eisaki and H. Hosono, Journal of the Physical Society of Japan, Vol. 77, No. 103715 (2008)

## 1.3.3 Large-Scale Simulations for the Fundamental Understanding of Superconductivity

### (1) Simulation Study for the Orientation of the Driven Vortex Lattice in an Amorphous Superconductor

Noriyuki Nakai, Nobuhiko Hayashi and Masahiko Machida

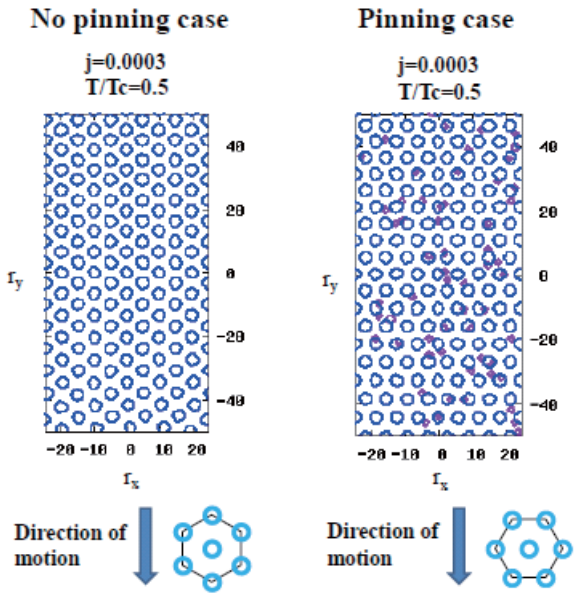


Fig. 1: Snapshot of a collective motion of vortices. The left figure shows no-vortex-pinning case. The right figure shows vortex-pinning case. Relative angles between the lattice-vector and direction of motion are different.

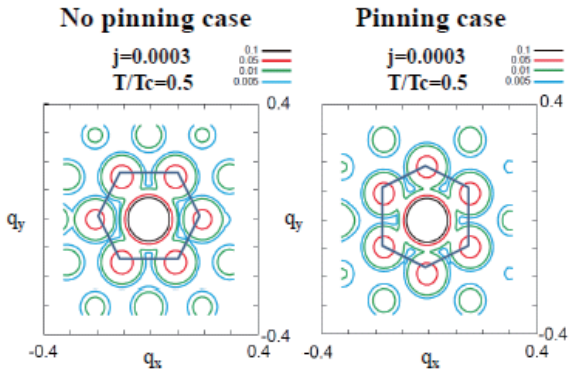


Fig. 2: Time-averaged structure factor of the superconducting order parameter. Periodicities of moving vortices are directly reflected in the left for the no-pinning case and right for the pinning case.

In some experimental measurements for type II superconductors, it was reported that vortices driven by an applied current show a collective motion. We studied driven vortices for the inhomogeneous superconductor with numerical simulations.

Here, our purpose was to investigate the orientation of the driven vortex-lattice by using the numerical simulation, which is on the basis of Time-Dependent-Ginzburg-Landau (TDGL) theory taking account of vortex pinnings as inhomogeneity.

As a result of the TDGL simulation, we confirmed the transformation from the static glass to the moving lattice with the increase of the applied current. Moreover, we found that the collective motions of vortices are different between no-pinning and pinning cases. It shows that vortex pinning affects not only stationary vortices but also moving them [1].

**References**

[1] N. Nakai, N. Hayashi and M. Machida, Physica C 469, 1106 (2009)

## 1.3.3 Large-Scale Simulations for the Fundamental Understanding of Superconductivity

### (2) Ginzburg-Landau Simulation for a Vortex around a Columnar Defect in a Superconducting Film

Noriyuki Nakai, Nobuhiko Hayashi and Masahiko Machida

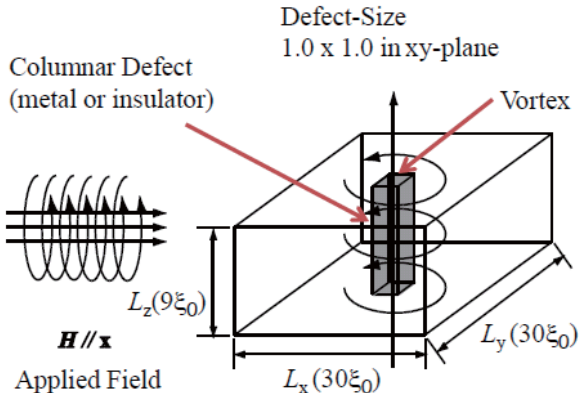


Fig. 1: Simulation model. The columnar defect in the superconductor captures one vortex.

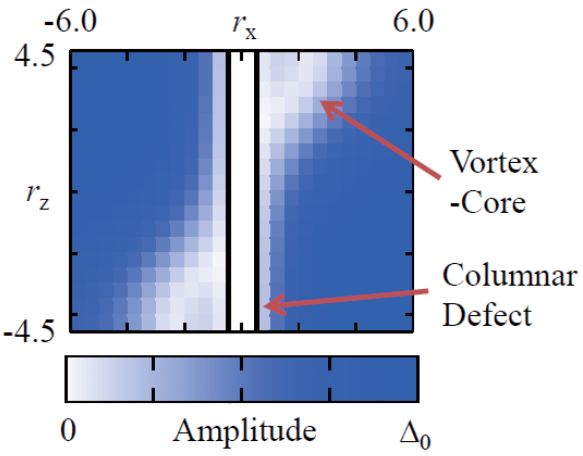


Fig. 2: Contour profile of the strength of the superconductivity. The superconductivity is suppressed at the columnar defect and flux-line (vortex-core). The vortex is partially depinning due to the external field which is perpendicular to the columnar defect.

Moving vortices driven by an applied supercurrent generate Ohmic heating. For applications it is necessary that vortices are pinned. Columnar defects are considered as strong vortex-pinning sources. It is important to study properties of a columnar defect as a vortex pinning source.

In order to investigate a vortex-pinning dynamics around a columnar defect, numerical simulations were performed. Our simulation considered a three-dimensional superconductor, which contained a single columnar defect. Our study was based on the Ginzburg-Landau (GL) theory. We focused on the simple problem, which is the depinning of the single vortex from the single columnar defect.

With numerical simulations we compared a metallic and insulator defects. It is found that the insulator case is stronger than the metallic case concerning the pinning force of a columnar defect [1].

**References**

[1] N. Nakai, N. Hayashi and M. Machida, J. Phys. Chem. Solids 69, 3301 (2008)

1.3.3 Large-Scale Simulations for the Fundamental Understanding of Superconductivity

## (3) Simulation Studies for the Vortex Depinning Dynamics around a Columnar Defect in Superconductors

Noriyuki Nakai, Nobuhiko Hayashi and Masahiko Machida

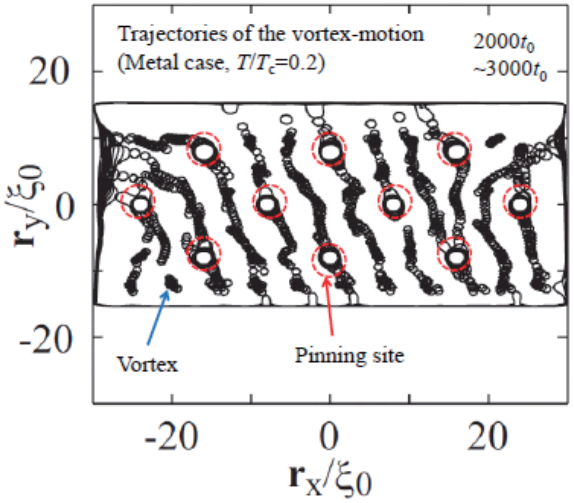


Fig. 1: Trajectries of moving vortices in the case of metallic pinning-sites. Contour lines indicate the weak superconductivity due to vortices.

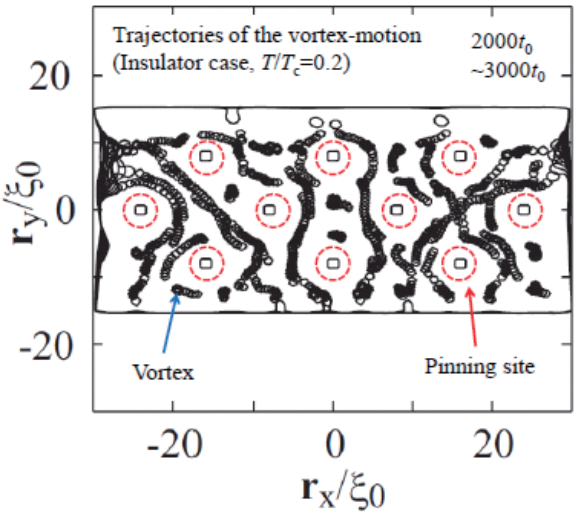


Fig. 2: Trajectries of moving vortices in the case of insulator pinning-sites. Counter lines indicate the weak superconductivity due to vortices.

The electric current drives vortices, and the induced vortex-motion gives rise to Ohmic heating. If one expects to use a large supercurrent, it is a serious problem that a vortex-motion is perfectly suppressed. The columnar defect has been a candidate as a strong vortex-pinning center. The modeling for numerical simulations is not a unique solution.

In this study, we compared two possible modeling. The first one is that the superconductor is strongly damaged inside the column, while the second one is that an empty space exists inside it. One expects that there is a difference in the vortex-pinning and –depinning dynamics for the two modeling.

In order to clarify the difference, we solved the time-dependent Ginzburg-Landau and Maxwell equations in the same time and simulated vortex-dynamics around a columnar defect. As seen in Fig. 1 and Fig. 2, this simulation revealed the depinning dynamics depending on the modeling of the columnar defect [1].

**References**

[1] N. Nakai, N. Hayashi and M. Machida, Physica C 468, 1270 (2008)

## 1.3.3 Large-Scale Simulations for the Fundamental Understanding of Superconductivity

### (4) Intergrain Josephson Currents in Multigap Superconductors; Microscopic Origin of Low Intergrain Critical Current and its Recovery Potential in Iron-Pnictide Materials

Yukihiro Ota, Masahiko Machida and Tomio Koyama [1)]

1) Institute for Materials Research, Tohoku University

Recently discovered iron-pnictide superconductors [1] have a lot of advantages for the application to superconducting tapes, cables, wires, etc. In particular, their rich material variety may lead to flexible material design depending on the application [2]. One of the important quantities for assessing application potential of a superconductor is superconducting critical current. A certain type of the iron-pnictides has been expected as a superconducting material with large critical current due to the weak anisotropy. However, their polycritalline samples showed an unexpected small critical current value [3-5]. More precisely, the intergrain critical current was much smaller than the intragrain one.

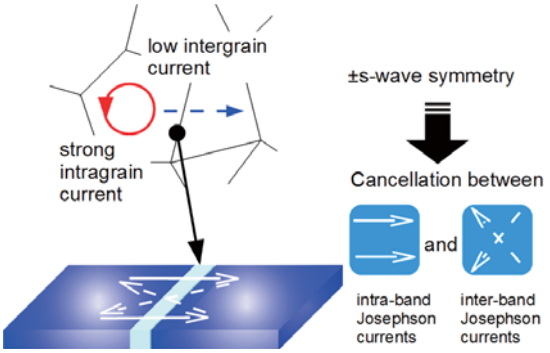


Fig. 1: Grain boundary junctions and mechanism of low intergrain Josephson current

The purpose of the present paper is to reveal a microscopic origin of the low intergrain critical current. As shown in Fig.1, we study the superconducting tunneling current at the grain boundaries in polycrystalline samples of two-band superconductors which corresponds to a minimal model for the iron-pinictide superconductor. We show [6] that the intergrain Josephson current is significantly suppressed when the Cooper pair symmetry is ±s-wave. Then, we propose that the bulk critical current is limited by the reduction mechanism due to the ±s-wave symmetry in the iron-pnictide superconductors.

The orign of the low intergrain current which we confirm in the present work is a cancellation between the currents in incoherent tunneling channels. The cancellation is predominant when the transport characters (e.g., the density of states and the superconducting gap amplitudes) between the two tunneling channels are identical each other. This consideration indicates that materials with the equivalent transport characters between the different tunneling channels are preferable in avoiding the large suppression. In addition, we show that, when coherent tunneling is active, the situation becomes quite different. Indeed, we find drastic recovery via the coherent tunneling of the intergrain current. Thus, we have shown several ways to solve a weak-link problem at the grain boundary of the iron-pnictide superconductors.

**References**

[1] Y. Kamihara, T. Watanabe, M. Hirano and H. Hosono, J. Am. Chem. Soc. 130, 3296 (2008)

[2] H. Nakamura, M. Machida, T. Koyama and N. Hamada, J. Phys.Soc. Jpn. 78, 123712 (2009)

[3] A. Yamamoto, A. A. Polyanskii, J. Jiang, F. Kametani, C. Tarantini, F. Hunte, J. Jaroszynski, E. E. Hellstrom, P. J. Lee, A. Gurevich, D. C. Larbalestier, Z. A. Ren, J. Yang, X. L. Dong, W. Lu and Z. X. Zhao, Supercond. Sci. Technol. 21, 095008 (2008)

[4] T. Tamegai, Y. Nakajima, Y. Tsuchiya, A. Iyo, K. Miyazawa, P. M. Shirage, H. Kito and H. Eisaki, Physica C 469, 915 (2009)

[5] E. S. Otabe, M. Kiuchi, S. Kawai, Y. Morita, J. Ge, B. Ni, Z. Gao, L. Wang, Y. Qi, X. Zhang and Y. Ma, Physica C 469, 1940 (2009)

[6] Y. Ota, M. Machida and T. Koyama, J. Phys. Soc. Jpn. 78, 103701 (2009)

1.3.3 Large-Scale Simulations for the Fundamental Understanding of Superconductivity

## (5) Theory of Vortex Structure in Josephson Junctions with Multiple Tunneling Channels: Vortex Enlargement as a Probe for ±s-wave Superconductors

Yukihiro Ota, Masahiko Machida, Tomio Koyama [1)] and Hideki Matsumoto [1)]

1) Institute for Materials Research, Tohoku University

Josephson junction is a sensitive superconducting device which exhibits various kinds of electromagnetic effects (i.e., Josephson effects) useful for investigating a fundamental property of unknown superconductivity. In 2008, a novel superconducting compound, iron-pnictide superconductor was found [1]. After this discovery, a large amount of the studies about such a material have been performed. An urgent issue of them is to confirm its superconducting pairing symmetry. Several theoretical works [2-5] have proposed that a sign change occurs between full gaps when a strong repulsion works between the quasiparticles on the disconnected Fermi surfaces. The symmetry with such a sign change has been called ±s-wave.

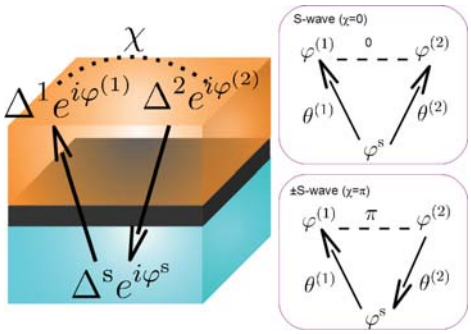


Fig.1: Schematics for a heterotic junction

The purpose of this paper [6] is to make a reliable probe to detect the pairing symmetry of the iron-pnictides on the basis of the observation of a Josephson vortex, which is one of the famous Josephson effects in the presence of magnetic field. The systems considered in this paper are shown in Figs. 1 and 2.

First, we derive a fundamental equation for the systems, coupled sine-Gordon equations, which are non-linear partial difference equations with several degrees of freedom. Numerically simulating these equations with a proper boundary condition, we successfully obtain the Josephson vortex solution. The size of the resultant Josephson vortex anomalously enlarges for ±s-wave compared to the size estimated without the sign change. The mechanism of the vortex core enlargement is simply explained by a cancellation of two Josephson current, as shown in Figs. 1 and 2. For the case of ±s-wave, π-shift between the two tunneling channels leads to the shown in Figs. 1 and 2. For the case of ±s-wave, π-shift

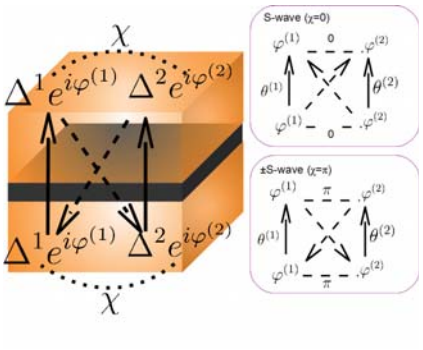


Fig.2: Schematics for a grain-boundary junction

between the two tunneling channels leads to the cancellation between the two Josephson currents. As a result, a characteristic spatial scale for the ±s-wave becomes longer than for the s-wave without the sign changes. The detection will be possible if one uses the scanning superconducting quantum interference devices.

### References

[1] Y. Kamihara, T. Watanabe, M. Hirano and H. Hosono, J. Am. Chem. Soc. 130, 3296 (2008)

[2] I. I. Mazin, D. J. Singh, M. D. Johannes and M. H. Du, Phys. Rev. Lett. 101, 057003 (2008)

[3] K. Kuroki, S. Onari, R. Arita, H. Usui, Y. Tanaka, H. Kontani and H. Aoki, Phys. Rev. Lett. 101, 087004 (2008); 102, 109902(E) (2009)

[4] Y. Nagai, N. Hayashi, N. Nakai, H. Nakamura, M. Okumura and M. Machida, New J. Phys. 10, 103026 (2008)

[5] K. Kuroki, H. Usui, S. Onari, R. Arita and H. Aoki, Phys. Rev. B 79, 224511 (2009)

[6] Y. Ota, M. Machida, T. Koyama and H. Matsumoto, Phys. Rev. B 81, 014502 (2010)

## 1.3.3 Large-Scale Simulations for the Fundamental Understanding of Superconductivity

### (6) Generation and Application of Multi-Path Cat States of Light

Natsuko Ishida[1)], Yukihiro Ota and Yoshihisa Yamamoto[2)]

1) National Institute of Informatics
2) Edward L. Ginzon Laboratory, Stanford University

Creation, manipulation, and detection of non-classical light provide remarkable application potential such as quantum communication [1] and quantum metrology [2]. Moreover, the combination of a photonic quantum state with the other quantum systems (e.g., trapped ions, superconducting Josephson qubits, etc) can be a key device to realize quantum control and quantum information processing. It is necessary for understanding and developing the related proposals to closely study quantumness of photon. Photon's quantum nature manifestly exhibits when one considers a multi-photon system. For example, the celebrated Hanbry-Brown-Twiss effect [3,4] observed in a two-body correlation experiment is directly brought about the fact that photon is boson. Indeed, superconductivity is closely related to such a bosonic many-body effect.

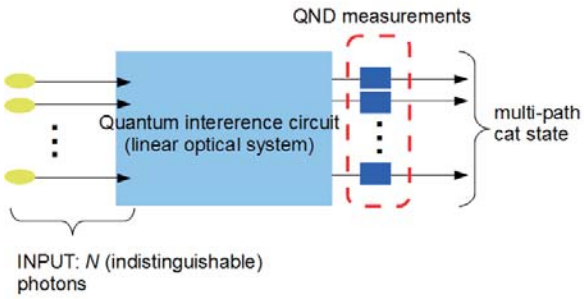


Fig.1: Schematics for a scheme to generate a multi-path cat state

Recently, various kinds of multi-photon entangled states have been proposed. One of the most famous examples is the NOON state [5], which is relevant to beating the standard quantum limit [6]. The purpose of this paper [7] is to propose a scheme to generate a complete new multi-path photonic entangled state, multi-path cat state. In contrast to the standard NOON state which has a similar structure to the Greenberger-Horne-Zeilinger state [8], the proposed state is similar to the W state [9]. We theoretically study the feasibility of converting indistinguishable single photons into the path-entangled photon number states, which are useful for the quantum lithography, using massive parallel indistinguishable single-photon sources and quantum interference circuits, as shown in Fig.1. The fidelity of the generated state is increased if the postselection based on a state preserving quantum non-demolition (QND) measurement of photon number is incorporated. The novel state will be useful for quantum lithography using multiple beams due to the improved spatial resolution and phase sensitivity.

**References**

[1] M. Nielsen and I. L. Chuang, Quantum Computation and Quantum Information (Cambridge University Press, Cambridge, 2000)
[2] V. Giovannetti, S. Lloyd and L. Maccone, Phys. Rev. Lett. 96, 010401 (2006)
[3] R. Loudon, The Quantum Theory of Light, 3rd ed. (Oxford, New York, 2000) Chap.5
[4] C. K. Hong, Z. Y. Ou and L. Mandel, Phys. Rev. Lett. 59, 2044 (1987)
[5] B. Yurke, S. L. McCall and J. R. Klauder, Phys. Rev. A 33, 4033 (1986)
[6] J. A. Jones, S. D. Karlen, J. Fitzsimons, A. Ardavan, S. C. Benjamin, G. Andrew D. Briggs and J. L. Morton, Science 324, 1166 (2009)
[7] N. Ishida, Y. Ota and Y. Yamamoto, New J. Phys. 11, 033007 (2009)
[8] D. M. Greenberger, M. A. Horn and A. Zeilinger, arXiv:0712.0921
[9] W. Dür, G. Vidal and J. I. Cirac, Phys. Rev. A 62, 062314 (2000)

## 1.3.3 Large-Scale Simulations for the Fundamental Understanding of Superconductivity

### (7) Theory of Heterotic Superconductor-Insulator-Superconductor Josephson Junctions between Single- and Multiple-Gap Superconductors

Yukihiro Ota, Masahiko Machida, Tomio Koyama [1)] and Hideki Matsumoto [1)]

1) Institute for Materials Research, Tohoku University

Superconductivity is one of the most drastic phenomena in condenced matter physics and Josephson junction is an intriguing devise sensitively and definitely depending on the superconductivity. A conventional theoretical description of such a device has been already established in 1960's. However, after the discovery of highly anisotropic layerd High-Tc copper oxide superconductors, extention and modification of the basic theory was highly desirable to explain intrinsic Josephson effects [1]. Thus, discovery of a new superconducting compound is a trigger of the development of novel theoretical description of Josephson junctions.

Since the recent discovery of iron-based superconductors [2], a theory of the Josephson junctions with such compounds has been intensively studied due to reveal their fundamental properties and their applicability to superconducting engineering [3-8]. A key feature of these compounds is multiband superconductivity, and, as a result, the coexistence of the multiple superconducting gaps [10]. Hence, a Josephson junction with the iron-based superconductors may be described by a Josephson junction with multiple tunneling channels, whose number of the channels is equivalent to the number of the bands.

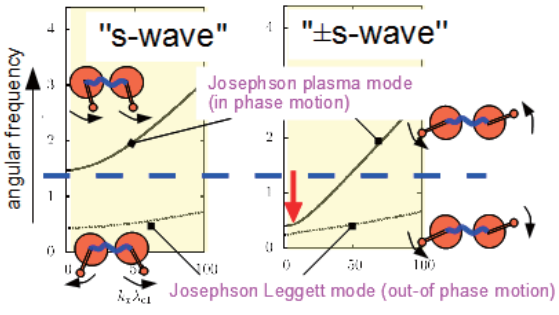


Fig.1: Collective excitation modes in a Josephson junction with multiple tunneling channels.

The purpose of this paper [3] is to construct a fundamental theory of the Josephson junction with multiple tunneling channels. The dynamical theory of the gauge invariant phase differences is derived on the basis of the time-dependent Ginzburg-Landau theory. The resultant dynamical equation exhibits rich junction dynamics.

The highlight of the present study is to clarify a collective excitation mode in this system. In particular, we show that a unique excitation, Leggett's mode [10] appears in addition to the standard mode, Josephson-plasma, as shown in Fig.1. The theory can predict the DC [7] and the AC Josephson effects [8] taking into account of such a new collective mode. Furthermore the results are effective to identify a fundamental property of the iron-based superconductor, its pairing symmetry.

**References**

[1] M. Machida, T. Koyama, A. Tanaka and M. Tachiki, Physica C 331, 85 (2000)

[2] Y. Kamihara, T. Watanabe, M. Hirano and H. Hosono, J. Am. Chem. Soc. 130, 3296 (2008)

[3] Y. Ota, M. Machida, T. Koyama and H. Matsumoto, Phys. Rev. Lett. 102, 237003 (2009)

[4] D. Inotani and Y. Ohashi, Phys. Rev. B 79, 224527 (2009)

[5] I. B. Sperstad, J. Linder and A. Sudbø, Phys. Rev. B 80, 144507 (2009)

[6] A. A. Golubov, A. Brinkman, Y. Tanaka, I. I. Mazin and O. V. Dolgov, Phys. Rev. Lett. 103, 077003 (2009)

[7] Y. Ota, N. Nakai, H. Nakamura, M. Machida, D. Inotani, Y. Ohashi, T. Koyama and H. Matsumoto, Phys. Rev. B 81, 214511 (2010)

[8] Y. Ota, M. Machida and T. Koyama, Phys. Rev. B 82, 140509(R) (2010)

[9] H. Ding, P. Richard, K. Nakayama, K. Sugawara, T. Arakane, Y. Sekiba, A. Takayama, S. Souma, T. Sato, T. Takahashi, Z. Wang, X. Dai, Z. Fang, G. F. Chen, J. L. Luo and N. L. Wang N, EPL 83, 47001 (2008)

[10] A. J. Leggett, Prog. Theor. Phys. 36, 901 (1966)

## 1.3.3 Large-Scale Simulations for the Fundamental Understanding of Superconductivity

### (8) Polarization Plateau in an Atomic Fermi Gas Loaded on a Three-Leg Triangular Optical Lattice

Masahiko Okumura, Susumu Yamada, Masahiko Machida and Toru Sakai [1)]

1) SPring-8, Japan Atomic Energy Agency; Department of Material Science, University of Hyogo

We study effects of spin-population imbalance on ultoracold Fermi atoms with two spin-components loaded on three-leg triangular optical lattice. We use the density-matrix renormalization-group method to include both effects of strong interaction and trapping potential. In strongly interacting case, we find that the ground state consists of a metallic and a Mott phases whose polarization shows plateaulike structure as a function of the input population imbalance. We also find characteristic spin structure in the Mott phase which is peculiar to the triangular Hesenberg models under the external magnetic field. This result suggests that the Mott phase is a suitable for systematic investigation of frustrated spin systems [1].

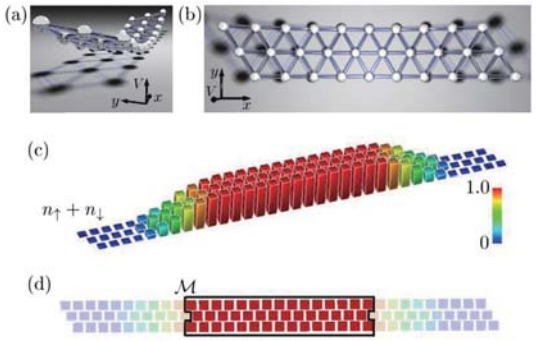


Fig. 1: (a), (b) Schematic figures of the system studied (c) A typical density distribution for 60 fermions (30↑,30↓) at $U/t$=10 and $V/t$=0.07. The Mott core is formed in the center of the system. (d) The definition of the Mott core region M, where the density $n\uparrow+n\downarrow$ is a unit.

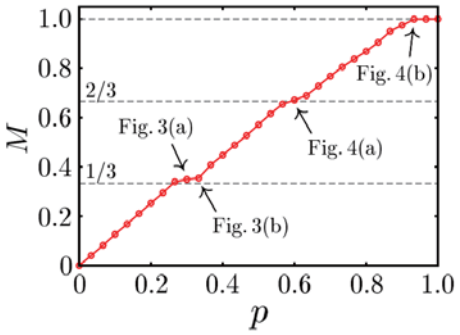


Fig. 2: The Mott-core polarization $M$ curve as a function of the population imbalance $p$. The spin distributions at the values of $p$ pointed by arrows are given in Figs. 3 and 4.

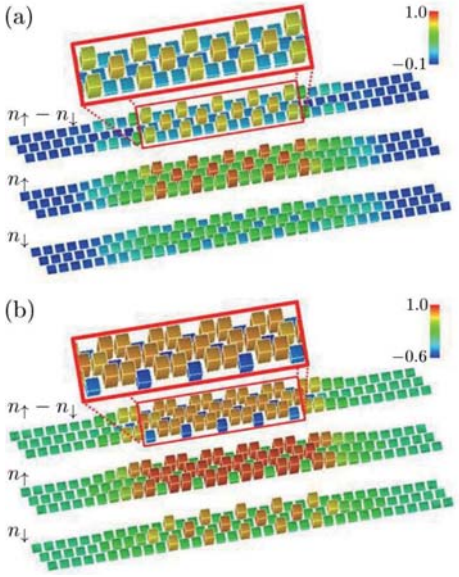


Fig. 3: Polarization ($n_\uparrow$−$n_\downarrow$), up-spin ($n_\uparrow$), and down-spin ($n_\downarrow$) density distributions at (a) $p$=0.30 and (b) $p$=0.33. The zoomed-in view is the spin distribution on the Mott core.

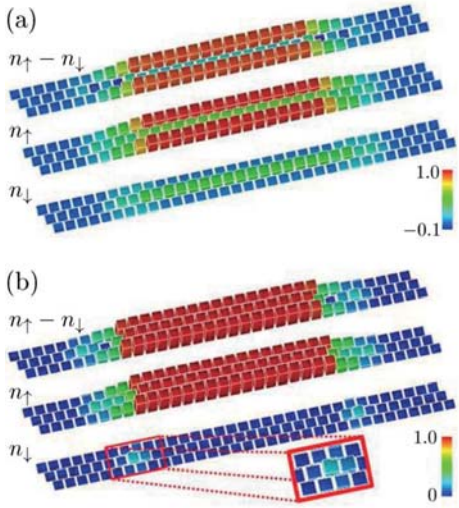


Fig. 4: Polarization ($n_\uparrow$−$n_\downarrow$), up-spin ($n_\uparrow$), and down-spin ($n_\downarrow$) density distributions at (a) $p$=0.60 and (b) $p$=0.93. The zoomed-in view is the down-spin distribution outside the Mott core.

**References**

[1] M. Okumura, S. Yamada, M. Machida and T. Sakai, Phys. Rev. A 79, 061602 (2009)

1.3.3 Large-Scale Simulations for the Fundamental Understanding of Superconductivity

## (9) Exact Diagonalization Studies on Two-Band Minimal Model for Iron-Based Superconductors

Masahiko Okumura, Noriyuki Nakai, Hiroki Nakamura, Nobuhiko Hayashi, Susumu Yamada and Masahiko Machida

We study a two-band minimal model for an iron-based superconductor with two degenerate $d_{xy}$ and $d_{yz}$ orbitals on Fe atom by using exact diagonaliation method. We consider 10 lattice sites with two-leg ladder structure, of which degree of freedom is equivalent a four leg ladder system (Fig.1). We evaluate the binding energy $E_b$ for several sets of parameters (Fig.2,3). As a result, a robust pairing is found when the intra-orbital repulsive interaction becomes smaller than the inter-orbital one. In addition, for several parameter sets, the obtained binding energies are largere than hat obtained in the single band Hubbard model [1].

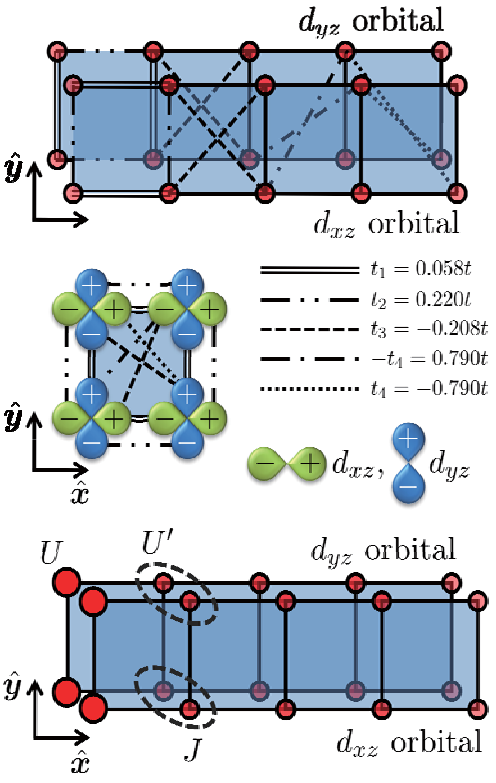


Fig. 1: Schematic figures of the simulated system, i.e., (a) $d_{xz}$ and $d_{yz}$ orbitals and the corresponding hopping parameters and (b) the interaction terms.

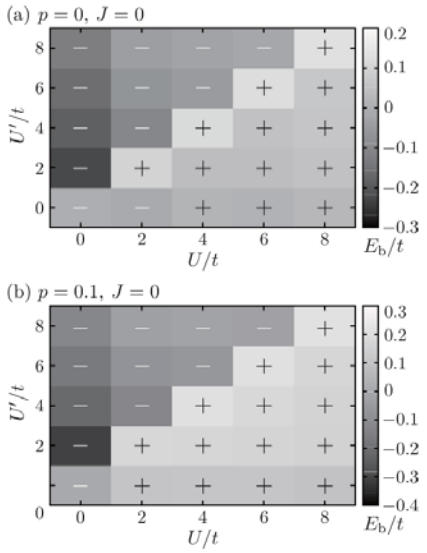


Fig. 2: Contour plots of $E_b$ with $J$=0 in (a) $p$=0 (half-filling) and (b) $p$=0.1 (2-hole doped) cases. The horizontal and the vertical axes indicate the intra-band repulsion $U$ and the inter-band repulsion $U'$, respectively. Signs of $E_b$ is depicted inside the plots.

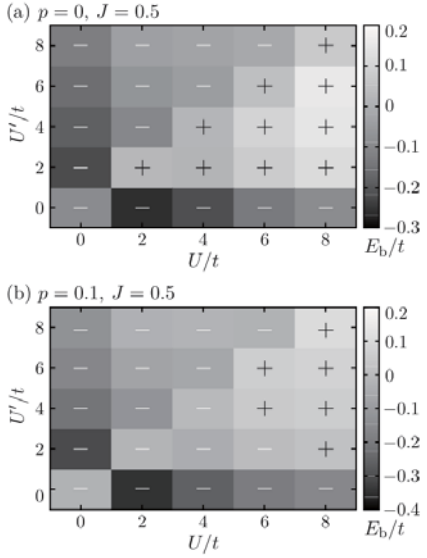


Fig. 3: Contour plots of $E_b$ with $J$=0.5 in (a) $p$=0 (half-filling) and (b) $p$=0.1 (2-hole doped) cases. The horizontal and the vertical axes indicate the intra-band repulsion $U$ and the inter-band repulsion $U'$, respectively. Signs of $E_b$ is depicted inside the plots.

**References**

[1] M. Okumura, N. Nakai, H. Nakamura, N. Hayashi, S. Yamada and M. Machida, Physica C: Superconductivity 469, 932 (2009)

## 1.3.3 Large-Scale Simulations for the Fundamental Understanding of Superconductivity

### (10) Magnetic Localization in the Spin-Polarized One-Dimensional Anderson-Hubbard Model

Masahiko Okumura, Susumu Yamada, Nobuhiko Taniguchi [1)] and Masahiko Machida

1) Institute of Physics, University of Tsukuba

We study an interplay of hat obtained in the single band Hubbard model by using the density-matrix renormalization-group method. We find that the antiferromagnetic spin-density wave is localized by disorders the increase in the disorder magnitude shrinks the areas of the localized antiferromagnetized regions (Fig.1,2). In addition, the antiferromagnetism disappears when the amplitude of the disorder exceed a critical value (Fig.1). These localization behaviors can be observed in atomic Fermi gases loaded on optical lattices as broadening of the momentum distribution of the spin density by using the Stern-Gerlach type of time-of-flight imaging (Fig.3) [1].

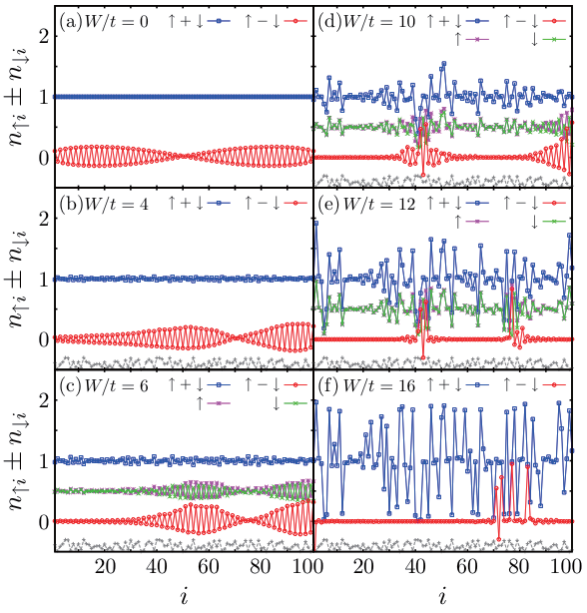


Fig. 1: The randomness magnitude $W$ depen- dence of the matter and spin-density profiles ($n_{\uparrow i}\pm n_{\downarrow i}$), respectively at the half filling for $U/t$=10 with ($N_\uparrow$,$N_\downarrow$) = (51,49). A profile of the selected random potential is depicted on the bottom of each figure in an arbitrary unit gray dashed line. In (c)-(e), up- and down-spin-density profiles are shown.

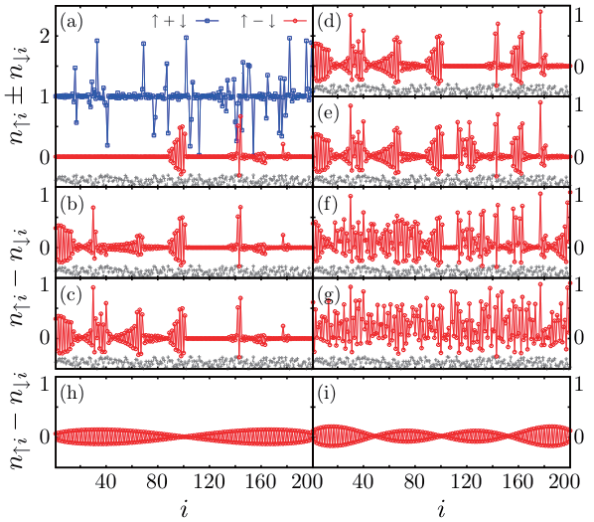


Fig. 2: The polarization dependence of the spin- density profiles (a)-(g) with $U/t$=$W/t$=20 and that without random potential (h) and (i) at $U/t$=20. The last two figures, (h) and (i), without the randomness are displayed for a comparison with disordered cases (a) and (b), respectively. The number of up- and down-spin particles ($N_\uparrow$,$N_\downarrow$) are (a) (101,99), (b) (102,98), (c) (103,97), (d) (104,96), (e) (105,95), (f) (110,90), (g) (120,80), (h) (101,99), and (i) (102,98), respectively.

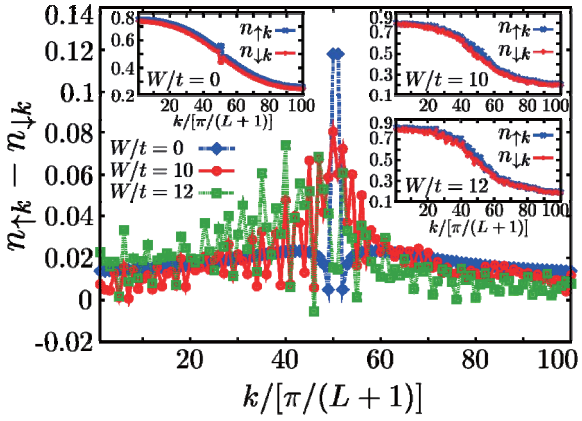


Fig. 3: The quasimomentum distributions of spin density ($n_{\uparrow k}$-$n_{\downarrow k}$) for Fig. 1(a) ($W/t$=0), Fig. 1(d) ($W/t$=10), and Fig. 1(e) ($W/t$=12). The insets show quasimomentum distributions for different spins $n_{\uparrow k}$ and $n_{\downarrow k}$, respectively in each case.

**References**

[1] M. Okumura, S. Yamada, N. Tanigushi, and M. Machida, Phys. Rev. B 79, 184417 (2009)

This is a blank page.

# 1.4 Computational Quantum Bioinformatics

This is a blank page.

## 1.4.1 Large-Scale Simulations for Molecular Biology

### (1) A Method for the Analysis of Domain Movements in Large Biomolecular Complexes

Guru Prasad Poornam [1], Atsushi Matsumoto, Hisashi Ishida and Steven Hayward [1]
1) School of Computing Sciences and School of Biological Sciences, University of East Anglia

It is now well-known that the conformational change of a biomolecule is often effential to its function. This is certainly true for allosteric mechanism where the binding of a ligand at one site affects binding affinities at distant sites. It is also true for domain enzymes where the binding of a substrate causes domain closure, isolating the substrate from the solvent. The mechanisms of some very large biomolecular complexes are beginning to be understood and for these, in particular, it is apparent that conformational change and function are intimately linked.

We have developed a new method for the analysis of conformational change in large, multichain, biomolecular complexes. The method is applicable to any molecule for which two atomic structures are available that represent a conformational change. The method is blind to atomic bonding and atom type and can, therefore, be applied to biomolecular complexes containing different constituent molecules such as protein, RNA or DNA [1].

At the heart of the method is the use of blocks located at grid points spanning the whole molecule. The rotation vector for the rotation of atoms from each block between the two conformations is calculated. Treating components of these vectors as coordinates means that each block is associated with a point in a "rotation space" and that blocks with atoms that rotate together, perhaps as part of the same rigid domain, will have colocated points. Thus a domain can be identified from the clustering of points from blocks that span it. Domain pairs are accepted for analysis of their relative movements in terms of screw axes based upon a set of reasonable criteria.

Here, we report on the application of the method to biomolecules covering a considerable size range: hemoglobin, liver alcohol dehydrogenase, S-Adenosylhomocysteine hydrolase, aspartate transcarbamylase, and the 70S ribosome. The results provide a depiction of the conformational change within each molecule that is easily understood, giving a perspective that is expected to lead to new insights.

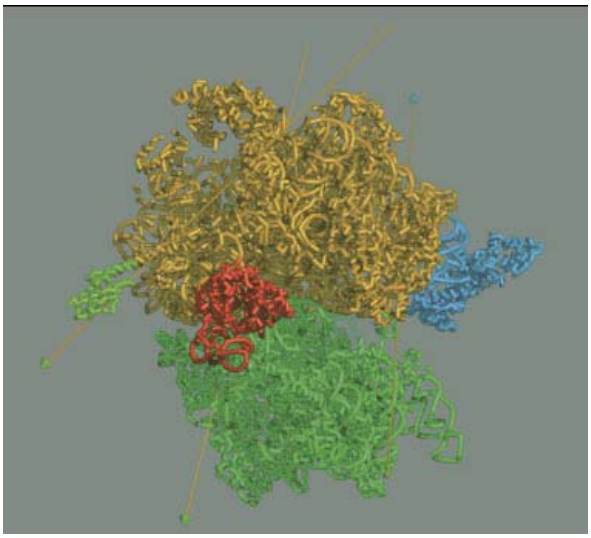

Fig. 1[1]: 70S Ribosome: DynDom3D analysis of 7th normal mode from elastic network model of ribosome [2]. It yielded six domains (only five are visible). The interdomain screw axis for the movement of the two large domains which comprise the 30S (green) and 50S (yellow) subunits suggests the possibility of a ratchet like movement [3]. The sticking out orange, cyan and green regions are the L1 stalk, L7/L12 stalk, and L9 protein, respectively.

**References**

[1] G. P. Poornam, A. Matsumoto, H. Ishida and S. Hayward, Proteins, Vol. 76, No.1, 201-212 (2009)
[2] A. Matsumoto and H. Ishida, Structure, Vol.17, No.12, 1605–1613 (2009)
[3] J. Frank and RK. Agrawal, Nature, Vol. 406, No.6793, 318-322 (2000)

## 1.4.1 Large-Scale Simulations for Molecular Biology

### (2) Global Conformational Changes of Ribosome Observed by Normal Mode Fitting for 3D Cryo-EM Structures

Atsushi Matsumoto and Hisashi Ishida

Ribosome is a huge macromolecular complex responsible for protein synthesis in all organisms. To understand the molecular mechanism of the protein synthesis, it is important to reveal the three-dimensional (3D) structures of ribosome in the functional states. Recent progress in electron microscopy (EM) has made it possible to capture 3D structures of ribosome at various functional states. As of Sep 2008, 44 data for the 3D-EM structures of the 70S ribosome were available in Electron Microscopy DataBank (EMDB) at the European Bioinformatics Institute (EBI). To analyze a 3D-EM structure, an atomic model, which fits into the EM structure well, is often built. However, because of its size, it is not so easy to build the atomic models for the EM structures of ribosome [1].

We have developed a new flexible-fitting approach to build an atomic model from a 3D-EM structure (Fig. 1). In this approach, a huge number of atomic models with different conformations are prepared by deforming the X-ray crystal structure. In this study, more than 1.5 million atomic models of ribosome with different conformations were prepared. Then, the best-fitting atomic model is selected from them for each EM structure by rigid-body fitting calculation.

In the usual flexible-fitting approach, which we call the “tailor-made” approach, the X-ray crystal structure is deformed for each EM structure so that it fits better. However, the computation for deforming a structure is very time-consuming, especially for large supra-molecule like ribosome. In our “ready-made” approach, on the other hand, once the deformed atomic models are prepared, only the rigid-body fitting calculation is necessary which require much less computational time. Thus, our approach is appropriate for analyzing many EM structures of the same target, because it can save computational time. At the same time, comparison of the best-fitting atomic models is straightforward (Fig. 2).

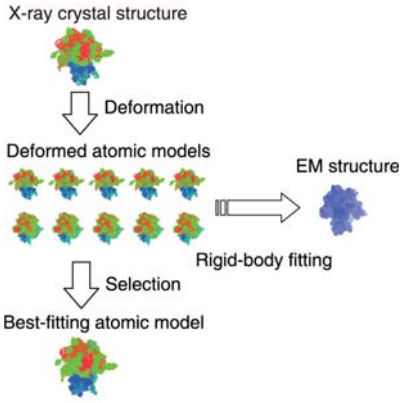


Fig.1: An overview of our ready-made flexible-fitting approach to build atomic models from EM structures. The molecular images were generated with a program VMD [2].

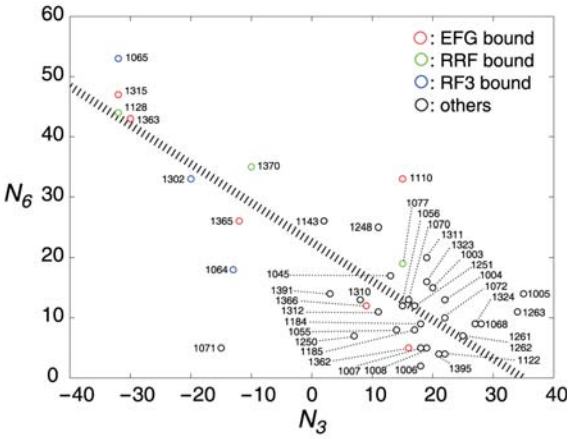


Fig. 2[1]: The distribution of the best-fitting atomic models. The structure of our atomic model is specified by the combination of integers $N_k$, which indicates the deviation from the X-ray crystal structure along the $k$th lowest frequency normal mode. The black dotted line is drawn in such a way that the sum of squared distances from the line to the points for all structures is smallest. The projection on the $N_3$-$N_6$ plane is shown. The IDs for the EM structures in the EMDB are shown for all structures.

**References**

[1] A. Matsumoto and H. Ishida, Structure, Vol.17, No.12, 1605–1613 (2009)

[2] W. Humphrey *et al.*, Journal of Molecular Graphics Vol. 14, No. 1, 33-38 (1996)

# 2. Publications & Presentations

List of Paper

## 1.1 Computer Science in Nuclear Engineering


1) Guehee Kim, Yoshio Suzuki, Naoya Teshima, Akemi Nishida, Tomonori Yamada, Fumimasa Araya, Hiroshi Takemiya, Norihiro Nakajima and Makoto Kondo, “A Script Generator API for the Full-Scale Three-Dimensional Vibration Simulation of an Entire Nuclear Power Plant within AEGIS”, Proceedings of 1st International Conference on Parallel, Distributed and Grid Computing for Engineering (PARENG) (Pécs, Hungary, 2009.4.6-8) (CD-ROM) (2009)
2) Guehee Kim, Yoshio Suzuki and Naoya Teshima, “Network Computing Infrastructure to Share Tools and Data in GNEP”, Proceedings of 17th International Conference on Nuclear Engineering (ICONE-17) (CD-ROM) (2009)
3) Kimiaki Saito, Naoya Teshima, Yoshio Suzuki, Norihiro Nakajima, Hidetoshi Saito, Etsuo Kunieda and Tatsuya Fujisaki, “Gridization of IMAGINE, Dose Calculation System, for the Remote Assistance of Radiation Therapy”, FUJITSU Family Association FY2008 (2008) (Japanese)
4) Kohei Nakajima, Yoshio Suzuki, Naoya Teshima, Shin-ichiro Sugimoto, Shinobu Yoshimura and Norihiro Nakajima, “Method to Unconsciously Use Grid Middleware; Proposal of Seamless API and Its Application to Mechanics System”, FY2008 Collected Papers of NEC C&C Systems Users Association (CD-ROM), p. 13 (2008) (Japanese)
5) Chiaki Kino, Yoshio Suzuki, Hiroko Nakamura Miyamura, Hiroshi Takemiya and Norihiro Nakajima, “Design of Scientific Concept Vocabulary for Cognitive Methodology Based on Data Analysis System”, Transaction of JSCES (Internet), Vol. 2009, No. 22, p. 12 (2009) (Japanese)
6) Hiroko Nakamura Miyamura, Yuji Shinano, Ryuhei Miyashiro and Takafumi Saito, “Visualization of Runtime Behavior of Branch-and-Bound Algorithms”, IPSJ; TOM, Vol. 12, No. 12, pp. 103-112 (2009) (Japanese)


## 1.2 Computational Mechanics


7) Tomonori Yamada and Toshio Nagashima, "An Integration Scheme of Boundary Elements for Meshfree Finite Element Analysis with Structured Grid", Transaction of JSCES (Internet), Vol. 2009, No. 6, p. 7 (2009) (Japanese)
8) Tomonori Yamada, Masao Ogino and Shinobu Yoshimura, ”Prediction and Numerical Validation of Optimal Number of Subdomains on Balancing Domain Decomposition Method", Transaction of JSCES (Internet), Vol. 2009, No. 14 p. 7 (2009) (Japanese)
9) Tomonori Yamada, “Parallel Distributed Seismic Analysis of an Assembled Nuclear Power Plant”, Parallel, Distributed and Grid Computing for Engineering, pp. 439-454 (2009)
10) Noriyuki Kushida, “High Speed Eigenvalue Solver on the Cell Cluster System for Controlling Nuclear Fusion Plasma”, Proceedings of 18th Euromicro International Conference on Parallel, Distributed and Network-Based Computing (PDP 2010) (Pisa, Italy, 2010.2.17-19), pp. 482-488 (2010)
11) Akemi Nishida, “Wave Propagation Analysis of Piping Structures”, Proceedings of 17th International Conference on Nuclear Engineering (ICONE-17) (CD-ROM), p. 7(2009)
12) Akemi Nishida, "Development of Physical Model Describing the Dynamic Interaction Characteristics of Component Connections for the Analysis of an Entire Nuclear Facility", Third Innovative Nuclear Research and Development Program (CD-ROM), p. 2 (2008) (Japanese)
13) Akemi Nishida, Fumimasa Araya, Tomonori Yamada, Noriyuki Kushida, Hiroshi Takemiya and Norihiro Nakajima, "Development and Application Research of Vibration Simulator for Full-Scale Nuclear Power Station”, Nuclear Safety Research Forum 2009, pp. 25-29 (2009) (Japanese)

1.3 Computational Materials Science


14) Ashwin Ramasubramaniam, Mitsuhiro Itakura and Emily Carter, "Interatomic Potentials for Hydrogen in Alpha-Iron Based on Density Functional Theory", Physical Review B, Vol. 79, No. 17, pp. 174101_1-174101_13 (2009)

15) Jordi Ribas-Arino, Motoyuki Shiga and Dominik Marx, "Understanding Covalent Mechanochemistry", Angewante Chemie International Edition, Vol. 48, No. 23, pp. 4190-4193 (2009)

16) Anna Kaczmarek, Motoyuki Shiga and Dominik Marx, "Quantum Effects on Vibrational and Electronic Spectra of Hydrazine Studied by "On-The-Fly" Ab Initio Ring Polymer Molecular Dynamics", Journal of Physical Chemistry A, Vol. 113, No. 10, pp. 1985-1994 (2009)

17) Akira Kakizaki, Haruki Motegi, Takehiro Yoshikawa, Toshiyuki Takayanagi, Motoyuki Shiga and Masanori Tachikawa, "Path-Integral Molecular Dynamics Simulations of Small Hydrated Sulfuric Acid Clusters $H_2SO_4(H_2O)_n$ (n=1-6) on Semiempirical PM6 Potential Surfaces", Journal of Molecular Structure (THEOCHEM), Vol. 901, No. 1-3, pp. 1-8 (2009)

18) Toshiyuki Takayanagi, Kenta Takahashi, Akira Kakizaki, Motoyuki Shiga and Masanori Tachikawa, "Path-Integral Molecular Dynamics Simulations of Hydrated Hydrogen Chloride Cluster $HCl(H_2O)_4$ on a Semiempirical Potential Energy Surface", Chemical Physics, Vol. 358, No. 3, pp. 196-202 (2009)

19) Alexander Witt, Sergei Ivanov, Motoyuki Shiga, Harald Forbert and Dominik Marx, "On the Applicability of Centroid and Ring Polymer Path Integral Molecular Dynamics for Vibrational Spectroscopy", Journal of Chemical Physics, Vol. 130, No. 19, pp. 194510_1-194510_15 (2009)

20) Akira Nakayama, Tetsuya Taketsugu and Motoyuki Shiga, "Speed-Up of Ab Initio Hybrid Monte Carlo and Ab Initio Path Integral Hybrid Monte Carlo Simulations by Using an Auxiliary Potential Energy Surface", Chemistry Letters, Vol. 38, No. 10, pp. 976-977 (2009)

21) Jordi Ribas, Motoyuki Shiga and Dominik Marx, "Unravelling the Mechanism of Force-Induced Ring-Opening of Benzocyclobutenes", Chemistry; A European Journal, Vol. 15, No. 48, pp. 13331-13335 (2009)

22) Toshiyuki Takayanagi, Takehiro Yoshikawa, Haruki Motegi and Motoyuki Shiga, "Path-Integral Molecular Dynamics Simulations for Water Anion Clusters $(H_2O)_5^-$ and $(D_2O)_5^-$", Chemical Physics Letters, Vol. 482, No. 4-6, pp. 195-200（2009）

23) Takehiro Yoshikawa, Haruki Motegi, Akira Kakizaki, Toshiyuki Takayanagi and Motoyuki Shiga, "Path-Integral Molecular Dynamics Simulations of Glycine-$(H_2O)_n$ (n=1-7) Clusters on Semi-Empirical PM6 Potential Energy Surfaces", Chemical Physics, Vol. 365, No. 1-2, pp. 60-68 (2009)

24) Kenichi Ebihara, Masatake Yamaguchi, Hideo Kaburaki and Yutaka Nishiyama, "Rate Theory Modeling of Irradiation-Induced Phosphorus Segregation in FCC Nickel Using First Principles Calculations", Materials Research Society Symposium Proceedings, Vol. 1125, pp. 133-138 (2009)

25) Kenichi Ebihara, Masatake Yamaguchi, Yutaka Nishiyama, Kunio Onizawa and Hiroshi Matsuzawa, "Numerical Simulation of Irradiation-Induced Grain-Boundary Phosphorous Segregation in Reactor Pressure Vessel Steels Using Rate Theory Model with First-Principles Calculations", Proceedings of 2009 ASME Pressure Vessels and Piping Division Conference (PVP 2009) (CD-ROM), PVP2009-77624, 8pages (2009)

26) Kenichi Ebihara, Hideo Kaburaki, Tomoaki Suzudo and Kenichi Takai, "A Numerical Study on the Validity of the Local Equilibrium Hypothesis in Modeling Hydrogen Thermal Desorption Spectra", ISIJ International, Vol. 49, No. 12, pp. 1907-1913 (2009)

27) Susumu Yamada, Toshiyuki Imamura and Masahiko Machida, "Communication Strategy of Parallel Density-Matrix Renormalization Group Method with Considering Architecture of Multi-Core Cluster," Transaction of JSCES (Internet), Vol. 2009, No. 15, pp. 12 (2009) (Japanese)

28) Susumu Yamada, Masahiko Okumura and Masahiko Machida, "Direct Extension of Density-Matrix Renormalization Group to Two-Dimensional Quantum Lattice Systems; Studies of Parallel Algorithm, Accuracy and Performance", Journal of the Physical Society of Japan, Vol. 78, No. 9, pp. 094004_1-094004_5 (2009)

29) Takao Morinari, Hiroki Nakamura, Masahiko Machida and Takami Tohyama, "Effect of Fermi Surface Topology on Inter-Layer Magnetoresistance in Layered Multiband Systems; Application to $LaFeAsO_{1-x}F_x$", Journal of the Physical Society of Japan, Vol. 78, No. 11, pp. 114702_1-114702_7 (2009)

30) Hiroki Nakamura and Masahiko Machida, "First-Principles Calculations of the Effect of Pressure on the Iron-Based Superconductor LaFeAsO", Physical Review B, Vol. 80, No. 16, pp. 165111_1-165111_5 (2009)
31) Hiroki Nakamura and Masahiko Machida, "Highly Two-Dimensional Electronic Structure and Strong Fermi-Surface Nesting of the Iron-Based Superconductor $Sr_2ScFePO_3$; A First-Principles Study", Journal of the Physical Society of Japan, Vol. 79, No. 1, pp. 013705_1-013705_4 (2010)
32) Hiroki Nakamura, Masahiko Machida, Tomio Koyama and Noriaki Hamada, "First-Principles Study for the Anisotropy of Iron-Based Superconductors toward Power and Device Applications", Journal of the Physical Society of Japan, Vol. 78, No. 12, pp. 123712_1-123712_4 (2009)
33) Hiroki Nakamura, Nobuhiko Hayashi, Noriyuki Nakai; Masahiko Okumura and Masahiko Machida, "First-Principle Electronic Structure Calculations for Magnetic Moment in Iron-Based Superconductors; An LSDA + Negative U Study", Physica C, Vol. 469, No. 15-20, pp. 908-911 (2009)
34) Hiroki Nakamura, Nobuhiko Hayashi, Noriyuki Nakai and Masahiko Machida, "First-Principle Calculation for the Phonon Structure on Iron-Based Superconductors", Physica C, Vol. 469, No. 15-20, pp. 1024-1026 (2009)
35) Noriyuki Nakai, Nobuhiko Hayashi and Masahiko Machida, "Simulation Study for the Orientation of the Driven Vortex Lattice in an Amorphous Superconductor", Physica C, Vol. 469, No. 15-20, PP. 1106-1109 (2009)
36) Noriyuki Nakai, Nobuhiko Hayashi and Masahiko Machida, "Ginzburg-Landau Simulation for a Vortex around a Columnar Defect in a Superconducting Film", Journal of Physics and Chemistry of Solids, Vol. 69, No. 12, pp. 3301-3303 (2008)
37) Noriyuki Nakai, Nobuhiko Hayashi and Masahiko Machida, "Simulation Studies for the Vortex Depinning Dynamics around a Columnar Defect in Superconductors", Physica C, Vol. 468, No. 15-20, PP. 1270-1273 (2008)
38) Yukihiro Ota, Masahiko Machida and Tomio Koyama, "Intergrain Josephson Currents in Multigap Superconductors; Microscopic Origin of Low Intergrain Critical Current and its Recovery Potential in Iron-Pnictide Materials", Journal of the Physical Society of Japan, Vol. 78, No. 10, pp. 103701_1-103701_4 (2009)
39) Yukihiro Ota, Masahiko Machida, Tomio Koyama and Hideki Matsumoto, "Theory of Vortex Structure in Josephson Junctions with Multiple Tunneling Channels: Vortex Enlargement as a Probe for ±s-wave Superconductors", Physical Review B, Vol. 81, No. 1, pp. 014502_1-014502_5 (2010)
40) Natsuko Ishida, Yukihiro Ota and Yoshihisa Yamamoto, "Generation and Application of Multi-Path Cat States of Light", New Journal of Physics (Internet), Vol. 11, pp. 033007_1-033007_15 (2009)
41) Yukihiro Ota, Masahiko Machida, Tomio Koyama and Hideki Matsumoto, "Theory of Heterotic Superconductor-Insulator-Superconductor Josephson Junctions between Single- and Multiple-Gap Superconductors", Physical Review Letters, Vol. 102, No. 23, pp. 237003_1-237003_4 (2009)
42) Masahiko Okumura, Susumu Yamada, Masahiko Machida and Toru Sakai, "Polarization Plateau in an Atomic Fermi Gas Loaded on a Three-Leg Triangular Optical Lattice", Physical Review A, Vol. 79, No. 6, pp. 061602_1-061602_4 (2009)
43) Masahiko Okumura, Noriyuki Nakai, Hiroki Nakamura, Nobuhiko Hayashi, Susumu Yamada and Masahiko Machida, "Exact Diagonalization Studies on Two-Band Minimal Model for Iron-Based Superconductors", Physica C, Vol. 469, No. 15-20, pp. 932-935 (2009)
44) Masahiko Okumura, Susumu Yamada, Nobuhiko Taniguchi and Masahiko Machida, "Magnetic Localization in the Spin-Polarized One-Dimensional Anderson-Hubbard Model", Physical Review B, Vol. 79, No. 18, pp. 184417_1-184417_5 (2009)

1.4 Computational Quantum Bioinformatics

45) Guru Prasad Poornam, Atsushi Matsumoto, Hisashi Ishida and Steven Hayward, "A Method for the Analysis of Domain Movements in Large Biomolecular Complexes", Proteins: Structure, Function, and Genetics, Vol. 76, No. 1, pp. 201-212 (2009)
46) Atsushi Matsumoto and Hisashi Ishida, "Global Conformational Changes of Ribosome Observed by Normal Mode Fitting for 3D Cryo-EM Structures", Structure, Vol. 17, No. 12, pp. 1605-1613 (2009)

List of Oral Presentation

1.1 Computer Science in Nuclear Engineering

1) Guehee Kim, Yoshio Suzuki, Akemi Nishida and Hiroshi Takemiya, "Development of APIs for Desktop Supercomputing", 9th Teraflop Workshop (Sendai, Japan, 2008.11.12-13）(2008)
2) Yoshio Suzuki, Sachiko Hayashi and Hiroko Nakamura Miyamura, "Cerebral Methodology Based Computing for Estimating Validity of Simulation Results", Proceedings of Computational Engineering Conference JSCES, Vol. 14 (Tokyo, Japan, 2009.5.13）(2009) (Japanese)
3) Hiroko Nakamura Miyamura, Yoshio Suzuki and Hiroshi Takemiya, "Spatio-Temporal Map for Time-Series Date Visualization," Proceedings of Computational Engineering Conference JSCES, Vol. 14, No. 1, pp. 157-160. (Tokyo, Japan, 2009.5.12）(2009) (Japanese)
4) Chiaki Kino, Yoshio Suzuki and Hiroshi Takemiya, "Semantic Information Processing of Physical Simulation Based on Scientific Concept Model", Proceegins of Electoronics, Information Systems Conference IEEJ (Tokushima, Japan, 2009.9.3-4）(2009) (Japanese)
5) Takayuki Tatekawa, Kohei Nakajima, Guehee Kim, Naoya Teshima, Yoshio Suzuki and Hiroshi Takemiya, "Development of Simple Orchestration Application Framework and its Application to Burning Plasma Simulation", 11th Teraflop Workshop (Tohoku Univ., Japan, 2009.10.19-20）(2009)
6) Guehee Kim, Kohei Nakajima, Takayuki Tatekawa, Naoya Teshima, Yoshio Suzuki and Hiroshi Takemiya, "3D Virtual Plant Vibration Simulator on Simple Orchestration Application Framework", 11th Teraflop Workshop (Sendai, Japan, 2009.10.19-20) (2009)
7) Hiroko Nakamura Miyamura, Yoshio Suzuki and Hiroshi Takemiya, "Visualization System for the Evaluation of Numerical Simulation Results", Mini-Symposium in SC09 (Portland, USA, 2009.11.14-20）(2009)
8) Takayuki Tatekawa, Kohei Nakajima, Guehee Kim, Naoya Teshima, Yoshio Suzuki and Hiroshi Takemiya, "Simple Orchestration Application Framework on AEGIS", Mini-Symposium in SC09 (Portland, USA, 2009.11.14-20）(2009)
9) Yoshio Suzuki, "Interoperation between Grid Infrastructures "AEGIS" and "DIET" for an International Sparse Linear Algebra Expert System", Mini-Symposium in SC09 (Portland, USA, 2009.11.14-20）(2009)
10) Hiroshi Takemiya, "Supercomputers in Japan Atomic Energy Agency", Mini-Symposium in SC09 (Portland, USA, 2009.11.14-20）(2009)
11) Takayuki Tatekawa, Kohei Nakajima, Guehee Kim, Naoya Teshima, Yoshio Suzuki and Hiroshi Takemiya, "Development of Simple Orchestration Application Framework and its Application to Burning Plasma Simulation", 2010 Annual Meeting of Atomic Energy Society of Japan (Ibaraki Univ., Japan, 2010.3.26-28）(2010) (Japanese)
12) Guehee Kim, Kohei Nakajima, Takayuki Tatekawa, Naoya Teshima, Yoshio Suzuki and Hiroshi Takemiya, "3D Virtual Plant Vibration Simulation on Simple Orchestration Application Framework", 2010 Spring Annual Meeting of Atomic Energy Society of Japan (Mito, Japan, 2010.3.26-28）(2010) (Japanese)
13) Yoshio Suzuki, "Current Status of ITBL Infrastructure Software and ITBL Communities", H21 ITBL Symposium (Yokohama, Japan, 2009.5.29）(2009) (Japanese)
14) Hiroko Nakamura Miyamura, Satoshi Ohzahata, Akihiro Nakao, Konosuke Kawashima and Yoshio Suzuki, "A Network Visualization System Focusing on Important Nodes", IEICE Technical Report; Network Systems, pp. 357-362 (Miyazaki, Japan, 2010.3.5）(2009) (Japanese)
15) Hiroko Nakamura Miyamura, Satoshi Ohzahata, Akihiro Nakao, Konosuke Kawashima and Yoshio Suzuki, "A Large Scale Network Visualization for Important Nodes Discovery", EICE Technical Report; Network Systems, pp. 85-90 (Sendai, Japan, 2009.9.11）(2009) (Japanese)
16) Chiaki Kino, Yoshio Suzuki and Hiroshi Takemiya, "Design of Scientific Concept Vocabulary for Annotation Method of Visualization System", Proceedings of Asia Simulation Conference 2009 (JSST 2009) (CD-ROM) (Shiga, Japan, 2009.10.7-9)(2009)

17) Hiroko Nakamura Miyamura, Satoshi Ohzahata, Akihiro Nakao, Konosuke Kawashima and Yoshio Suzuki, “A Network Visualization System with Interactive Operations for Important Nodes Discovery”, The Papers of Technical Meeting on Industrial Instrumentation and Control, IEE Japan IIC-10-079, 080,082-087, pp. 27-32 (Koganei, Japan, 2010.3.8）(2010)
18) Hiroko Nakamura Miyamura, Masatoshi Kureta, Mariko Segawa, Jun Kubo, Takafumi Saito, Yoshio Suzuki and Hiroshi Takemiya, “Visualization for Atomizing Liquid by Using Multi Scale Decomposition”, The Papers of Technical Meeting on Industrial Instrumentation and Control, IEE Japan IIC-10-071,073-078, pp. 7-12 (Koganei, Japan, 2010.3.8）(2010)

1.2 Computational Mechanics

19) Tomonori Yamada and Fumimasa Araya, "Construction of Computing Framework for Vibration Simulation of Nulcear Power Plant in Its Entirety”, Proceedings of 2009 Fall Meeting of the Atomic Energy Society of Japan (Sendai, Japan, 2009.9.16）(2009) (Japanese)
20) Tomonori Yamada and Toshio Nagashima, "A Simple and Efficient Hybrid Numerical Quadrature Scheme for Structured Extended FEM”, 10th US National Congress on Computational Mechanics (USNCCM-10) (Columbus, USA, 2009.7.17）(2009)
21) Michiya Sakai, Akemi Nishida, Fumimasa Araya and Noriyuki Kushida, “Seismic Evaluation of Support Stracture for Components and Piping Systems”, 2009 Fall Meeting of AESJ (Sendai, Japan, 2009.9.16-18）(2009) (Japanese)
22) Akemi Nishida, Fumimasa Araya, Noriyuki Kushida, Makoto Kondo, Michiya Sakai and Yuzo Shiogama, “Development of a Simple Elastic-Plastic Connection Model Describing the Dynamic Interaction Characteristics of Component Connections”, 2009 Fall Meeting of AESJ (Sendai, Japan, 2009.9.16-18）(2009) (Japanese)
23) Akemi Nishida, Tomonori Yamada, Noriyuki Kushida, Fumimasa Araya, Hiroshi Takemiya and Norihiro Nakajima, “Vibration Simulation for Component and Piping Structures of Nuclear Plants”, PD09 (Osaka, Japan, 2009.2.12）(2009) (Japanese)
24) Akemi Nishida, “Vibration Simulation for Piping Structures of a Nuclear Plant”, Workshop about the Building Structure Analysis in Near Future (GA09) (Yokohama, Japan, 2009.5.28）(2009) (Japanese)
25) Michiya Sakai, Akemi Nishida, Fumimasa Araya and Noriyuki Kushida, “Hybrid Seismic Testing of Support Structure for Components and Piping Systems”, 2008 Fall Meeting of AESJ (Kochi, Japan, 2008.9.4-6）(2008) (Japanese)
26) Akemi Nishida, Yoshio Suzuki, Sachiko Hayashi, Ken Hasegawa, Takahiro Kunitomo, Mineo Kumazawa and Yoko Hasada, “Damping Measurement Method by Using Acoustic Frequency Comb”, Symposium on Response Control and Damping on Shell and Spatial Structures; Current Status and the Future (Tokyo, Japan, 2009.12.9) (2009) (Japanese)
27) Noriyuki Kushida, "Eigenvalue Solution on the Heterogeneous Multi-Core (Cell Processor) for International Thermo-Nuclear Experimental Reactor (ITER) Monitoring System”, Mini-Symposium in SC '09 (Portland, USA, 2009.11.14-20）(2009)
28) Tomonori Yamada, "Preliminary Study on a Matrix-Coupling Framework for Huge Assembled Structures", Proceedings of the Conference on Computational Engineering and Science, Vol. 14, No. 1, pp. 247-248 (Tokyo, Japan, 2009.5.13）(2009) (Japanese)
29) Akemi Nishida, Yoshio Suzuki, Sachiko Hayashi, Mineo Kumazawa, Takahiro Kunitomo and Yoko Hasada, "Frequency Comb Spectroscopy for Reliable Evaluation of Vibration Characteristics of Nuclear Facilities by Means of ACROSS Part 1: Basic Line of Approach for System Identification and Health Monitoring”, Proceedings of the 58th National Congress of Theoretical and Applied Mechanics (Tokyo, Japan, 2010.6.10）(2009)
30) Akemi Nishida, Yoshio Suzuki, Sachiko Hayashi, Mineo Kumazawa, Takahiro Kunitomo and Yoko Hasada, "Frequency Comb Spectroscopy for Reliable Evaluation of Vibration Characteristics of Nuclear Facilities by Means of ACROSS Part 2: Accurate Measurements and Monitoring”, Proceedings of the 58th National Congress of Theoretical and Applied Mechanics (Tokyo, Japan, 2010.6.10）(2009)

31) Akemi Nishida, Yoshio Suzuki, Sachiko Hayashi, Mineo Kumazawa, Takahiro Kunitomo and Yoko Hasada, "Frequency Comb Spectroscopy for Reliable Evaluation of Vibration Characteristics of Nuclear Facilities by Means of ACROSS Part 3: Data Processing Method to Estimate the Vibration Characteristics in Multi-Scales by Means of SOMPI Method", Proceedings of the 58th National Congress of Theoretical and Applied Mechanics (Tokyo, Japan, 2010.6.10）(2009)
32) Noriyuki Kushida, Hiroshi Takemiya and Shinji Tokuda, "Eigenvalue Solution on the Heterogeneous Multicore Cluster for Nuclear Fusion Reator Monitoring" Proceedings of International Conference for Highperformance Computing, Networking, Storage and Analysis (SC09) (Portland, USA, 2009.11.14-20）(2009)
33) Tadashi Watanabe, "Accurate Measurement of Surface Tension Using a Levitated Liquid Droplet", Proceedings of 6th International Conference on Electromagnetic Processing of Materials (EPM 2009), pp. 403-406 (Dresden, Germany, 2009.10.19-23) (2009)

1.3 Computational Materials Science

34) Yukihiro Ota, Masahiko Machida, Tomio Koyama and Hideki Matsumoto, "Theory of Josephson Junctions between Single- and Two-Gap Superconductors; Identification of ±s-wave Symmetry via Basic Josephson Effects", International Workshop on the Search for New Superconductors; Frontier and Future（Hayama, Japan, 2009.5.12-16）(2009)
35) Hiroki Nakamura, Masahiko Machida, Baron Alfred, Tatsuo Fukuda and Shinichi Shamoto, "Crystalline and Magnetic Structures of Iron-Based Superconductors; A First-Principle Study", International Workshop on the Search for New Superconductors; Frontier and Future (Hayama, Japan, 2009.5.12-16) (2009)
36) Motoyuki Shiga, "Ab Initio Path Integral Hybrid Monte Carlo Method", 12nd Theoretical Chemistry Symposium (Sapporo, Japan, 2009.5.23-25）(2009) (Japanese)
37) Motoyuki Shiga, "Basic of Path Integral Molecular Dynamic", RIKEN Seminar (Wako, Japan, 2009.4.27）(2009) (Japanese)
38) Motoyuki Shiga, "Ab Initio Path Integral Simulations; Nuclear Quantum Effect", 13th International Congress of Quantum Chemistry (ICQC-13) (Helsinki, Finland, 2009.6.22-27）(2009)
39) Ryo Igarashi and Masao Ogata, "Partial Order of Frustrated Potts Model", International Conference on Magnetism 2009 (ICM 2009) (Karlsruhe, Germany, 2009.7.26-31）(2009)
40) Motoyuki Shiga, "Ab Initio Path Integral Simulations; Nuclear Quantum Effect", 7th International Conference of Computational Methods in Sciences and Engineering 2009 (ICCMSE 2009) (Rhodes, Greece, 2009.9.29-10.4）(2009)
41) Yukihiro Ota, Masahiko Machida, Tomio Koyama and Hideo Aoki, "Leggett's Modes in Multi-Band Superconductors", New Developments in Theory of Superconductivity（NDTS09）(Kashiwa, Japan, 2009.7.8-10) (2009)
42) Yukihiro Ota, Masahiko Machida, Tomio Koyama and Hideki Matsumoto, "Heterotic Josephson Junctions between Single- and Two-Gap Superconductors; Identification of ±s-wave in Iron-Based Superconductors", The 2nd Symposium on Transformative Research Project on Iron Pnictides (TRIP) (Tokyo, Japan, 2009.7.10-11) (2009) (Japanese)
43) Susumu Yamada, Masahiko Okumura and Masahiko Machida, "Parallelization of Dynamical DMRG for N-Leg Hubbard Model", Supercomputing in Solid State Physics 2009 (Kashiwa, Japan, 2009.2.18）(2009)
44) Susumu Yamada, Masahiko Okumura and Masahiko Machida, "Parallelization of Dynamical DMRG Method for 2-Dimensional Model", Recent Progress in Density Matrix Renormalization Group (DMRG) (Kyoto, Japan, 2008.12.17）(2008) (Japanese)
45) Susumu Yamada, Masahiko Okumura and Masahiko Machida, "Analysis of Single-Particle Excitation Spectrum of Fermions in Two-dimensional Optical Lattice Using Dynamical DMRG Method", The Physical Society of Japan 64th Annual Meeting (Tokyo, Japan, 2009.3.28）(2009) (Japanese)

46) Hiroki Nakamura, Masahiko Machida, Alfred Baron, Tatsuo Fukuda and Shin-ichi Shamoto, "Crystalline and Electronic Structures of Iron-Based Superconductors; A First-Principle Study", New Developments in Theory of Superconductivity (Kashiwa, Japan, 2009.7.8-10) (2009)

47) Susumu Yamada, Toshiyuki Imamura, Masahiko Okumura and Masahiko Machida, "Parallelization of Density Matrix Renormalization Group Method Using Communication Strategy for Multicore Cluster", Summer United Workshops on Parallel, Distributed and Cooperative Processing (Sendai, Japan, 2009.8.6) (2009)

48) Masahiko Okumura, Hiroaki Onishi, Susumu Yamada and Masahiko Machida, "Non-equilibrium Dynamics of Spin-Imbalanced Fermions in Optical Lattice", New Developments in Theory of Superconductivity (Kashiwa, Japan, 2009.7.8-10) (2009)

49) Yukihiro Ota, Masahiko Machida, Tomio Koyama and Hideki Matsumoto, "Peculiar Josephson Vortex Structure for ±s-wave in Josephson Junctions with Multiple Tunneling Channels", New Directions of Superconducting Nanostructures 2009 (NDSN 2009) (Nagoya, Japan, 2009.9.4-5) (2009)

50) Noriyuki Nakai, Yukihiro Ota, Nobuhiko Hayashi and Masahiko Machida, "Direct Numerical Simulations for the Time-Dependent Ginzburg-Landau Equation in the Vortex-Flow Stage of a Two-Gap Superconductor", Nanoscience and Engineering in Superconductivity (Tsukuba, Japan, 2009.3.23-26）(2009)

51) Noriyuki Nakai, Hiroki Nakamura, Yuki Nagai, Yukihiro Ota, Nobuhiko Hayashi and Masahiko Machida, "Temperature Dependence of Specific Heat and Nuclear Magnetic Relaxation Rate for Multi-Gap Superconductors", New Developments in Theory of Superconductivity（Kashiwa, Japan, 2009.7.8-10）(2009)

52) Masahiko Machida and Yukihiro Ota, "Theory of Josephson Vortices and Collective Modes in Multi-Bands Superconductors", 12th International Workshop on Vortex Matter in Superconductors (Lake Yamanaka, Japan, 2009.9.12-16) (2009)

53) Ryo Igarashi, Susumu Yamada, Masahiko Machida and Masao Ogata, "Analysis of "One-Dimensionalization" in Heisenberg Model", The Physical Society of Japan 2009 Autumn Meeting (Kumamoto, Japan, 2009.9.25-28) (2009) (Japanese)

54) Yukihiro Ota, Masahiko Machida, Tomio Koyama and Hideki Matsumoto, "Vortex Solutions in Josephson Junctions with Multiple Tunneling Channels", The Physical Society of Japan 2009 Autumn Meeting (Kumamoto, Japan, 2009.9.25-28) (2009) (Japanese)

55) Yukihiro Ota, Masahiko Machida and Tomio Koyama, "Microscopic Analysis of Inter-Grain Josephson Currents in Polycrystalline Iron-Pnicide Superconductors" The Physical Society of Japan 2009 Autumn Meeting (Kumamoto, Japan, 2009.9.25-28) (2009) (Japanese)

56) Hiroki Nakamura and Masahiko Machida, "Anisotropies in Iron-Based Superconductors: A First-Principles Study", The Physical Society of Japan 2009 Autumn Meeting (Kumamoto, Japan, 2009.9.25-28) (2009) (Japanese)

57) Noriyuki Nakai, Hiroki Nakamura, Michiyasu Miyashita, Yuki Nagai, Yukihiro Ota, Nobuhiko Hayashi and Masahiko Machida, "Temperature Dependence of Specific Heat and Nuclear Magnetic Relaxation Rate for Multi-Gap Superconductors", The Physical Society of Japan 2009 Autumn Meeting (Kumamoto, Japan, 2009.9.25-28) (2009) (Japanese)

58) Noriyuki Nakai and Masahiko Machida, "Simulation Study on the Vortex-Penetration with the Square Pinning Array", The Physical Society of Japan 2009 Autumn Meeting (Kumamoto, Japan, 2009.9.25-28) (2009) (Japanese)

59) Masahiko Okumura, "Non-Equilibrium Dynamics of Fermi Gases Loaded on Optical Lattices in Metallic, Insulating, and Superfluid Phases", The Physical Society of Japan 2009 Autumn Meeting (Kumamoto, Japan, 2009.9.25-28) (2009) (Japanese)

60) Susumu Yamada, Masahiko Okumura and Masahiko Machida, "Development of Massively Parallel Dynamical DMRG Method: Direct Extension to Ladder System and Acceleration", The Physical Society of Japan 2009 Autumn Meeting (Kumamoto, Japan, 2009.9.25-28) (2009) (Japanese)

61) Masahiko Okumura, Hiroaki Onishi, Susumu Yamada and Masahiko Machida, "Center of Mass Motion of an Attractive Interacting Fermi Gas in an Optical Lattice", The Physical Society of Japan 2009 Autumn Meeting (Kumamoto, Japan, 2009.9.25-28) (2009) (Japanese)

62) Yukihiro Ota, Masamitu Bando, Yasushi Kondo and Mikio Nakahara, “Holonomic Quantum Computing in a Dimer-Chain Model via Ising-Type Interaction”, 2nd International Workshop on Dynamics and Manipulation of Quantum Systems 2009 (Tokyo, Japan, 2009.10.13-16）(2009)
63) Yukihiro Ota and Yasushi Kondo, “Composite Pulses in NMR as Non-Adiabatic Geometric Quantum Gates: Classification of Fluctuations from Robustness of Geometric Phases”, The 21th Quantum Information Technology Symposium (QIT21) (Tokyo, Japan, 2009.11.4-5）(2009) (Japanese)
64) Mitsuhiro Itakura, Hideo Kaburaki, Masatake Yamaguchi and Kenichi Ebihara, “Multiscale Simulation of Hydrogen Segregation and Decohesion”, Materials Research Society 2009 Fall Meeting (Boston, USA, 2009.12.4) (2009)
65) Susumu Yamada, Toshiyuki Imamura, Masahiko Okumura, Ryo Igarashi and Masahiko Machida, “Next-Generation Quantum Many-Body Simulation Project toward Petaflops Computing; Density Matrix Renormalization Group Method on Massively Parallel Computer”, Mini-Symposium in SC '09 (Portland, USA, 2009.11.17-19）(2009)
66) Yukihiro Ota, Noriyuki Nakai, Hiroki Nakamura, Masahiko Machida, Daisuke Inotani, Yoji Ohashi, Tomio Koyama and Hideki Matsumoto, “Shapiro Steps in Heterotic SIS Multi-Tunneling-Channel Josephson Junctions: Identification of ±s-wave in Iron-Pnictide Superconductors”, RIEC Workshop on Superconducting Computing Devices (Sendai, Japan, 2009.11.26-27) (2009) (Japanese)
67) Yukihiro Ota, Masahiko Machida, Noriyuki Nakai, Hiroki Nakamura, Tomio Koyama and Hideki Matsumoto, “Theory of Josephson Effects in Heterotic S-I-S Junctions with Iron-Pnictide Superconductors”, The 3rd Symposium on Transformative Research Project on Iron Pnictides (TRIP) (Tokyo, Japan, 2009.12.12-13) (2009)
68) Noriyuki Nakai, Yukihiro Ota, Nobuhiko Hayashi and Masahiko Machida, “TDGL Simulation of Flux-Flow Voltage in Two-Band Models”, 17th Workshop on Vortex Physics (Osaka, Japan, 2009.12.1-3) (2009) (Japanese)
69) Noriyuki Nakai, Hiroki Nakamura, Yukihiro Ota, Yuki Nagai, Nobuhiko Hayashi and Masahiko Machida, “Superconducting State of Iron Pnictides by a Phenomenological Approach”, Transformative Research-Project on Iron Pnictides 3rd Meeting (Tokyo, Japan, 2009.12-13) (2009) (Japanese)
70) Yukihiro Ota, Masahiko Machida, Tomio Koyama and Hideo Aoki, “Collective Excitation Modes in Multi-Band Superconductors”, The 17th Workshop on Vortex Physics (VPWJ2009) (Osaka, Japan, 2009.12.1-3) (2009) (Japanese)
71) Hideo Kaburaki, Masatake Yamaguchi, Mitsuhiro Itakura, Kenichi Ebihara, Tomoko Kadoyoshi and Tomoaki Suzudo, “Computational Science Research on the Atomistic Crack Initiation in the Grain Boundary Due to Hydrogen”, The 1st Symposium of Fundamental Studies on Technologies for Steel Materials with Enhanced Strength and Functions（Tokyo, Japan, 2009.4.14) (2009) (Japanese)
72) Tomoko Kadoyoshi, Hideo Kaburaki, Mitsuhiro Itakura and Masatake Yamaguchi, “Hydrogen Embrittlement of a Grain Boundary in Alpha-Iron; A Molecular Dynamics Study”, 14th International Conference on Fusion Reactor Materials (ICFRM-14) (Sapporo, Japan, 2009.9.7-12) (2009)
73) Hideo Kaburaki, Tomoko Kadoyoshi, Mitsuhiro Itakura and Masatake Yamaguchi, “Molecular Dynamics Simulation on the Grain Boundary Embrittlement of Iron Crystal”, 19th MRS-Japan Academic Symposium (Yokohama, Japan, 2009.12.7-9) (2009)
74) Tomoko Kadoyoshi, Hideo Kaburaki, Mitsuhiro Itakura and Masatake Yamaguchi, “A Molecular Dynamics Study on Hydrogen Embrittlement of a Grain Boundary in Alpha-Iron”, Materials Research Society 2009 Fall Meeting (Boston, USA, 2009.11.30-12.04) (2009)
75) Masatake Yamaguchi, Kenichi Ebihara, Yutaka Nishiyama, Kunio Onizawa and Hiroshi Matsuzawa, “First-Principles Calculations of the Elemental Processes of Irradiation-Induced Phosphorous Segregation at Grain Boundary”, 2009 Research Meeting at the Research Institute for Applied Mechanics of Kyushu University, “Clarification of the Basic Process of Material Irradiation Effects; It Aims at the Improvement of Light-Water Nuclear Reactor Aging Technology” (Fukuoka, Japan, 2009.7.9) (2009) (Japanese)
76) Kenichi Ebihara, Masatake Yamaguchi, Yutaka Nishiyama, Kunio Onizawa and Hiroshi Matsuzawa, “Numerical Simulation of Irradiation-Induced Grain-Boundary Phosphorous Segregation in Reactor Pressure Vessel Steels Using Rate Theory Model with First-Principles Calculations”, 2009 Research Meeting at the Research Institute for Applied Mechanics of Kyushu University, "Clarification of the Basic Process of Material Irradiation Effects; It Aims at the Improvement of Light-Water Nuclear Reactor Aging Technology" (Fukuoka, Japan, 2009.7.9) (Japanese)

77) Tomoaki Suzudo, Hideo Kaburaki and Mitsuhiro Itakura, “Computational Study of Recovery Process in UO2/CeO2”, 5th International Workshop of New Crossover Project (Tokyo, Japan, 2009.2.2）(2009)
78) Tomoaki Suzudo, “Mesoscopic Computational Science and its Application to Microstructural Evolution of Nuclear Materials”, AESJ 2009 Summer Seminar for Fuels, Materials and Water Chemistry of Light-Water Reactor (Matsue, Japan, 2009.7.3) (Japanese)
79) Masatake Yamaguchi, “First-Principles Study on the Decohesion of Iron (Fe) Grain Boundary by Solute (B, C, P, S) Segregation”, International Symposium on Stress Corrosion Cracking in Stractural Materials at Ambient Temperatures (Padova, Italy, 2009.8.31-9.4) (2009)
80) Masatake Yamaguchi, Kenichi Ebihara, Mitsuhiro Itakura, Tomoaki Suzudo, Hideo Kaburaki and Tomoko Kadoyoshi, “First-Principles Study on the Decohesion of Grain Boundaries in Metals by Hydrogen Trapping”, International Symposium on Stress Corrosion Cracking in Stractural Materials at Ambient Temperatures (Padova, Italy, 2009.8.31-9.4) (2009)
81) Masatake Yamaguchi, Kenichi Ebihara, Mitsuhiro Itakura, Tomoaki Suzudo, Hideo Kaburaki and Tomoko Kadoyoshi, “First-Principles Calculations of Grain Boundary Cohesive Energy: Hydrogen Embrittlement of Iron”, The Japan Institute of Metals (JIM) 2009 Autumn Meeting (Kyoto, Japan, 2009.9.16) (2009) (Japanese)
82) Masatake Yamaguchi, Kenichi Ebihara, Yutaka Nishiyama, Kunio Onizawa and Hiroshi Matsuzawa, “First-Principles Calculations of the Formation and Migration Energies of Defect-Phosphorous Complexes in Bcc Fe and Fcc Ni”, 15th Meeting of the International Group on Radiation Damage Mechanisms in Pressure Vessel Steels (IGRDM-15) (Budapest, Hungary, 2009.10.12-16) (2009)
83) Masatake Yamaguchi, “First-Principles Study of the Grain Boundary Embrittlement of Metals”, The 140th Meeting of the Japan Society for Research on Superplasticity（Tsukuba, Japan, 2010.1.19）(2010) (Japanese)
84) Masatake Yamaguchi, Yutaka Udagawa, Hiroaki Abe and Naoto Seikimura, “Study on Hydrogenation and Radiation Effects in Zr-Nb Alloys(4) Modelling: First-Principles Calculations for the Energies of Lattice Defects in Zr”, 2010 Annual Meeting of Atomic Energy Society of Japan (AESJ) (Mito, Japan, 2010.3.28) (2010) (Japanese)
85) Tomoaki Suzudo, Masatake Yamaguchi and Hideo Kaburaki, “Computer Simulation of Helium Segregation Using Ab Initio and Kinetic Monte Carlo Calculations”, The Japan Institute of Metals (JIM) 2010 Spring Meeting (Tsukuba, Japan, 2010.3.30) (2010) (Japanese)
86) Susumu Yamada, Toshiyuki Imamura, Masahiko Okumura, Ryo Igarashi and Masahiko Machida, “Parallel Solver for Large Eigenvalue Problems on Density Matrix Renormalization Group Method”, RIMS Workshop “Recent Developments of Numerical Analysis and Numerical Computation Algorithms” (Kyoto, Japan, 2009.12.14）(2009) (Japanese)
87) Ryo Igarashi, Masahiko Okumura, Susumu Yamada and Masahiko Machida, “Spin Ladder System as an Application of the Parallelized DMRG”, Supercomputer Joint Use Activity Report 2009 (ISSP Workshop) (Kashiwa, Japan, 2009.12.10-11) (2009) (Japanese)
88) Noriyuki Nakai, Hiroki Nakamura, Yukihiro Ota, Yuki Nagai, Nobuhiko Hayashi and Masahiko Machida, “Temperature Dependence of the Superfluid Density for Iron Pnictide Superconductors”, The Physical Society of Japan 65th Annual Meeting (Okayama, Japan, 2010.3.20-23) (2010) (Japanese)
89) Noriyuki Nakai, Masahiko Machida and Nobuhiko Hayashi, “Vortex-Dynamics Simulation by Using Ginzburg-Landau Theory”, The Physical Society of Japan 65th Annual Meeting (Okayama, Japan, 2010.3.20-23) (2010) (Japanese)
90) Yukihiro Ota, Noriyuki Nakai, Hiroki Nakamura, Masahiko Machida, Daisuke Inotani, Youji Ohashi, Tomio Koyama and Hideki Matsumoto, “Theory of Ac Josephson Effects in Multiple Tunneling Junctions; A Probe of ±s-wave in Iron-Based Superconductors”, American Physical Society 2010 March Meeting (Portland, USA, 2010.3.15-19) (2010)
91) Yukihiro Ota, Masahiko Machida, Tomio Koyama and Hideo Aoki, “Leggett's Collective Modes in Multi-Band Superconductors; Multiple Dynamical Classes”, American Physical Society 2010 March Meeting (Portland, USA, 2010.3.15-19) (2010)

92) Yukihiro Ota, Masahiko Machida, Tomio Koyama and Hideo Aoki, “Leggett's Modes in Multi-Band Superconductivity”, The Physical Society of Japan 65th Annual Meeting (Okayama, Japan, 2009.3.20-23) (2009) (Japanese)
93) Susumu Yamada, Toshiyuki Imamura, Masahiko Okumura, Ryo Igarashi and Masahiko Machida, “Parallelization Strategy for Density Matrix Renormalization Group toward Peta-Flops Parallel Computer”, Supercomputer Workshop 2010 (Okazaki, Japan, 2010.1.13) (2010) (Japanese)
94) Masahiko Okumura, Susumu Yamada, Masahiko Machida and Hideo Aoki, “DMRG Study for Ultracold Fermionic Atoms Loaded on an Optical Ladder - Spin Polarization Structure”, The Physical Society of Japan 65th Annual Meeting (Okayama, Japan, 2009.3.20-23) (2009) (Japanese)
95) Susumu Yamada, Masahiko Okumura, Ryo Igarashi and Masahiko Machida, “High Performance Algorithm of Dynamical DMRG Method for Quasi-Two-Dimensional Hubbard Mode”, The Physical Society of Japan 65th Annual Meeting（Okayama, Japan, 2009.3.20-23) (2009) (Japanese)
96) Mitiyasu Miyashita, Katsuhiko Higuchi and Masahiko Higuchi, “An Alternative Scheme for Calculating the Unrestricted Hartree-Fock Equation”, The Physical Society of Japan 65th Annual Meeting (Okayama, Japan, 2010.3.20-23) (2010) (Japanese)
97) Motoyuki Shiga, “Ab Initio Path Integral Simulations”, 69th Okazaki Conference on "New Frontier in Quantum Chemical Dynamics" (Okazaki, Japan, 2009.2.21-23) (2009)
98) Ryo Igarashi, Masahiko Okumura, Susumu Yamada and Masahiko Machida, “Evaluation of the Energy Gap of the Various Spin-Tube Systems Using Parallelized DMRG”, Ministry of Education, Culture, Sports, Science and Technology (MEXT) the “Advanced, High-Performance General-Purpose Supercomputer Development” Project Next-Generation Integrated Nanoscience Simulation Software Research and Development 4th Open Symposium (Okazaki, Japan, 2010.3.3-4) (2010) (Japanese)
99) Ryo Igarashi, Masahiko Okumura, Susumu Yamada and Masahiko Machida, “Systematic Research of Energy Gap in the Spin Tube Systems”, The Physical Society of Japan 65th Annual Meeting (Okayama, Japan, 2010.3.20-23) (2010) (Japanese)
100) Ryo Igarashi, Masahiko Okumura, Susumu Yamada and Masahiko Machida, “Ground State Phase Diagram of the Asymmetric Spin Tube up to 6 Legs”, American Physical Society 2010 March Meeting (Portland, USA, 2010.3.15-19) (2010)
101) Ryo Igarashi, Masahiko Okumura, Susumu Yamada and Masahiko Machida, “Evaluation of Spin Gap Using Parallelized DMRG”, Next-Generation Integrated Nanoscience Simulation Software Research and Development Condensed Matter Area Conference “New Materials and Energy” (Tokyo, Japan, 2010.3.10-11) (2010) (Japanese)
102) Masahiko Machida, “Computational Approach to Structural and Fuel Materials”, 2009 Fall Meeting of the Atomic Energy Society of Japan (Sendai, Japan, 2009.9.16-18) (2009) (Japanese)
103) Masahiko Machida and Narimasa Sasa, “Bottleneck Effects of Energy Cascade in Quantum Turbulence”, The Physical Society of Japan 65th Annual Meeting (Okayama, Japan, 2010.3.20-23) (2010) (Japanese)
104) Hiroki Nakamura and Masahiko Machida, “Anisotropies in Iron-Based Superconductors: A First-Principles Study”, The Physical Society of Japan 65th Annual Meeting (Okayama, Japan, 2009.3.20-23) (2009) (Japanese)
105) Hiroki Nakamura and Masahiko Machida, “Electronic Structure of Iron-Based Superconductors with Thick Perovskite-Blocking Layers”, American Physical Society 2010 March Meeting (Portland, USA, 2010.3.15-19）(2010)
106) Masahiko Machida and Narimasa Sasa, “Massively-Parallel Simulations for Quantum Turbulence: Current Status and Problems”, VPWJ2009 (Osaka, Japan, 2009.12.1-3) (2009) (Japanese)
107) Masahiko Okumura, Hiroaki Onishi, Susumu Yamada and Masahiko Machida, “Breakdown and Relaxation of Mott Phase in Optical Lattice System”, Photoinduced Phenomena in Correlated Electron System (Kyoto, Japan, 2009.12.10-11) (2009) (Japanese)
108) Yukihiro Ota, Masahiko Machida, Tomio Koyama and Hideki Matsumoto, “Propagation and Reflection Properties of External Electromagnetic Waves in Josephson Junctions”, 1st JST-DFG Workshop on Terahertz Superconductor Electronics (Tsukuba, Japan, 2010.2.21-24) (2010)

109) Masahiko Okumura, Hiroaki Onishi, Susumu Yamada and Masahiko Machida, “Time Dependent DMRG Study of Relaxation Processes of Fermi Atoms Loaded in an Optical Lattice”, Thermal Quantum Field Theory and their Applications (Kyoto, Japan, 2009.9.3) (2009)
110) Masatake Yamaguchi, Kenichi Ebihara, Mitsuhiro Itakura, Tomoaki Suzudo, Hideo Kaburaki and Tomoko Kadoyoshi, “First-Principles Study on the Decohesion of Grain Boundary by Hydrogen Trapping in Aluminum and Other Metals”, Proceedings of PFAM18 (Sendai, Japan, 2009.12.12-14) (2009)
111) Masatake Yamaguchi, Atsushi Matsumoto and Masahiko Machida, “Introduction of the Numerical Simulation Group in Center for Computational Science and E-Systems (CCSE)”, Japan Journal of Industrial and Applied Mathematics (JJIAM) (2010)
112) Masahiko Machida, Mitiyasu Miyashita and Hiroki Nakamura, “First-Principle Calculation Studies for Electronic and Magnetic Structures of Iron-Based Superconductors”, The Physical Society of Japan 2009 Autumn Meeting (Kumamoto, Japan, 2009.9.25-28) (2009)

1.4 Computational Quantum Bioinformatics

113) Atsushi Matsumoto, "Structural Analysis of Bound Molecules to Ribosome by Em-Fitting”, Biophysical Society 54th Annual Meeting (San Francisco, USA, 2010.2.20-24）(2010)
114) Hisashi Ishida, "Analysis of Dynamic Properties of DNA Repair Protein MutS and DNA Complexes Using Molecular Dynamics Simulations”, Biophysical Society 54th Annual Meeting (San Francisco, USA, 2010.2.20-24）(2010)

# 3. Awards

1) Winning essays, FY2009 Collected Papers of NEC C&C Systems Users Association (November 2009), Hiroko Nakamura Miyamura, Kohei Nakajima, Yoshio Suzuki and Hiroshi Takemiya, "Data Exploration System for the Evaluation of Numerical Simulation Results" (Japanese)

2) Incentive Award, FUJITSU Family Association FY2009 (January 2010, Award Ceremony in May 2010), Hiroko Nakamura Miyamura, Sachiko Hayashi, Yoshio Suzukii and Hiroshi Takemiya, "Overview Visualization of Time-Series Dataset" (Japanese)

3) Young Investigator Award, Computational Science and Engineering Division of the Japan Atomic Energy Society (March 2010), Tomonori Yamada

## 4. External Funds

1) "Research and Development of International Matrix Solver Prediction System on French-Japan International GRID Computing Environment" (REDIMPS) (JST), 4,500K Yen (FY2006-FY2009)

2) "Simulation for Predicting Quake-Proof Capability of Nuclear Power Plants", Core Research for Evolutional Science and Technology (JST), 40,430K Yen (FY2007-FY2012)

3) "Development of Real Time Monitoring System of ITER" (MEXT: Grant-in-Aid for Young Scientists (B)), 3,380K Yen (FY2009)

4) "High-Dimensional Data Pocket: Analysis and Visualize Technique of Large-Scale Time-Series Volume Datasets" (MEXT：Grant-in-Aid for Young Scientists (B)), 3,250K Yen (FY2009)

5) "Quasi-Equilibrium Evolution in Self-Gravitating and Long-Range Interacting Systems" (MEXT: Grant-in-Aid for Young Scientists (B)), 3,900K Yen (FY2009)

6) A Study on File Distribution Control in P2P Network over a Large Scale Distributed System (JSPS : Grant-in-Aid for Scientific Research (B)), 390K Yen (FY2009)

7) "Construction of Simulation Research Foundation for Micro, Meso and Macro Scales, and Research for Multiscale and Multiphysics Simulation Scheme in Superconductivity Funadamentals and Application", CREST(JST), 55,692K Yen (FY2009).

8) "The Prediction of the Irradiation-Induced Embrittlement of Reactor Pressure Vessel Steels in High-Irradiation Region" (JNES), 1,110K Yen (FY2009)

9) "Fundamental Studies on Technologies for Steel Materials with Enhanced Strength and Functions" (JRCM), 24,898K Yen (FY 2009)

10) "Large-Scale Simulation Studies for Quantum Turbulence II" (MEXT), 1,000K Yen (FY2009)

11) "Research and Development of Parallel Simulation Method for Quantum Many-Body Problem" (JSPS: Grant-in-Aid for Scientific Rearch (C)), 1,820K Yen (FY2009)

12) "Studies for Bifurcation Structure and Transition Dynamics in Mathematical Modeling on Superconductivity and BEC Phenomena" (JSPS: Grant-in-Aid for Scientific Rearch (B)), 130K Yen (FY2009)

13) "Neutron Imaging by Nano-Fabricated Superconducting-Detector Array" (JSPS: Grant-in-Aid for Scientific Research (A)), 104K Yen (FY2009)

14) "A Microscopic Perspective of Supra-Functional Biological Molecules with Quantum and Thermal Fluctuations" (Grant-in-Aid for Scientific Research on Priory Areas), 800K (FY2009)

15) "Nuclear Quantum Effects on the Solvation Stuctures Studied by Hybrid QM/MM Path Integral Simualtion" (Grant-in-Aid for Young Scientists B), 200K Yen (FY2009)

# 5. Staff List of CCSE (R&D Office) in FY2009

| | |
|---|---|
| Director: | Toshio Hirayama |
| Deputy Director: | Norihiro Nakajima |
| Deputy Director: | Masayuki Tani |

- Computer Science Research and Development Office

| | |
|---|---|
| General Manager: | Hiroshi Takemiya |
| Deputy General Manager: | Tetsuo Aoyagi |

- R&D Team for Computer Science

| | |
|---|---|
| Team Leader (Principal Researcher): | Yoshio Suzuki |
| Senior Post-Doctoral Fellow: | Hiroko Nakamura Miyamura |
| Collaborating Engineer: | Sachiko Hayashi |
| | Kohei Nakajima (until August 2009) |
| | Naoya Teshima |
| Post-Doctoral Fellow: | Chiaki Kino |
| | Guehee Kim |
| | Takayuki Tatekawa |
| | Ken Uzawa (from January 2010) |

- R&D Team for Full-Scale Simulation Technology

| | |
|---|---|
| Team Leader (Assistant Principal Researcher): | Akemi Nishida |
| Assistant Principal Researcher: | Fumimasa Araya (until September 2009) |
| Research Engineer: | Noriyuki Kushida |
| Senior Post-Doctoral Fellow: | Tomonori Yamada |
| | Ken Uzawa (from January 2010) |

- Concurrent Post

Tadashi Watanabe
Toshiharu Muramatsu
Yasuhiro Idomura
Fumimasa Araya (from October 2009)

- Simulation Technology Research and Development Office

| | |
|---|---|
| General Manager: | Masahiko Machida |
| Deputy Director: | Hideo Kaburaki |
| Invited Researcher: | Kei Yura |

- Material Simulator Team

| | |
|---|---|
| Team Leader (Principal Researcher): | Masahiko Machida |
| Assistant Principal Researcher: | Susumu Yamada |
| Research Engineer: | Narimasa Sasa |
| Senior Post-Doctoral Fellow: | Hiroki Nakamura |
| Post-Doctoral Fellow: | Mitiyasu Miyashita |
| Assistant Principal Researcher: | Tomoaki Suzudo |
| Assistant Principal Researcher: | Kenichi Ebihara |

| | |
|---|---|
| Principal Researcher: | Masatake Yamaguchi |
| Assistant Principal Researcher: | Motoyuki Shiga |
| Assistant Principal Researcher: | Mitsuhiro Itakura |
| Special Topic Researcher: | Tomoko Kadoyoshi |

- CREST Special-Topic Research Team

| | |
|---|---|
| Special Topic Researcher: | Ryo Igarashi |
| Special Topic Researcher: | Masahiko Okumura |
| Special Topic Researcher: | Noriyuki Nakai |
| Special Topic Researcher: | Yukihiro Ohta |

- Quantum Bioinformatics Team

| | |
|---|---|
| Team Leader (Assistant Principal Researcher): | Atsushi Matsumoto |

- Concurrent Post

Hideo Kaburaki
Hidetoshi Kono
Hisashi Ishida

# 国際単位系（SI）

表１．SI 基本単位

| 基本量 | SI 基本単位 | |
|---|---|---|
| | 名称 | 記号 |
| 長さ | メートル | m |
| 質量 | キログラム | kg |
| 時間 | 秒 | s |
| 電流 | アンペア | A |
| 熱力学温度 | ケルビン | K |
| 物質量 | モル | mol |
| 光度 | カンデラ | cd |

表２．基本単位を用いて表されるSI組立単位の例

| 組立量 | SI 基本単位 | |
|---|---|---|
| | 名称 | 記号 |
| 面積 | 平方メートル | $m^2$ |
| 体積 | 立法メートル | $m^3$ |
| 速さ，速度 | メートル毎秒 | m/s |
| 加速度 | メートル毎秒毎秒 | $m/s^2$ |
| 波数 | 毎メートル | $m^{-1}$ |
| 密度，質量密度 | キログラム毎立方メートル | $kg/m^3$ |
| 面積密度 | キログラム毎平方メートル | $kg/m^2$ |
| 比体積 | 立方メートル毎キログラム | $m^3/kg$ |
| 電流密度 | アンペア毎平方メートル | $A/m^2$ |
| 磁界の強さ | アンペア毎メートル | A/m |
| 量濃度(a)，濃度 | モル毎立方メートル | $mol/m^3$ |
| 質量濃度 | キログラム毎立法メートル | $kg/m^3$ |
| 輝度 | カンデラ毎平方メートル | $cd/m^2$ |
| 屈折率(b) | （数字の） 1 | 1 |
| 比透磁率(b) | （数字の） 1 | 1 |

(a) 量濃度（amount concentration）は臨床化学の分野では物質濃度（substance concentration）ともよばれる。
(b) これらは無次元量あるいは次元１をもつ量であるが、そのことを表す単位記号である数字の１は通常は表記しない。

表３．固有の名称と記号で表されるSI組立単位

| 組立量 | SI 組立単位 | | | |
|---|---|---|---|---|
| | 名称 | 記号 | 他のSI単位による表し方 | SI基本単位による表し方 |
| 平面角 | ラジアン(b) | rad | 1 (b) | m/m |
| 立体角 | ステラジアン(b) | sr(c) | 1 (b) | $m^2/m^2$ |
| 周波数 | ヘルツ(d) | Hz | | $s^{-1}$ |
| 力 | ニュートン | N | | m kg $s^{-2}$ |
| 圧力，応力 | パスカル | Pa | $N/m^2$ | $m^{-1}$ kg $s^{-2}$ |
| エネルギー，仕事，熱量 | ジュール | J | N m | $m^2$ kg $s^{-2}$ |
| 仕事率，工率，放射束 | ワット | W | J/s | $m^2$ kg $s^{-3}$ |
| 電荷，電気量 | クーロン | C | | s A |
| 電位差（電圧），起電力 | ボルト | V | W/A | $m^2$ kg $s^{-3}$ $A^{-1}$ |
| 静電容量 | ファラド | F | C/V | $m^{-2}$ $kg^{-1}$ $s^4$ $A^2$ |
| 電気抵抗 | オーム | Ω | V/A | $m^2$ kg $s^{-3}$ $A^{-2}$ |
| コンダクタンス | ジーメンス | S | A/V | $m^{-2}$ $kg^{-1}$ $s^3$ $A^2$ |
| 磁束 | ウエーバ | Wb | Vs | $m^2$ kg $s^{-2}$ $A^{-1}$ |
| 磁束密度 | テスラ | T | $Wb/m^2$ | kg $s^{-2}$ $A^{-1}$ |
| インダクタンス | ヘンリー | H | Wb/A | $m^2$ kg $s^{-2}$ $A^{-2}$ |
| セルシウス温度 | セルシウス度(e) | ℃ | | K |
| 光束 | ルーメン | lm | cd sr(c) | cd |
| 照度 | ルクス | lx | $lm/m^2$ | $m^{-2}$ cd |
| 放射性核種の放射能(f) | ベクレル(d) | Bq | | $s^{-1}$ |
| 吸収線量, 比エネルギー分与, カーマ | グレイ | Gy | J/kg | $m^2$ $s^{-2}$ |
| 線量当量, 周辺線量当量, 方向性線量当量, 個人線量当量 | シーベルト(g) | Sv | J/kg | $m^2$ $s^{-2}$ |
| 酸素活性 | カタール | kat | | $s^{-1}$ mol |

(a)SI接頭語は固有の名称と記号を持つ組立単位と組み合わせても使用できる。しかし接頭語を付した単位はもはやコヒーレントではない。
(b)ラジアンとステラジアンは数字の１に対する単位の特別な名称で、量についての情報をつたえるために使われる。実際には、使用する時には記号radおよびsrが用いられるが、習慣として組立単位としての記号である数字の１は明示されない。
(c)測光学ではステラジアンという名称と記号srを単位の表し方の中に、そのまま維持している。
(d)ヘルツは周期現象についてのみ、ベクレルは放射性核種の統計的過程についてのみ使用される。
(e)セルシウス度はケルビンの特別な名称で、セルシウス温度を表すために使用される。セルシウス度とケルビンの単位の大きさは同一である。したがって、温度差や温度間隔を表す数値はどちらの単位で表しても同じである。
(f)放射性核種の放射能（activity referred to a radionuclide）は、しばしば誤った用語で"radioactivity"と記される。
(g)単位シーベルト（PV,2002,70,205）についてはCIPM勧告2（CI-2002）を参照。

表４．単位の中に固有の名称と記号を含むSI組立単位の例

| 組立量 | SI 組立単位 | | |
|---|---|---|---|
| | 名称 | 記号 | SI 基本単位による表し方 |
| 粘度 | パスカル秒 | Pa s | $m^{-1}$ kg $s^{-1}$ |
| 力のモーメント | ニュートンメートル | N m | $m^2$ kg $s^{-2}$ |
| 表面張力 | ニュートン毎メートル | N/m | kg $s^{-2}$ |
| 角速度 | ラジアン毎秒 | rad/s | m $m^{-1}$ $s^{-1}$=$s^{-1}$ |
| 角加速度 | ラジアン毎秒毎秒 | $rad/s^2$ | m $m^{-1}$ $s^{-2}$=$s^{-2}$ |
| 熱流密度，放射照度 | ワット毎平方メートル | $W/m^2$ | kg $s^{-3}$ |
| 熱容量，エントロピー | ジュール毎ケルビン | J/K | $m^2$ kg $s^{-2}$ $K^{-1}$ |
| 比熱容量，比エントロピー | ジュール毎キログラム毎ケルビン | J/(kg K) | $m^2$ $s^{-2}$ $K^{-1}$ |
| 比エネルギー | ジュール毎キログラム | J/kg | $m^2$ $s^{-2}$ |
| 熱伝導率 | ワット毎メートル毎ケルビン | W/(m K) | m kg $s^{-3}$ $K^{-1}$ |
| 体積エネルギー | ジュール毎立方メートル | $J/m^3$ | $m^{-1}$ kg $s^{-2}$ |
| 電界の強さ | ボルト毎メートル | V/m | m kg $s^{-3}$ $A^{-1}$ |
| 電荷密度 | クーロン毎立方メートル | $C/m^3$ | $m^{-3}$ sA |
| 表面電荷 | クーロン毎平方メートル | $C/m^2$ | $m^{-2}$ sA |
| 電束密度，電気変位 | クーロン毎平方メートル | $C/m^2$ | $m^{-2}$ sA |
| 誘電率 | ファラド毎メートル | F/m | $m^{-3}$ $kg^{-1}$ $s^4$ $A^2$ |
| 透磁率 | ヘンリー毎メートル | H/m | m kg $s^{-2}$ $A^{-2}$ |
| モルエネルギー | ジュール毎モル | J/mol | $m^2$ kg $s^{-2}$ $mol^{-1}$ |
| モルエントロピー, モル熱容量 | ジュール毎モル毎ケルビン | J/(mol K) | $m^2$ kg $s^{-2}$ $K^{-1}$ $mol^{-1}$ |
| 照射線量（X線及びγ線） | クーロン毎キログラム | C/kg | $kg^{-1}$ sA |
| 吸収線量率 | グレイ毎秒 | Gy/s | $m^2$ $s^{-3}$ |
| 放射強度 | ワット毎ステラジアン | W/sr | $m^4$ $m^{-2}$ kg $s^{-3}$=$m^2$ kg $s^{-3}$ |
| 放射輝度 | ワット毎平方メートル毎ステラジアン | $W/(m^2$ sr) | $m^2$ $m^{-2}$ kg $s^{-3}$=kg $s^{-3}$ |
| 酵素活性濃度 | カタール毎立方メートル | $kat/m^3$ | $m^{-3}$ $s^{-1}$ mol |

表５．SI 接頭語

| 乗数 | 接頭語 | 記号 | 乗数 | 接頭語 | 記号 |
|---|---|---|---|---|---|
| $10^{24}$ | ヨタ | Y | $10^{-1}$ | デシ | d |
| $10^{21}$ | ゼタ | Z | $10^{-2}$ | センチ | c |
| $10^{18}$ | エクサ | E | $10^{-3}$ | ミリ | m |
| $10^{15}$ | ペタ | P | $10^{-6}$ | マイクロ | μ |
| $10^{12}$ | テラ | T | $10^{-9}$ | ナノ | n |
| $10^9$ | ギガ | G | $10^{-12}$ | ピコ | p |
| $10^6$ | メガ | M | $10^{-15}$ | フェムト | f |
| $10^3$ | キロ | k | $10^{-18}$ | アト | a |
| $10^2$ | ヘクト | h | $10^{-21}$ | ゼプト | z |
| $10^1$ | デカ | da | $10^{-24}$ | ヨクト | y |

表６．SIに属さないが、SIと併用される単位

| 名称 | 記号 | SI 単位による値 |
|---|---|---|
| 分 | min | 1 min=60s |
| 時 | h | 1h =60 min=3600 s |
| 日 | d | 1 d=24 h=86 400 s |
| 度 | ° | 1°=(π/180) rad |
| 分 | ’ | 1’=(1/60)°=(π/10800) rad |
| 秒 | ” | 1”=(1/60)’=(π/648000) rad |
| ヘクタール | ha | $1ha=1hm^2=10^4m^2$ |
| リットル | L, l | $1L=11=1dm^3=10^3cm^3=10^{-3}m^3$ |
| トン | t | $1t=10^3$ kg |

表７．SIに属さないが、SIと併用される単位で、SI単位で表される数値が実験的に得られるもの

| 名称 | 記号 | SI 単位で表される数値 |
|---|---|---|
| 電子ボルト | eV | $1eV=1.602\ 176\ 53(14)\times10^{-19}J$ |
| ダルトン | Da | $1Da=1.660\ 538\ 86(28)\times10^{-27}kg$ |
| 統一原子質量単位 | u | 1u=1 Da |
| 天文単位 | ua | $1ua=1.495\ 978\ 706\ 91(6)\times10^{11}m$ |

表８．SIに属さないが、SIと併用されるその他の単位

| 名称 | 記号 | SI 単位で表される数値 |
|---|---|---|
| バール | bar | 1 bar=0.1MPa=100kPa=$10^5$Pa |
| 水銀柱ミリメートル | mmHg | 1mmHg=133.322Pa |
| オングストローム | Å | 1 Å=0.1nm=100pm=$10^{-10}$m |
| 海里 | M | 1 M=1852m |
| バーン | b | $1\ b=100fm^2=(10^{-12}cm)2=10^{-28}m^2$ |
| ノット | kn | 1 kn=(1852/3600)m/s |
| ネーパ | Np | SI単位との数値的な関係は、対数量の定義に依存。 |
| ベル | B | |
| デジベル | dB | |

表９．固有の名称をもつCGS組立単位

| 名称 | 記号 | SI 単位で表される数値 |
|---|---|---|
| エルグ | erg | $1\ erg=10^{-7}$ J |
| ダイン | dyn | $1\ dyn=10^{-5}$N |
| ポアズ | P | 1 P=1 dyn s $cm^{-2}$=0.1Pa s |
| ストークス | St | 1 St =$1cm^2$ $s^{-1}$=$10^{-4}m^2$ $s^{-1}$ |
| スチルブ | sb | 1 sb =1cd $cm^{-2}$=$10^4$cd $m^{-2}$ |
| フォト | ph | 1 ph=1cd sr $cm^{-2}$ $10^4$lx |
| ガル | Gal | 1 Gal =1cm $s^{-2}$=$10^{-2}ms^{-2}$ |
| マクスウェル | Mx | 1 Mx = 1G $cm^2$=$10^{-8}$Wb |
| ガウス | G | 1 G =1Mx $cm^{-2}$ =$10^{-4}$T |
| エルステッド(c) | Oe | 1 Oe≙ $(10^3/4\pi)$A $m^{-1}$ |

(c) ３元系のCGS単位系とSIでは直接比較できないため、等号「 ≙ 」は対応関係を示すものである。

表10．SIに属さないその他の単位の例

| 名称 | 記号 | SI 単位で表される数値 |
|---|---|---|
| キュリー | Ci | $1\ Ci=3.7\times10^{10}Bq$ |
| レントゲン | R | $1\ R = 2.58\times10^{-4}C/kg$ |
| ラド | rad | $1\ rad=1cGy=10^{-2}Gy$ |
| レム | rem | $1\ rem=1\ cSv=10^{-2}Sv$ |
| ガンマ | γ | 1γ=1 nT=10-9T |
| フェルミ | | 1フェルミ=1 fm=10-15m |
| メートル系カラット | | 1メートル系カラット = 200 mg = 2×10-4kg |
| トル | Torr | 1 Torr = (101 325/760) Pa |
| 標準大気圧 | atm | 1 atm = 101 325 Pa |
| カロリー | cal | 1cal=4.1858J（「15℃」カロリー），4.1868J（「IT」カロリー）4.184J（「熱化学」カロリー） |
| ミクロン | μ | 1 μ =1μm=$10^{-6}$m |

（第8版，2006年改訂）

この印刷物は再生紙を使用しています